ACCELERATION OF PARTICLES AND PRESSURE DROPS ENCOUNTERED IN HORIZONTAL PNEUMATIC CONVEYING

A THESIS

Presented to

the Faculty of the Division of Graduate Studies

Georgia Institute of Technology

In Partial Fulfillment

of the Requirements for the Degree

Doctor of Philosophy in the School of Chemical Engineering

by

Barton L. Hinkle

June 1953

ACCELERATION OF PARTICLES AND PRESSURE DROPS ENCOUNTERED

IN HORIZONTAL PNEUMATIC CONVEYING

Approved:

Thesis Adviser

Date Approved by Chairman: May 27, 1953

PREFACE

Years ago, authorities stated that the underlying mechanics of pneumatic conveying were so complex that it would never be possible to establish a sound, comprehensive theory which could be applied to design problems. Considerable progress, however, has been achieved in recent studies. The present investigation was designed as an examination of the horizontal transport process, with emphasis devoted to the importance of the particle velocity in the evaluation of the energy requirements.

The author is particularly indebted to Prof. J.M. DallaValle, whose advice and encouragement were indispensable to the direction of the project, and to Prof. M.J. Goglia, whose discussions clarified many of the details of the analysis. In addition, the author wishes to express his gratitude to the School of Chemical Engineering of the Georgia Institute of Technology, for the ready assistance in procuring equipment, and to the Koppers Company, which graciously supplied the polystyrene beads.

SYMBOLS

a. Latin Letter Symbols

A	Pipe cross-sectional area, ft.^{2}
A_p	Particle cross-sectional area, ft.^{2}
a	Acceleration, ft./sec.^{2}
C_r	Coefficient of resistance
D	Pipe diameter, ft.
d_p	Particle diameter, ft.
f	Friction factor
G	Mass rate, lb./min.
g	Acceleration of gravity, ft./sec.^{2}
g_c	Conversion factor, lb. mass, ft./lb. force, sec.^{2}
K	Constant
L	Pipe length, ft.
m	Particle weight, lb. mass
P	Pressure, lb. force/ft.^{2}
R	Specific loading
Re	Air Reynolds number
Re_p	Particle Reynolds number
s	Specific gravity of solid
t	Time, min.
u	Velocity, ft./sec.

b. Greek Letter Symbols

β	Functional relation
Δ	Finite difference
μ	Dynamic viscosity of air, lb. mass/hr., ft.
ρ	Density, lb. mass/ft.^{3}
ψ	Sphericity
σ_g	Geometric standard deviation

c. Latin Letter Subscripts

a	Air
p	Particle
r	Relative
aa	Acceleration, air
ap	Acceleration, particle
fa	Friction, air
fp	Friction, particle
ft	Friction, total
sa	Static, air
sp	Static, particle
mc	Minimum conveying
T	Total

SYMBOLS

d. Superscripts

b	Constant
*	Equilibrium condition

TABLE OF CONTENTS

(Continued)

TABLE OF CONTENTS (Concluded)

LIST OF FIGURES

LIST OF FIGURES

LIST OF FIGURES

LIST OF TABLES

ACCELERATION OF PARTICLES AND PRESSURE DROPS ENCOUNTERED IN HORIZONTAL PNEUMATIC CONVEYING

I. SUMMARY

The importance of pneumatic transport systems has increased remarkably during recent years, especially since the widespread application of fluidized catalyst processes. In addition, pneumatic conveying is being used more and more in problems involving the transport of hazardous substances and in cases requiring the transport of heavy concentrations of granular materials.

Early investigations, based upon a few specific materials, led to empirical equations for estimation of the energy requirements in a pneumatic process. Recent studies have dealt with methods whereby the constants of the empirical equations could be evaluated in terms of such properties as particle size and density. The importance of particle velocity was recognized in many cases, but the difficulties of measurement precluded its use in developing equations, and experimental data were rectified through diverse correlating factors. It is not surprising that the various correlations proposed were accurate for only a few specific systems and that no single correlation has found wide applicability and acceptance.

The present investigation was concerned with a re-examination of the fundamental principles and a re-evaluation of the principal forces involved in pneumatic conveying, with special emphasis devoted to the importance of particle velocity. The primary objective was the develop-

ment of a generalized method for predicting the pressure drop encountered in the horizontal pneumatic transport of any material at any loading rate. Secondary objectives were: (1) a method for estimating the necessary length of pipe to attain equilibrium particle velocity; (2) estimation of the equilibrium particle velocity; (3) estimation of the pressure drop encountered during the acceleration of the solids; (4) the effect of loading on the ultimate particle velocity and on the resulting pressure drop; and (5) the effect of particle size and shape on the velocity and pressure drop.

All experiments were conducted using horizontal glass pipes two inches and three inches in diameter. Pressure drops were measured at intervals of five feet along a total pipe length of thirty feet. Particle velocities at various distances from the solids inlet were measured by high-speed photographic techniques. The solid materials examined were polystyrene beads, Tenite plastic pellets, Alundum catalyst supports and Catalin spheres. The four materials provided a particle size range from 0.014 to 0.33 inch diameter and a specific gravity range from 1.05 to 1.82.

A theoretical analysis of the problem led to a method for predicting particle velocity from pressure drop measurements, and the results so obtained were found to agree with the data obtained from the high-speed photographs. The length of pipe necessary for the attainment of an equilibrium particle velocity was found to be a function of the loading, and an equation is presented which permits calculation of the necessary pipe length from pressure drop data. The ultimate particle

velocity is shown to be independent of the loading but of course is strongly influenced by the air velocity.

The pressure drop due to the acceleration of the solids was a significant fraction of the total pressure drop in the thirty foot length of pipe. An equation for calculating the acceleration pressure drop, derived from a momentum balance across the accelerating section, was found to agree with experimental observations.

The widely used method of presenting friction pressure drop data (a plot of specific pressure drop versus loading) has been re-examined. The solids friction effects were treated by a method analogous to the Fanning equation for fluids, and through consideration of the continuity equations for both the solids and the air, studies have shown that the slope of the line resulting from a plot of specific pressure drop versus loading is a function of particle velocity, air velocity, air friction factor and solids friction factor. Methods of presenting friction pressure drop data for both horizontal and vertical conveying are developed which satisfy both theoretical considerations and observed results. For the case of horizontal pneumatic conveying,

$$\frac{\Delta P_{ft}}{\Delta L} = 1 + \frac{f_p u_p^*}{f_a u_a} R$$

and for vertical transport,

$$\frac{\Delta P_{ft}}{\Delta L} = 1 + \frac{f_p u_p^*}{f_a u_a} R + \frac{2 g_c D}{f_a u_a u_p^*} R$$

The validity of the method for horizontal transport was established by data of the present investigation, and for vertical transport, by data

presented in the literature. Whereas the method of presenting data as specific pressure drop against loading gives a single linear relationship only for a specific material and a specific air velocity, the method developed in this study gives a single linear relationship for all materials and all air velocities.

The total pressure drop, obtained by adding the calculated friction and acceleration pressure drops, was found to give precise agreement with the observed total pressure drop.

An empirical equation is presented for estimating the equilibrium solids velocity in a horizontal pipe in the absence of experimental values or pressure drop measurements. Thus,

$$u_r = 1.41\ u_a d_p^{0.3} s^{0.5}$$

The dependence of particle velocity on saltation or "slugging" velocity and the necessity for more accurate methods of estimating the minimum conveying velocity are recognized.

II. INTRODUCTION

A. Literature Review

Interest in the pneumatic conveying of granular solids has increased steadily during the past three decades, and the recent developments of fluidized catalyst systems have led to more incisive studies of the dynamics of the transported particles. While pneumatic conveying is not the cheapest method of transportation with regard to energy requirements, it has distinct advantages in systems dealing with expensive or hazardous materials, and in cases where ease of solids charging and removal is desired. Many examples of pneumatic installations are available. Culgan (6) mentions the pneumatic tube used during the construction of Boulder Dam, where up to seventy six tons per hour of dry cement were transported through a conduit nearly a mile in length. Sadler (23) discusses various applications, such as the transport of flour, granular chemicals, lime, soda ash, plastic chips and coal. One of the earlier widespread uses of pneumatic conveying was the unloading of grain from ships, and Gasterstadt's work is devoted to quantitative studies of the pressure drops encountered in the transport of suspensions of grain in air. Gasterstadt (11) defined a dimensionless factor α as the ratio of the pressure drop of the solid suspension to the pressure drop for air alone at the same velocity. From studies on wheat, he concluded that a linear relationship existed between α and the specific loading R, defined as the weight ratio of solid flow to air flow. The slope of the line resulting from a plot of α versus R was found to vary with air velocity. Segler (24) confirmed the results of Gasterstadt, but

others, e.g. Farbar (10), have found that no such simple relation exists, particularly in the case of horizontal conveying.

Cramp (4) presented a detailed analysis of the force terms to be considered in the estimation of pressure drops in pneumatic conveying systems. According to Cramp the following effects must be evaluated: (1) the differential pressure on the two ends of the column, multiplied by the cross-sectional area of the pipe; (2) the friction between the pipe and the material being conveyed; (3) in vertical pipes, the force required to support the column of material; (4) the friction of air on the pipe; (5) the forces required to support and accelerate the air; and (6) the force required to accelerate the material. An example in conveyor design is presented, with demonstrations of calculations of the various terms. Cramp also describes an experiment for the estimation of the solids velocity in a horizontal pipe. Evidently the necessity for pressure drop estimation and the dependence of pressure drop on the solids velocity was recognized at an early date. Jennings (15) and Chatley (3) give theoretical treatments of the evaluation of the forces discussed by Cramp, and disagreement regarding the estimation of particle velocity is evident. Wood and Bailey (31) gave a detailed analysis of the momentum transfer between the conveying air and the solids, using an injector system. The objective of their investigation was the determination of the optimum position of the injector; hence their pressure drop data includes the pressure drop across the injector, thus complicating any comparison with data from other studies. It is of interest to note the conclusions of Wood and Bailey: (1) that the optimum position for an air

injector is in the middle of the transport tube; (2) that a conical diffuser at the outlet of a conveyor system improves the performance of the conveyor by the conversion of kinetic energy to pressure energy by a reduction of velocity; and (3) that the path of the particles in the pipe appears to be a series of leaps: as the particle is picked up by the air and carried downstream, gravitation causes it to fall to the bottom of the pipe.

This last conclusion raises questions regarding the minimum air velocity necessary to pick up a particle at rest on the bottom of a pipe, which has been examined by Davis (9), and the nature of solids flow, which has been discussed by Korn (17). Davis presented a thorough analysis of the minimum fluid velocity necessary to raise a particle of fixed size and keep it in suspension for the cases of clear and saturated streams. He suggests that a slightly higher air velocity is required to keep a heavy concentration of solids in suspension than is predicted from theory, and consequently introduces an empirical "safety factor" to the proposed formula. The data of the present investigation show that Davis' theoretical equation for the "saturation" velocity is quite accurate, however, if proper account is taken of the relative velocity of the solids with respect to the air. Regarding the nature of solid flow, Korn (17) suggested three separate classifications. In the first case, solid particles may advance by successive leaps with consequent saltation, i.e., contact with pipe walls. If the solids are light and are acted upon by a steep velocity gradient, however, there is little contact with the pipe walls, as the bulk of the material is carried by the central (higher

velocity) portions of the air in the pipe. In the third case, if the particles are extremely small, the terminal velocity of their free fall will be negligible, there will be an insignificant difference between the air velocity and the particle velocity, and consequently the mixture will behave as a true fluid.

The importance of particle terminal velocity in pneumatic conveying studies is mentioned by Gasterstadt and is discussed in detail by Wagon (29). Application of terminal velocity data to vertical transport has been successful; in horizontal transport, however, the relationship of terminal velocity to particle velocity is somewhat obscure.

Whereas the earlier theoretical studies, e.g. Cramp, Gasterstadt, and Wood and Bailey, contain empirical factors to be evaluated for every solid, recent investigations have attempted to derive generalized correlations through the introduction of new variables. Vogt and White (27) used the dimensionless pressure drop ratio α suggested by Gasterstadt, and correlated their data by the equation

$$\alpha - 1 = A\left(\frac{D}{d}\right)^2 \left[\frac{w_g}{w_s} \cdot \frac{R}{Re}\right]^k \qquad (1)$$

where D is the pipe diameter, d the particle diameter, w_g and w_s the densities of the gas and of the solids, respectively, R the weight ratio of the solids flow per unit time to the air flow per unit time, and Re the air Reynolds number. The constants A and k are functions of the dimensionless group

$$\left[\frac{(\rho_s - \rho_g)\rho_g g d^3}{3\mu^2}\right]^{0.5}$$

which is the product of the Reynolds number and the square root of the drag coefficient for a spherical particle under free-settling conditions. No velocity term is involved, and the derivation ignores the effect of particle shape. Experiments were conducted using a loop constructed of one-half inch pipe. The horizontal test section was located nine feet from a bend, and the authors state that this distance was not always a sufficient allowance for the attainment of equilibrium particle velocity. Materials used were wheat, clover seed, sand and steel shot.

Hariu and Molstad (12) studied the transport of closely sized silica-alumina catalysts and sand in vertical pipes 0.267 and 0.532 inch in diameter. Particle size ranged from 0.0043 to 0.0198 inch. They recognized the importance of a knowledge of particle velocity for the correlation of data, and calculated the particle velocity through measurements of the "disperse-density" of the solids. The continuity equation applied to the solids is:

$$G_s/A = u_s \rho_{ds} \qquad (2)$$

where G_s is the mass flow of the solids, A the pipe cross-sectional area, u_s the particle velocity, and ρ_{ds} the weight of solids dispersed per unit volume.

Hence particle velocity was easily calculated, once the mass rate and the disperse-density were known. The authors observed that the equilibrium velocity of the solids was independent of the loading; that the pressure drop due to acceleration of the solids was a significant portion of the total pressure drop; and that the average particle

velocity for the material used (Ottawa sand) was approximately one-half the gas velocity. Good correlation was achieved by considering the total pressure drop as a sum of the pressure drop due to the carrier gas plus a solids pressure drop. Attempts to consider the individual pressure drops jointly rather than separately have met with more difficulty.

Belden and Kassel (2) also studied pneumatic conveying in vertical tubes. Data are presented for the transport of spherical catalysts approximately 0.04 and 0.08 inch in diameter in transfer lines 0.473 and 1.023 inches in diameter. The correlation developed in this work expresses the total pressure drop as a function of a static term based upon actual particle density in the transfer line, and a friction term which involves the particle mass velocity, but which is independent of particle diameter and density. The greater part of the data presented can be related by the equation

$$f(Re)^{0.2} = 0.049 + 0.22 \frac{G_g G_c}{(G_g + G_c)^2} \qquad (3)$$

where f is the friction factor, Re the Reynolds number, G_g the mass velocity of the carrier gas, and G_c the mass velocity of the solids. According to these authors, the correlation proposed by Vogt and White involves an incorrect dependence on the ratio of tube diameter to particle diameter. Korn (17) confirms Belden's and Kassel's findings that the pressure drop is nearly independent of this ratio. Acceleration losses, however, were not determined, and the measured pressure drops were corrected for acceleration on a speculative basis. The statement

that the correction for acceleration losses is small does not agree with the results of other investigators, and the effect of the "speculative" corrections may account in part for the anomalous negative friction factors which appear in a few of the experiments.

Farbar (10) investigated the flow characteristics of an alumina-silica catalyst mixture with a particle size spectrum ranging from 10 to 220 microns. The glass conveying tube was 17 mm. inside diameter, and the air velocity was varied from 50 to 150 feet per second. No measurement of particle velocity was attempted; in fact, Farbar avoids the use of the word "velocity" on the basis that the term is meaningless when applied to the mixture. Several types of nozzles for feeding the solids were investigated, and qualitative observations are presented on the flow in the solids feed line, the mixing nozzle, the horizontal and vertical test sections, bends, and the behavior of a cyclone separator. The data obtained in this study are not included, but a plot of the specific pressure drop versus specific loading for both the horizontal and vertical conduits is offered.

Lapple (18) discussed the contributions of Gasterstadt and DallaValle (7), reviewed the various force ters to be considered in the pneumatic design problem, and suggested the following equation for the calculation of the pressure drop due to the friction of both the air and the solids:

$$P_f = \frac{4fLG^2}{2g_c D} (1 + R) \left(\frac{1}{\rho_a} + \frac{R}{\rho_s}\right) \qquad (4)$$

where f is the Fanning friction factor, L the length of pipe in feet,

G is the air mass velocity in pounds per second per square foot, D is the pipe diameter in feet, R the specific loading, and ρ_a and ρ_s the densities of the air and of the solid, respectively. Friction factors are determined from plots of f versus Re, using Re as defined by the relation

$$Re = \frac{DG}{\mu}(1 + R) \tag{5}$$

where μ is the viscosity of the air.

The pressure drops predicted from equation (4) are somewhat lower than the actual pressure drops encountered.

The recent study of Khudyakov and Chukhanov (16) deals with the movement of sand particles of average size 70, 200 and 845 microns in a stream of gas. Pipes of diameters 14, 20 and 32 mm. were used. No pressure drop data is presented. Particle velocity data were obtained by high-speed photographic techniques, as in the present investigation. The differential equation relating particle velocity to length of pipe is integrated by assuming that contact of the solid with the pipe walls is negligible. The validity of this assumption is doubtful, considering the particle size and density of the larger sample and the relatively small tube diameters of the conduits. The authors have counterbalanced the questionable assumption, however, by redefining the coefficient of resistance as

$$C_r = 0.7\ Re^{-0.18} \tag{6}$$

where C_r is the coefficient of resistance. Although no definition is

included in the article, Re in equation (6) is evidently the particle Reynolds number for pneumatic conveying, defined as

$$Re_p = \frac{d_p(u_a - u_p)\rho_a}{\mu} \qquad (7)$$

Examination will show that the values of C_r obtained from equation (6) are considerably lower than the values given by the established C_r vs. Re_p curve which is presented in almost any standard text dealing with particle motion (8,14), and is included as Figure 30 in the Appendix. A decreased C_r results in decreased particle acceleration; and since particle contact with the walls of a pipe also results in a reduced acceleration, the use of C_r as defined by equation (6) will approximate actual conditions during the acceleration period even though particle-to-wall collisions are neglected. The applicability of Khudyakov and Chukhanov's work is limited to the early phase of the acceleration period, as their equation predicts an ultimate particle velocity equal to the gas velocity. Experimental evidence contradicts this prediction.

Uspenskii (26) has also considered the velocity of particles and the coefficients of resistance in pneumatic conveying; in fact, his work is prefaced by the statement that all energy losses in the pneumatic conveying of granular solids are functions of the particle velocity. Calculations of particle velocity were accomplished in the same manner as discussed by Hariu and Molstad (12). Particles of 0.82, 0.105 and 0.142 mm. average diameter were transported in a tube 41 mm. in diameter, and pressure drops were measured. The ratio of particle velocity to gas velocity for coal dust of diameter 0.105 mm. was found to decrease

from a value of 0.94 at high gas velocities to a value of 0.57 at a gas velocity just sufficient to move the particles along the bottom of the tube. The friction coefficient was assumed to be the same in the accelerating region as in the uniform velocity region. The data of the present study do not support this assumption. The principal contribution of this work is the thorough graphical analysis of a plot of pressure drop versus length of pipe.

Albright et al. made an interesting study of the flow of dense air-coal mixtures with specific loadings up to 200 pounds of coal per pound of air. The coal particles were sized so that 90 per cent would pass through 200 mesh, and were conveyed through tubing 3/8, 5/16 and 1/2 inch diameter. No particle velocity data was obtained. None of the methods of correlation proposed thus far was found to be adaptable to the data of this investigation, although the authors felt that a modification of the Vogt and White correlation might be useful.

Zenz (32) obtained pressure drop data for the flow of three samples of essentially uniform particles 0.231, 0.0366 and 0.066 inch in diameter, and a material of 0.0066 inch mean diameter with a five-fold variation in particle size. All experiments were carried out in a 1.75 inch inside diameter lucite tube. Again, particle velocity was not measured. Correlation is offered in the form of two graphs, one a plot of specific pressure drop versus fluid velocity divided by choking velocity for vertical pipes, the other a plot of specific pressure drop versus fluid velocity minus saltation velocity for horizontal pipes. Saltation velocity is defined as the fluid velocity at which particles begin to

settle out of the air stream and collide with the tube walls in horizontal conveying. Choking velocity is an analogous situation with vertical pipes: it is the fluid velocity at which the particles begin to choke up and to travel in distinct slugs. It is interesting to note that the saltation velocity was found to be equal to the choking velocity for comparable solid loadings. Zenz criticizes Vogt and White for neglecting to account for saltation and choking velocities, and Cramp and Priestly for failing to note an effect of loading on the choking velocity. The pressure drop data reported by Zenz are high, owing to the short accelerating section provided, and while the graphical correlations offered are limited in general application, the dependence of pressure drop on saltation or choking velocity is evident.

Culgan (6) examined the horizontal conveying of materials of approximately unit specific gravity, average particle size ranging from 0.03 to 0.33 inches, in a three inch pipe. Only a few measurements of particle velocity were made. Correlation of data was achieved through the use of an empirical correlating factor, and the pressure drop per unit length of pipe in which the solids were conveyed was expressed by an equation of the form

$$\frac{2g_c D h_m}{u_a^2 L}\left(\frac{\rho_m}{\rho_s}\right)^{0.25} = f\,(Re)_m \qquad (8)$$

where h_m is the head loss in feet of air, ρ_m the density of the mixture of air and solids, ρ_s the density of the solid, and Re_m the Reynolds number based on the air velocity and the mixture density. The other

terms are defined as in the present study. The mixture density, ρ_m, is calculated by the equation

$$\rho_m = \frac{W_s}{Q_a} + \rho_a \tag{9}$$

where W_s is the feed rate of the solids in pounds per minute, Q_a the volumetric air rate in c.f.m., and ρ_a the density of the conveying air. Since the mixture density, ρ_m, in pounds per cubic foot is equal to the pounds of solids dispersed per cubic foot, ρ_{ds}, plus the pounds of air per cubic foot, ρ_a, Culgan is effectively defining the disperse-density as

$$\rho_{ds} = \frac{W_s}{Q_a} \tag{10}$$

Continuity equations for the solids and for the air may be expressed as

$$W_s = Au_s\rho_{ds} \tag{11}$$

and

$$W_a = Au_a\rho_a \tag{12}$$

where **A** is the cross-sectional area of the pipe. Dividing equation (11) by equation (12) and solving for ρ_{ds} leads to

$$\rho_{ds} = \frac{W_s\rho_a}{Q_a} \cdot \frac{u_a}{u_s} \tag{13}$$

Substituting Q_a for its equivalent, W_a/ρ_a, reduces equation (13) to

$$\rho_{ds} = \frac{W_s}{Q_a} \cdot \frac{u_a}{u_s} \tag{14}$$

Reference to equation (10) shows that Culgan's calculated values of the disperse-density are low by the amount of the prevailing slip factor, u_a/u_s. For the Tenite particles used in both Culgan's studies and the author's, the slip factor is approximately 1.5, thus indicating that the disperse-densities of Culgan are nearly 50 per cent lower than the actual disperse-densities.

The correlating factor introduced by Culgan evidently well compensates for his neglecting the slip factor, since equation (8), proposed for pressure drop estimations, was found to express the observed data of the present study within ten per cent.

Due to some arithmetic errors in the studies of the relative velocity of the solids, it appears that the equilibrium particle velocity is dependent on the solids loading and is independent of the conveying air velocity. Actually the opposite is true: the equilibrium particle velocity is strongly influenced by the air velocity and is not affected by the solids loading rate.

Perhaps the most significant of Culgan's recommendations was the suggestion that knowledge of the relative velocity of the solids with respect to the conveying air is of fundamental importance in the solution of design problems.

B. Objectives of Investigation

The preceding review of the major contributions to the knowledge of pneumatic conveying shows that, while significant advances have been made, there still remains much confusion and apparent disagreement.

Most of the investigators have recognized a need for information on the velocity of the solids, yet there is little data of this nature. Many of the experimental results are of doubtful value because of failure to allow for an adequate accelerating section. In view of these shortcomings, it is not surprising that the generalized correlations proposed have not found wide acceptance.

This thesis work involved a study of pneumatic transport encompassing particle velocity as well as pressure drop measurements, to the end that the following objectives might be realized: (1) knowledge of the length of pipe required for equilibrium particle velocity to be attained; (2) methods for estimating the equilibrium particle velocity; (3) estimation of the pressure drop encountered during the acceleration of the solids; (4) the effect of particle size, density and shape on the equilibrium velocity and on the pressure drops; (5) the effect of solids loading on the equilibrium particle velocity and on the pressure drops; (6) estimation of the pressure drop due to friction effects; and (7) estimation of the total pressure drop, including the pressure drops due to accelerating the conveying air and the solids, and due to air and solids friction.

III. EXPERIMENTAL METHODS

A. Apparatus

The essential features of the apparatus used for the pneumatic conveying studies are presented in Figure 1.

Material to be conveyed was charged to the feed hopper. A helical screw conveyor in a trough at the bottom of the hopper fed the solids to a cylindrical shaft connected with the conveyor line. Control of the rate of solid feed was adjustable by means of a Master Speed Ranger gear reducer attached to the drive motor of the helical screw. Two type 2-RE blowers manufactured by the Buffalo Forge Company were connected in series to provide the air flow through the transport tube. Flow of air was regulated with a gate valve located on the low pressure side of the blowers. After passage through the conveyor line the solids were removed from the air stream in a centrifugal separator.

The conveyor line was constructed from sections of Pyrex Brand "Double-Tough" glass pipe, manufactured by the Corning Glass Works, Corning, New York. The sections of pipe were carefully aligned and joined together in the manner shown in detail in Figure 2. The interface gaskets were the Neoprene Type R-2, also manufactured by the Corning Glass Works. The metal flange sets and inserts were obtained with the pipe. The pressure tap insert was made of 3/8 inch brass and was shaped according to the design of the interface gaskets. During assembly, the interface gaskets and pressure tap insert were aligned with the pipe so that there would be no obstruction at the junction of the pipe sections.

Pipes of two inches and three inches inside diameter were used in

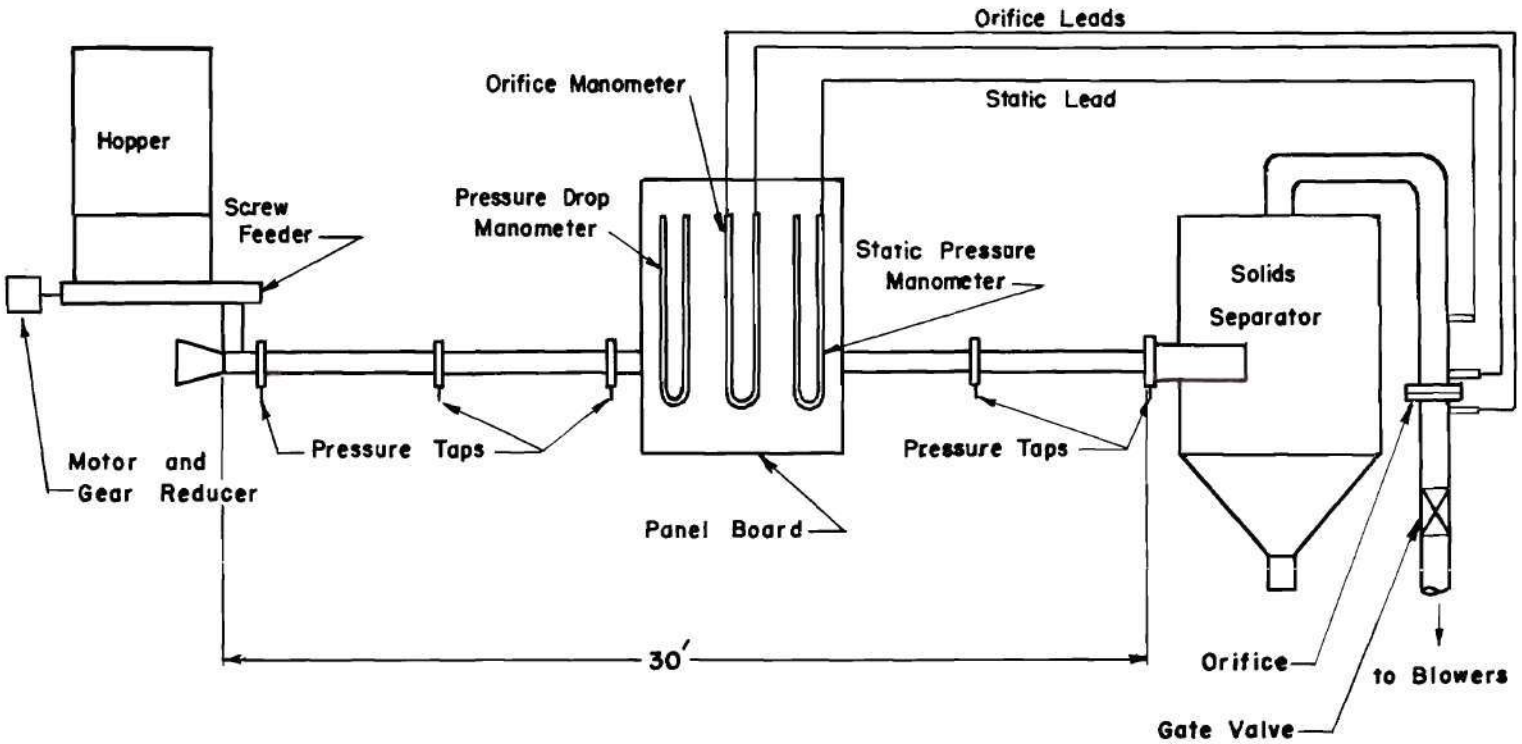

Figure 1. Diagram of Experimental Apparatus.

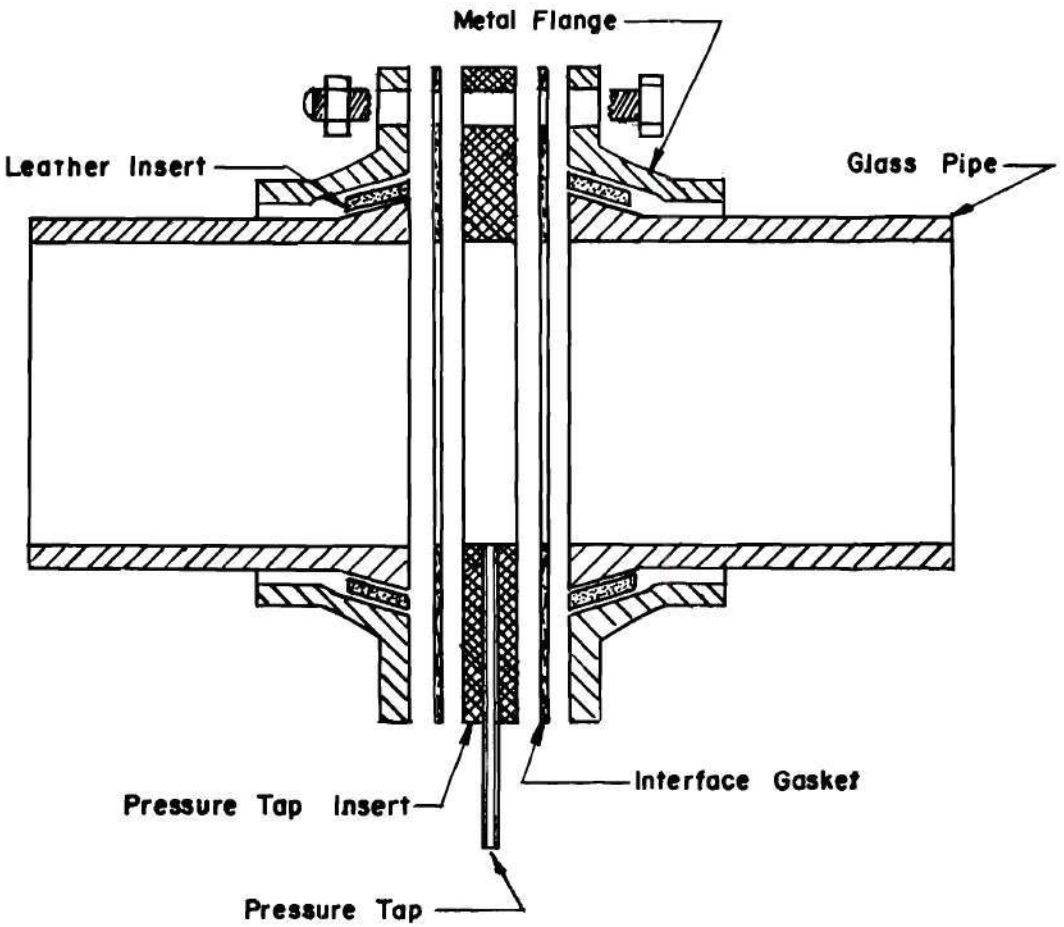

Figure 2. Diagram of Pipe Coupling and Pressure Tap Insert.

the study. Six sections, each five feet in length, constituted the conveyor line. Since the pressure taps were located between adjoining pipe sections, the spacing between taps was fixed at five feet.

The flow rate of the air through the pipe was measured by the use of an orifice 2.174 inches in diameter, located in the standard three inch line between the solids separator and the blowers. The installation of the orifice was made in accordance with the specifications of Stearns et al. (25), and hence the orifice coefficients used in subsequent calculations were evaluated by the methods outlined by Stearns. For purposes of calibration, a pitot tube was installed in a line on the high pressure side of the blowers. Such pitot tube measurements, made over the range of air velocities used in this study, gave excellent agreement with the orifice measurements. A plot of air velocity calculated from orifice measurements versus air velocity calculated from pitot tube measurements is given in Figure 27 in the Appendix.

An indirect check of the accuracy of orifice measurements was obtained through pressure drop measurements. The pressure drop of air in the pipe was calculated by the familiar Fanning equation, using a roughness factor suggested for smooth glass tubing and friction factors corresponding to the air Reynolds number. The agreement between calculated and experimentally determined pressure drops for the two-inch and the three-inch pipes is given in Figures 28 and 29 in the Appendix. For convenience, the accepted Reynolds number-Fanning friction factor relation for smooth glass tubing is included in Figure 31. Pitot tube, static pressures and differential pressures across the orifice were meas-

ured by means of simple U-tube manometers. Distilled water containing a small amount of dye served as the manometer fluid. More accurate devices for measuring differential pressures were not justified because of the pulsations which occurred during air and air-solid flow.

Manometers were located on the panel board as shown in Figure 1. Electrical connections were routed through switches on the panel board so that the blowers and the solids feed motor could be actuated when desired.

The particle velocity measurements were made with a Western Electric high-speed motion picture camera using 16 mm. Eastman Super-XX film from the Eastman Kodak Company, Rochester, New York. A small ruler was taped to the bottom of the pipe at the point where pictures were taken so that the distance of movement of a particle downstream could be measured. A neon timing-light in the body of the camera provided a means for calculating the rate at which photographs were taken. Calculations of particle velocity were based upon a knowledge of the camera speed and the rate at which particles moved past the ruler. The method of analysis is presented in more detail later.

B. Materials

Four different materials were used in this study: Tenite particles supplied by the Tennessee Eastman Corporation, Kingsport, Tennessee; type 8X polystyrene beads, supplied by the Koppers Company, Pittsburg, Penna.; Catalin spheres, purchased from the Ace Plastic Company, Jamaica, New York; and Alundum spheres, obtained from the Norton Company, Worcester,

Massachusetts. These solids were chosen to give a wide range of particle size and density. Properties of the four different materials are presented in Table I.

The polystyrene beads were small, colorless spheres. Specific gravity and other properties were furnished by the Koppers Company in Technical Bulletin No. 1-0-137. Particle size was determined by microscopic measurement using the method outlined by DallaValle (8). The diameters of two hundred beads were measured and the results plotted on logarithmic probability coordinates as shown in the lower curve of Figure 32; the geometric median particle diameter d_g was then obtained by noting the size corresponding to 50 per cent on the probability scale. Standard deviation was also obtained from the curve by a relationship derived from the probability plots. The geometric standard deviation is given by

$$\sigma_g = \frac{84.13 \text{ per cent size}}{50 \text{ per cent size}} = \frac{50 \text{ per cent size}}{15.87 \text{ per cent size}} \qquad (15)$$

where σ_g is the standard deviation. The median diameter obtained by microscopic measurement is based upon number or count. Since the relations developed for pneumatic conveying deal with weights rather than numbers, it was necessary to convert the median diameter by count to a median diameter on a weight basis. The necessary conversion equation is given by DallaValle (8). Thus

$$\ln d_g' = \ln d_g + 3 \ln^2 \sigma_g \qquad (16)$$

where d_g and σ_g are the statistical parameters of the size-frequency curve by count and d_g' is the geometric median diameter by weight. The size-frequency curve by weight is given in the upper curve of Figure 32. The curves are parallel owing to the fact that the geometric standard deviations by count and weight are equal.

The Tenite particles were shaped in the form of cubes, with rounded edges and corners. The sieve analysis is noted in Table I. The maximum size observed was 0.12 inch, and 93 per cent by weight was greater than 0.0661 inch. Thus the standard deviation of the material was small, and the average size was taken as 0.1 inch. Average sphericity was estimated using the method discussed by Wadell (28). Sphericity is defined as the ratio of the surface area of a sphere having the same volume as the particle to the actual surface area of the particle. The limiting value of sphericity is 1.0, which occurs when the particle is a sphere. Unfortunately, measurement of sphericity is quite difficult for particles having irregular shapes; however, Wadell suggests two methods by which sphericity may be readily estimated. A closely correlated measurement is the degree of circularity, defined as the ratio of the circumference of a circle having the same cross-sectional area as the particle to the actual perimeter of the cross-section. Another measurement can be obtained by dividing the nominal diameter of the particle by the diameter of the smallest sphere circumscribing the particle. The sphericities reported in Table I represent the average values obtained from experiments using both the methods described above.

The Catalin particles were red spheres exceptionally uniform in

TABLE I

PROPERTIES OF THE SOLID MATERIALS

Material	TENITE	
Specific Gravity	1.13	
Particle Density	70.5 lb./ft.^{3}	
Bulk Density	45.5 lb./ft.^{3}	
Per cent Voids	35.7	
Sphericity	0.93	
Sieve Analysis		
	Retained on No. 8 (0.0939 in.)	67.3%
	Retained on No. 12(0.0661 in.)	25.7%
	Retained on No. 16(0.0469 in.)	4.2%
	Less than No. 16	2.8%
Maximum Size Observed	0.12 in.	
Terminal Velocity	21.2 ft./sec.	
Material	CATALIN	
Specific Gravity	1.12	
Particle Density	69.7 lb./ft.^{3}	
Bulk Density	49.0 lb./ft.^{3}	
Per cent Voids	0.30	
Particle Diameter	0.25 in.	
Sphericity	1.00	
Terminal Velocity	44.5 ft./sec.	

TABLE I

PROPERTIES OF THE SOLID MATERIALS

Material	POLYSTYRENE
Specific Gravity	1.05
Particle Density	65.5 lb./ft.^{3}
Bulk Density	40.0 lb./ft.^{3}
Per cent Voids	0.39
Sphericity	0.962
Mean Particle Size	0.00805 in. (count)
Mean Particle Size	0.014 (weight)
Maximum Size Observed	0.035 in.
Terminal Velocity	8.65 ft./sec.
Material	ALUNDUM
Specific Gravity	1.82
Particle Density	113 lb./ft.^{3}
Bulk Density	71 lb./ft.^{3}
Per cent Voids	0.37
Sphericity	1.00
Mean Particle Size	0.33 in.
Maximum Size Observed	0.36 in.
Terminal Velocity	65.3 ft./sec.

size, having been manufactured for use as ball bearings. Particle density was determined by weighing a specified number of the spheres and dividing the weight obtained by the total particle volume. After several runs the material had been degraded to an extent such that a number of the spheres had been split in half. Since particle velocity and friction calculations were dependent on particle shape, the remainder of the experiments were performed with materials which did not suffer such drastic degradation.

The Alundum spheres (alumina catalyst supports) were also uniform in size and had porous, gritty surfaces. The average diameter was determined from a number of measurements with a micrometer, and the particle density was again obtained by the weighing technique described in connection with the Catalin spheres.

C. Methods of Investigation

Preliminary runs were devoted to calibration of the screw conveyor feeder. A brief discussion of the characteristics of screw feeders is given by Perry (20). Such a feeder was ideally suited for use with studies of horizontal pneumatic conveying, since a uniform stream of material is delivered even though the head of material above the screw may vary over a wide range. Screw feeders have the additional advantage that material cannot flood through the outlet. In view of these characteristics, it is not surprising that the calibration of weight solids conveyed versus time of conveying, given in Figure 33, is a linear relation. Conveying time was determined with a stopwatch; the weight delivered was measured on a one-half ton capacity Howe scale. For

convenience, the speed regulator of the screw feeder was calibrated against the weight delivered per unit time for all materials studied. These curves are presented in Figure 34.

Periodically the glass pipe was examined for roughness which might have developed due to contacts of the particles with the pipe walls. No such abrasive effects were evident, however, even in the case of the gritty Alundum spheres. Furthermore, the air pressure drops in the line remained constant throughout the series of tests, indicating that, even if the pipe had been roughened somewhat, the effect was negligible. Experimental pressure drop data for the air alone are presented in Table II.

The experimental procedure used in these studies was as follows: first, the variable speed drive of the screw feeder was adjusted to give the desired solids feed rate; next, the blowers were actuated and the gate valve adjusted to give the desired air flow in the line. The motor driving the screw conveyor was then started. After the manometers had attained a constant reading, thus indicating equilibrium conditions, the orifice and static pressure readings and the pressure drop measurements were recorded. Usually less than ten seconds was required for the attainment of equilibrium after the solids flow was initiated, and all readings could be noted within three minutes. The experimental pressure drop data for all runs are given in Table III, and the calculated pressure drop, particle velocity and loading data are given in Table IV.

Theoretical studies led to the development of a method for calculating the equilibrium particle velocities based on pressure drop measure-

TABLE II

PRESSURE DROP DATA FOR THE CONVEYING AIR

Run	Orifice Reading in. H_2O	Orifice Static Pressure in. H_2O	Bar. Pressure mm. Hg	Temp. ^oF	$\frac{\Delta P_{fa}}{\Delta L}$ $\frac{\text{in.}H_2O}{\text{ft.}}$	u_a ft./sec.
		Two-Inch Pipe				
A2	4.80	15.0	740	74	0.330	120
B2	4.30	13.9			0.303	114
C2	3.95	12.7			0.272	109
D2	3.65	12.0			0.255	105
E2	3.30	11.1			0.233	100
F2	2.90	10.0			0.207	94
G2	2.75	9.60			0.196	91
H2	2.45	8.65			0.173	86
I2	2.25	8.05			0.157	82
J2	2.00	7.40			0.145	78
K2	1.80	6.75			0.120	74
L2	1.65	6.15			0.110	70
		Three-Inch Pipe				
A3	14.20	7.80	743	79	0.0968	80
B3	12.80	7.20			0.0870	76
C3	11.50	6.70			0.0782	72
D3	10.90	6.50			0.0740	70
E3	10.20	6.25			0.0695	68
F3	9.40	5.92			0.0638	65
G3	8.55	5.62			0.0580	62
H3	8.00	5.40			0.0545	60
I3	12.15	6.95			0.0825	74
J3	13.05	7.35			0.0895	77

TABLE III

EXPERIMENTAL DATA

Run No.	Material	Solids Mass Rate, lb./min.	Orifice Air Velocity, ft./sec.	Air Velocity in Pipe, ft./sec.	Equil. Friction Loss, in. H_2O/ft.	Total Head Loss, in. H_2O (25 ft.)	Bar. Press., mm. Hg	Temperature °F
1	Tenite	12.0	100	118	0.390	16.3	740	80
2	Tenite	17.5	91	108	0.373	17.0	739	70
3	Tenite	10.0	90	106	0.305	12.9	739	70
4	Tenite	10.0	101	119	0.370	15.5	742	80
5	Tenite	17.5	100	118	0.435	19.9	742	80
6	Tenite	13.8	91	108	0.337	15.0	742	80
8	Tenite	9.2	92	109	0.310	12.9	742	80
9	Tenite	9.2	101	119	0.365	15.1	740	90
10	Tenite	8.8	68	79	0.175	8.3	740	90
11	Tenite	9.2	95	112	0.320	13.5	740	90
12	Tenite	13.8	99	117	0.385	16.5	740	90
13	Tenite	13.8	97	115	0.380	17.4	740	90
14	Tenite	13.8	95	112	0.365	16.0	740	90
15	Tenite	13.8	90	107	0.325	14.9	740	90
16	Tenite	13.8	78	92	0.255	12.3	740	90
17	Tenite	17.6	94	111	0.385	17.5	740	90
18	Tenite	17.6	93	110	0.385	17.5	740	90
19	Tenite	17.6	90	107	0.370	17.3	740	90
20	Tenite	17.6	89	106	0.355	16.4	740	90
21	Tenite	17.6	83	97	0.305	14.4	740	90
22	Tenite	23.8	90	107	0.410	19.4	740	90
23	Tenite	23.8	88	104	0.390	18.5	740	90
24	Tenite	23.8	80	94	0.340	16.4	740	90
25	Tenite	35.0	87	103	0.410	22.0	740	90

TABLE III

EXPERIMENTAL DATA

Run No.	Material	Solids Mass Rate, lb./min.	Orifice Air Velocity, ft./sec.	Air Velocity in Pipe, ft./sec.	Equil. Friction Loss, in. H_2O/ft.	Total Head Loss, in. H_2O (25 ft.)	Bar. Press., mm. Hg	Temperature, °F
26	Tenite	35.0	85	101	0.415	22.0	740	90
27	Tenite	35.0	81	95	0.400	20.5	740	90
28	Polysty.	4.0	100	118	0.385	14.5	740	60
29	Polysty.	4.0	95	112	0.340	13.1	740	60
31	Polysty.	6.0	97	115	0.370	14.5	740	60
32	Polysty.	6.0	90	107	0.340	13.3	740	60
33	Polysty.	8.5	93	110	0.365	14.6	740	60
34	Polysty.	8.5	88	104	0.350	14.3	740	60
35	Polysty.	12.5	88	104	0.370	16.1	740	60
36	Polysty.	12.5	85	100	0.360	15.2	740	60
37	Polysty.	17.0	83	97	0.375	17.0	740	60
38	Polysty.	17.0	80	94	0.360	16.7	740	60
39	Tenite	9.0	98	116	0.355	14.6	741	78
40	Tenite	13.5	95	113	0.340	15.4	741	78
41	Tenite	17.5	89	106	0.360	16.2	741	78
42	Tenite	24.5	85	101	0.390	18.5	741	78
43	Tenite	33.0	81	95	0.400	19.0	741	78
44	Tenite	48.5	73	86	0.360	22.1	741	78
45	Catalin	7.0	98	116	0.315	12.5	741	78
46	Catalin	7.0	86	102	0.247	10.4	741	78
47	Catalin	15.0	85	101	0.265	12.9	741	78
48	Catalin	15.0	82	97	0.255	12.2	741	78
49	Polysty.	8.5	88	104	0.350	14.0	741	78
50	Polysty.	8.5	85	101	0.320	13.5	745	76
51	Polysty.	6.0	90	106	0.360	13.3	745	76

TABLE III

EXPERIMENTAL DATA

Run No.	Material	Solids Mass Rate, lb./min.	Orifice Air Velocity, ft./sec.	Air Velocity in Pipe, ft./sec.	Equil. Friction Loss, in. H_2O/ft.	Total Head Loss, in. H_2O (25 ft.)	Bar. Press., mm. Hg	Temperature °F
52	Polysty.	6.0	89	105	0.330	13.0	745	80
53	Polysty.	4.0	97	115	0.360	13.0	745	80
54	Polysty.	4.0	92	109	0.340	12.0	745	80
55	Polysty.	17.0	76	90	0.315	15.6	745	82
56	Polysty.	17.0	73	86	0.300	14.2	745	82
57	Polysty.	12.5	81	95	0.320	14.6	745	82
58	Polysty.	12.5	78	92	0.310	13.0	745	82
59	Alundum	15.5	94	111	0.340	13.9	747	77
60	Alundum	15.5	90	107	0.320	13.3	747	77
61	Alundum	21.5	88	104	0.340	14.4	747	77
62	Alundum	21.5	85	101	0.330	13.8	747	77
63	Alundum	29.0	82	97	0.370	14.8	747	77
64	Alundum	40.0	74	88	0.400	15.6	747	77
65	Tenite	9.0	138	72	0.094	4.70	735	70
66	Tenite	9.0	130	68	0.080	4.00	735	70
67	Tenite	12.5	128	67	0.095	4.55	735	70
68	Tenite	12.5	136	71	0.105	5.00	735	70
69	Tenite	17.5	133	70	0.111	5.55	735	70
70	Tenite	24.5	131	69	0.138	6.30	735	70
71	Tenite	33.5	126	66	0.158	7.50	735	70
72	Catalin	7.0	138	72	0.084	3.70	743	75
73	Catalin	7.0	133	70	0.081	3.55	743	75
74	Catalin	15.0	130	68	0.085	4.20	743	75
75	Catalin	15.0	126	66	0.081	3.80	743	75

TABLE IV

CALCULATED DATA

Run	R	$\frac{\Delta P_{ft}}{\Delta P_{fa}}$	ΔP_{fp}	u_p^*	f_p	$\frac{f_p u_p^*}{f_a u_a} R$	u_r/u_a	ΔP_{ap}	ΔP_{aa}	ΔP_T (25 ft.)
			in.H_2O/ft.	ft./sec.	x10^3			in. H_2O	in. H_2O	in. H_2O
1	1.08	1.25	0.080	77	6.30	0.252	0.348	4.27	2.90	16.75
2	1.71	1.41	0.220	71	6.47	0.413	0.343	5.68	2.44	17.39
3	0.98	1.20	0.050	72	5.17	0.196	0.320	3.28	2.34	13.18
4	0.90	1.19	0.060	80	5.48	0.188	0.328	3.65	2.96	15.86
5	1.58	1.41	0.125	77	6.77	0.397	0.348	6.15	2.90	19.75
6	1.35	1.32	0.082	72	6.03	0.305	0.335	4.53	2.44	15.47
8	0.91	1.19	0.050	73	5.47	0.186	0.335	3.07	2.48	13.33
9	0.83	1.18	0.055	80	5.47	0.174	0.328	3.29	2.96	15.35
10	1.20	1.27	0.037	54	5.80	0.252	0.316	2.17	1.31	8.03
11	0.88	1.16	0.045	72	4.97	0.159	0.358	3.03	2.61	13.63
12	1.22	1.31	0.090	78	6.10	0.285	0.333	4.93	2.86	16.26
13	1.29	1.32	0.093	76	6.48	0.316	0.338	4.78	2.76	17.01
14	1.32	1.33	0.090	73	6.52	0.315	0.348	4.60	2.61	16.24
15	1.38	1.30	0.075	71	5.58	0.290	0.338	4.47	2.40	14.92
16	1.60	1.34	0.065	61	5.64	0.328	0.336	5.02	1.77	12.99
17	1.70	1.43	0.117	72	6.75	0.423	0.352	5.92	2.57	18.04
18	1.71	1.47	0.123	71	7.20	0.450	0.355	5.83	2.53	17.84
19	1.76	1.48	0.120	69	7.22	0.467	0.355	5.67	2.40	17.23
20	1.78	1.45	0.110	69	6.62	0.432	0.350	5.67	2.34	16.81
21	1.95	1.49	0.100	63	6.58	0.462	0.350	5.18	1.98	14.66
22	2.38	1.64	0.160	69	7.10	0.613	0.356	7.50	2.40	20.00
23	2.45	1.66	0.155	66	7.10	0.626	0.356	7.17	2.26	18.98
24	2.72	1.74	0.145	58	7.67	0.707	0.382	6.30	1.85	16.45
25	3.65	1.78	0.180	70	5.37	0.745	0.320	11.20	2.22	23.42
26	3.70	1.89	0.195	67	6.07	0.827	0.337	10.70	2.13	22.83
27	3.94	2.05	0.205	62	6.88	0.972	0.348	9.90	1.90	21.45
28	0.36	1.26	0.080	90	16.6	0.254	0.255	1.64	2.91	14.10

TABLE IV

CALCULATED DATA

Run	R	$\frac{\Delta P_{ft}}{\Delta P_{fa}}$	ΔP_{fp}	u_p^*	f_p	$\frac{f_p u_p^*}{f_a u_a} R$	u_p/u_a	ΔP_{ap}	ΔP_{aa}	ΔP_T (25 ft.)
			in. H_2O/ft.	ft./sec.	x 10^3			in. H_2O	in. H_2O	in. H_2O
29	0.38	1.24	0.065	86	13.8	0.240	0.232	1.57	2.62	13.04
31	0.56	1.30	0.085	90	11.5	0.286	0.218	2.46	2.74	14.35
32	0.60	1.36	0.090	85	12.8	0.345	0.205	2.33	2.40	13.13
33	0.83	1.40	0.105	87	10.4	0.386	0.210	3.36	2.53	14.91
34	0.88	1.46	0.110	81	11.5	0.440	0.221	3.14	2.26	13.88
35	1.29	1.54	0.130	83	9.25	0.525	0.212	4.68	2.26	16.07
36	1.34	1.64	0.140	78	10.5	0.610	0.220	4.45	2.09	15.39
37	1.87	1.83	0.170	77	9.60	0.770	0.205	5.98	1.98	17.02
38	1.93	1.80	0.160	75	9.50	0.775	0.202	5.82	1.86	16.13
39	0.83	1.21	0.063	76	6.77	0.209	0.345	3.12	2.81	14.98
40	1.28	1.22	0.063	78	4.37	0.220	0.310	4.82	2.67	15.94
41	1.78	1.47	0.115	69	6.95	0.453	0.350	5.52	2.34	16.76
42	2.57	1.77	0.170	64	7.97	0.722	0.365	7.13	2.13	18.73
43	3.70	2.00	0.200	61	7.30	0.955	0.358	9.20	1.90	20.87
44	6.02	2.25	0.200	59	5.10	1.14	0.315	13.10	1.54	23.19
45	0.65	1.07	0.020	66	3.26	0.069	0.430	2.10	2.81	12.81
46	0.74	1.09	0.020	56	3.72	0.083	0.452	1.78	2.18	10.11
47	1.59	1.20	0.045	54	4.05	0.190	0.465	3.70	2.13	12.38
48	1.65	1.24	0.050	50	4.87	0.229	0.483	3.42	1.98	11.70
49	0.87	1.49	0.114	81	12.2	0.462	0.220	3.14	2.36	14.03
50	0.90	1.46	0.100	79	10.9	0.427	0.218	3.06	2.13	13.04
51	0.61	1.47	0.115	79	17.7	0.452	0.255	2.16	2.34	13.40
52	0.61	1.38	0.090	80	13.7	0.355	0.238	2.19	2.31	12.63
53	0.37	1.26	0.075	85	16.1	0.250	0.260	1.55	2.76	13.21
54	0.39	1.33	0.085	80	19.4	0.315	0.265	1.46	2.48	12.32
55	2.02	1.80	0.140	72	8.25	0.762	0.200	5.58	1.69	14.99
56	2.11	1.88	0.140	69	8.73	0.790	0.198	5.36	1.54	14.05

TABLE IV

CALCULATED DATA

Run	R	$\frac{\Delta P_{ft}}{\Delta P_{fa}}$	ΔP_{fp}	u_p^*	f_p	$\frac{f_p u_p^*}{f_a u_a} R$	u_r/u_a	ΔP_{ap}	ΔP_{aa}	ΔP_T (25 ft.)
			in. H_2O/ft.	ft./sec.	x 10^3			in. H_2O	in. H_2O	in. H_2O
57	1.41	1.60	0.120	76	9.23	0.572	0.200	4.34	1.90	14.11
58	1.45	1.67	0.125	72	10.2	0.630	0.220	4.12	1.77	13.44
59	1.50	1.28	0.075	41	8.62	0.270	0.630	2.90	2.57	13.87
60	1.55	1.28	0.070	37	8.68	0.260	0.655	2.62	2.40	12.89
61	2.21	1.45	0.105	34	10.5	0.425	0.673	3.34	2.26	11.05
62	2.28	1.50	0.110	32	11.7	0.470	0.684	3.14	2.13	13.37
63	3.22	1.80	0.165	29	14.3	0.760	0.702	3.84	1.98	14.82
64	4.90	2.42	0.235	24	17.9	1.29	0.728	4.38	1.63	15.46
65	0.61	1.22	0.0168	47	9.28	0.218	0.348	0.85	1.08	4.30
66	0.64	1.16	0.0110	48	6.25	0.158	0.294	0.87	0.97	3.85
67	0.90	1.42	0.0282	42	13.1	0.412	0.374	1.02	0.90	4.30
68	0.85	1.40	0.0298	44	13.3	0.395	0.380	1.06	1.05	4.75
69	1.21	1.52	0.380	44	12.2	0.517	0.372	1.55	1.02	5.35
70	1.71	1.91	0.0680	41	16.6	0.950	0.405	2.03	0.99	6.47
71	2.46	2.43	0.930	40	17.0	1.41	0.394	2.70	0.86	7.52
72	0.47	1.09	0.0068	38	6.36	0.089	0.472	0.54	1.08	3.72
73	0.48	1.10	0.0075	36	7.03	0.0983	0.487	0.51	1.02	3.54
74	1.06	1.23	0.0160	34	7.90	0.234	0.500	1.03	0.97	4.12
75	1.10	1.24	0.0155	33	7.90	0.240	0.500	1.00	0.86	3.87

ments. The experimental determinations of particle velocity data from high speed motion pictures served as a check on, and as justification for, the theoretical development. The agreement between observed and calculated particle velocities is shown in Table V. The expense of high speed photography prohibited the taking of pictures at each section of the pipe for every run, but sufficient photographs were made at various sections of the pipe and of each material to establish the validity of the theoretical equation. Typical photographs of the Tenite, polystyrene, Catalin and Alundum particles are given in Figures 3 through 6. Through enlargement and reproduction, the small polystyrene beads shown in Figure 4 have lost the necessary resolution to permit tracking the path of the particles. Even with the aid of a wide-field microscope, following the motion of the polystyrene particles was difficult. The large sphere appearing in Figure 4 is extraneous material.

The analysis of the high speed photographs was accomplished with a wide-field microscope manufactured by Bausch and Lomb, Rochester, New York. A neon timing-light, synchronized with the camera, registered flashes which appeared as white streaks at the edge of the film negative. Since the light flashed on and off twice per cycle (1/60 second), the speed of the camera, measured as frames per second, could be calculated by counting the number of frames exposed per half cycle (i.e., the number of frames from the beginning of a flash to the beginning of the next flash) and multiplying this number by 120. Next, the path of the particles was examined with the aid of the microscope. The particle speed was measured as the number of frames of the film negative required for

TABLE V

PARTICLE VELOCITY DATA

Material	Air Velocity, ft./sec.	Solids Rate, lb./min.	Distance from Solids Inlet, ft.	Particle Velocity, ft./sec. Calculated	Observed
Tenite	118	9.2	4.5	34	36
Tenite	115	13.8	4.5	34	33
Tenite	110	17.6	4.5	29	28
Tenite	104	23.8	4.5	25	24
Tenite	97	35.0	4.5	19	19
Tenite	118	12.0	7.0	55	55
Tenite	118	12.0	12.0	65	63
Tenite	118	12.0	22.0	77	73
Tenite	108	17.5	7.0	43	45
Tenite	108	10.0	20.0	70	67
Tenite	106	10.0	7.0	45	47
Tenite	106	10.0	20.0	71	66
Tenite	119	10.0	7.0	60	59
Tenite	119	10.0	20.0	77	79
Tenite	101	24.5	20.0	64	64
Tenite	95	33.0	20.0	61	62
Polystyr.	109	6.0	4.5	38	38
Polystyr.	111	4.0	20.0	80	75
Polystyr.	104	8.5	20.0	79	79
Polystyr.	90	17.0	20.0	72	70
Catalin	116	7.0	4.5	28	28
Catalin	116	7.0	20.0	66	67
Catalin	101	15.0	4.5	20	22
Catalin	101	15.0	20.0	54	56
Alundum	104	21.5	20.0	34	34
Alundum	88	40.0	20.0	25	29
Alundum	107	15.5	20.0	38	37
Alundum	107	15.5	4.5	26	28
Alundum	104	21.5	4.5	24	22

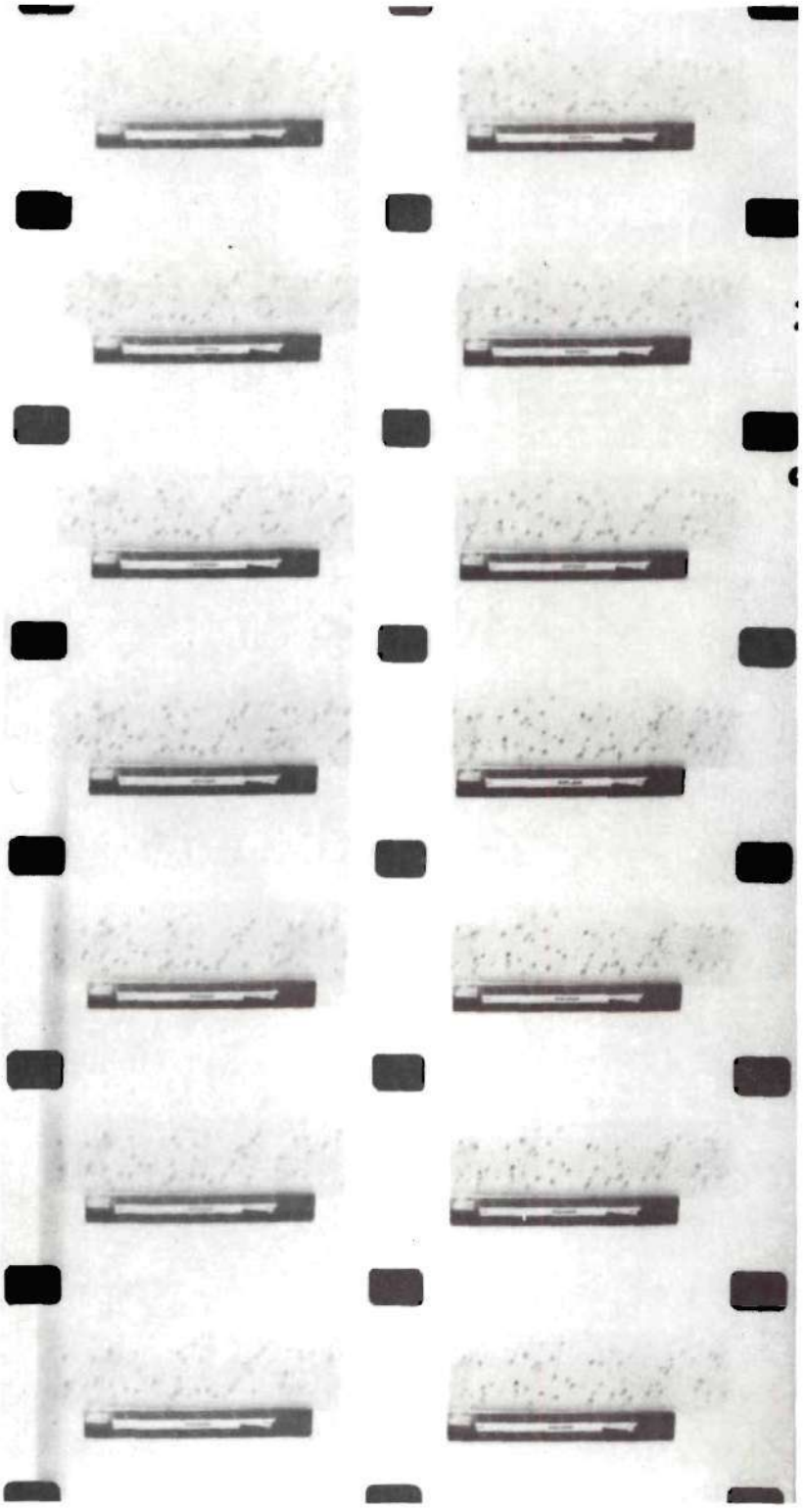

Figure 3. Successive Pictures Showing the Motion of Tenite Particles in a Two-Inch Pipe.

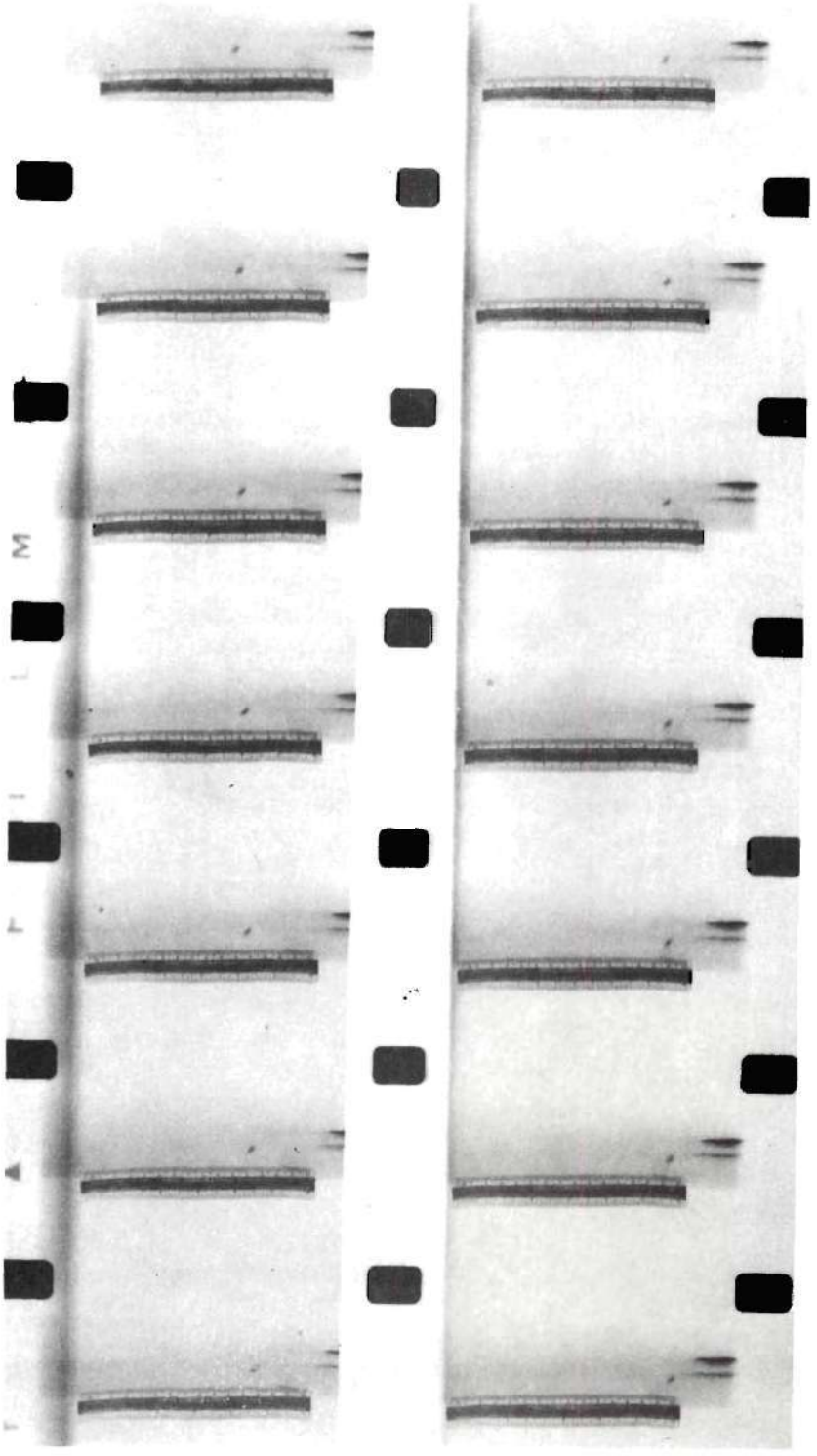

Figure 4. Successive Pictures Showing the Motion of Polystyrene Beads in a Two-Inch Pipe.

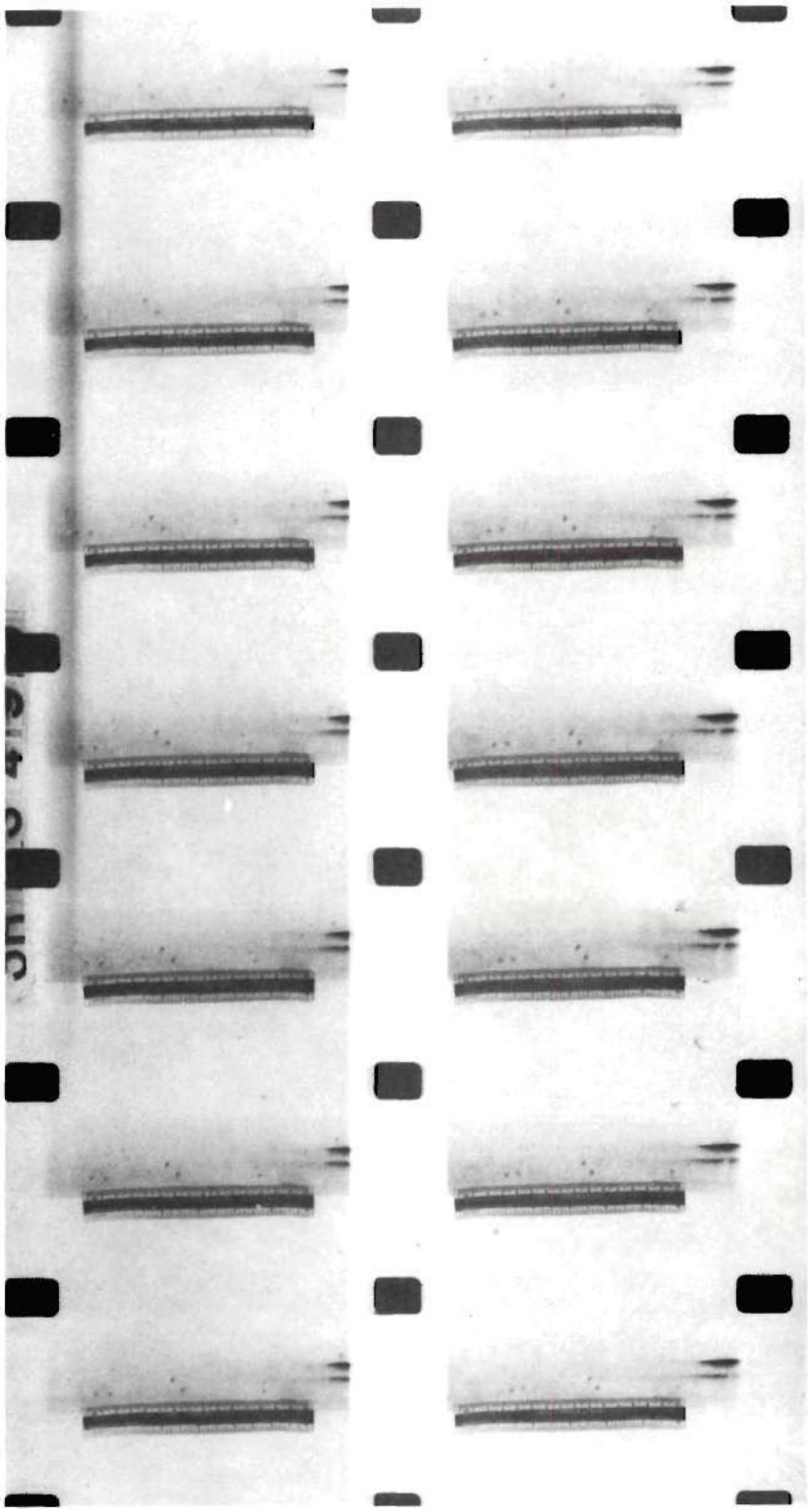

Figure 5. Successive Pictures Showing the Motion of Catalin Spheres in a Two-Inch Pipe.

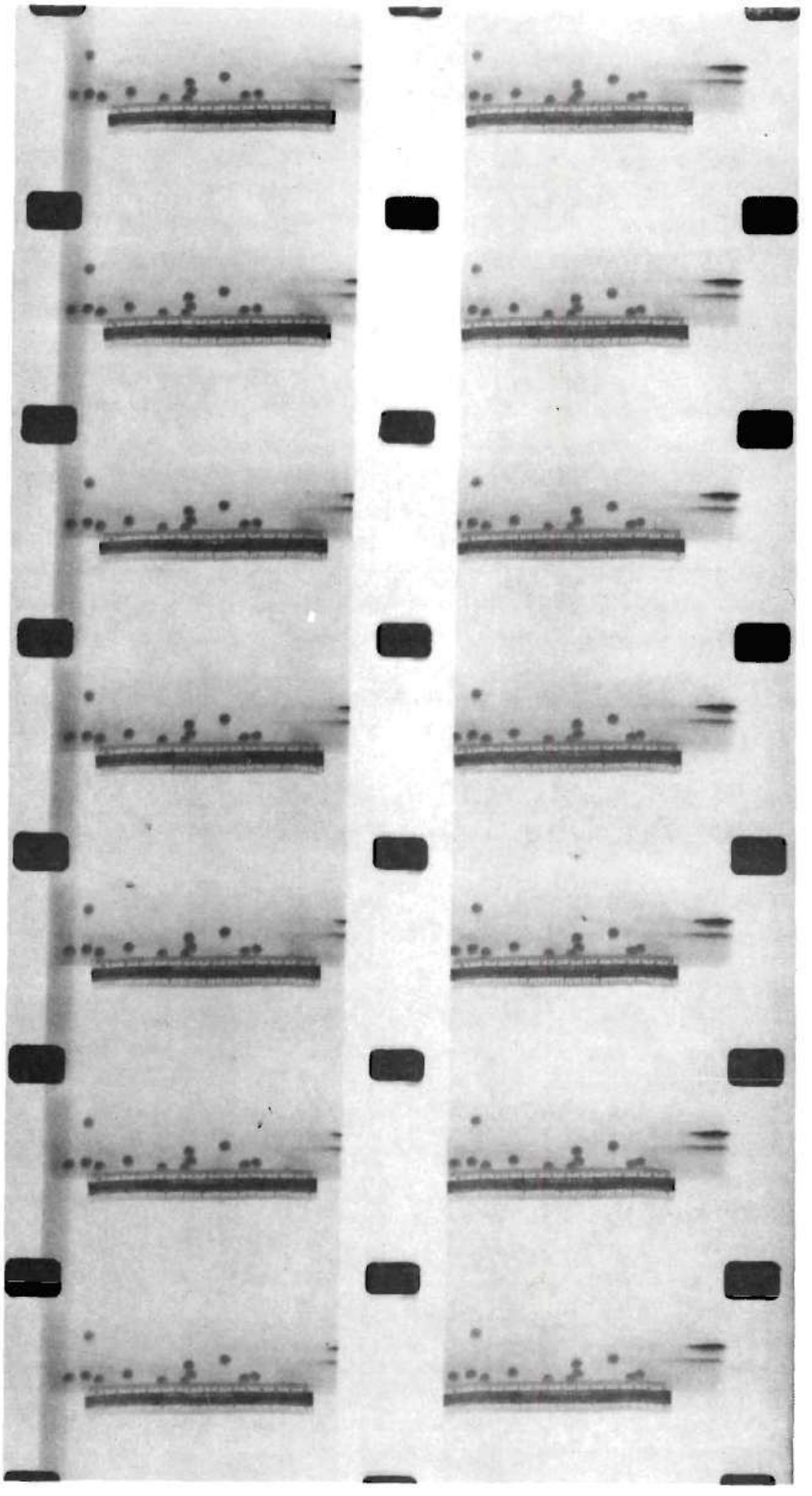

Figure 6. Successive Pictures Showing the Motion of Alundum Spheres in a Two-Inch Pipe.

a particle to move the distance of the six-inch ruler which was taped to the bottom of the pipe. This value, multiplied by two, gave the number of frames exposed while the particle travelled a distance of one foot. The particle velocity in the pipe measured as feet per second was then obtained by dividing the camera speed in frames per second by the particle speed in frames per foot. The values of observed particle velocity reported in Table V represent the average velocity of at least twenty particle measurements. Deviation of ± 10 per cent from the average value was not uncommon.

Care had to be exercised in the analysis of the film negatives. Each roll contained 100 feet of film which had been exposed in less than three seconds, corresponding to camera speeds of 3000-4000 frames per second. Although the motors driving the roll of film necessarily accelerated very quickly, a sufficient portion of the film had to be allotted for the motors to attain an equilibrium speed, and therefore all particle velocity measurements were made at approximately the middle of the roll.

Considerable static electricity was developed as the particles were transported through the pipe to the separator. Adequate grounding of the pipe and separator at strategic points reduced the static electricity effects to a minimum.

IV. DISCUSSION OF RESULTS

A. Particle Velocity and Pipe Length

From the discussion of previous work, it is apparent that a knowledge of particle velocity is necessary for the analysis of acceleration losses and friction losses in a pneumatic conveying system. Accordingly, initial studies were devoted to the theoretical treatment of the motion of a particle. Since high speed photography gave particle velocities at points where the camera was located, it was evident that a relation between particle velocity and the length of pipe would be desirable.

Suppose a particle initially at rest is injected into a moving fluid. The drag of the fluid slipping past the particles will cause them to be accelerated, and the resulting motion of a particle may be expressed as

$$m\frac{du_p}{dt} = \pm mg + 1/2\ (u_a - u_p)^2\ C_r A_p \rho_a \qquad (17)$$

where $1/2(u_a - u_p)^2 C_r A_p \rho_a$ is the well-known resistance or drag force. For the case of horizontal pneumatic conveying, the mg term drops out and the equation reduces to

$$m\frac{du_p}{dt} = 1/2\ (u_a - u_p)^2\ C_r A_p \rho_a \qquad (18)$$

Since experimental observations were concerned with relations involving velocity and pipe length from the solids inlet rather than velocity and time, dt in equation (18) was replaced by its equivalent

value given by

$$dL = u_p dt \tag{19}$$

and thus equation (18) becomes

$$u_p \frac{du_p}{dL} = \frac{(u_a - u_p)^2 C_r A_p \rho_a}{2m} \tag{20}$$

Rearrangement and separation of the variables leads to the relation between particle velocity and length of pipe.

$$dL = \frac{u_p du_p}{\frac{(u_a - u_p)^2 C_r A_p \rho_a}{2m}} \tag{21}$$

The right side of equation (21) is not directly integrable since the coefficient of resistance C_r is a function of the relative velocity, $(u_a - u_p)$, as shown in Figure 30. The relation between C_r and the particle Reynolds number, Re_p, is given in many sources (8,14,19), where C_r and Re_p are defined by the following expressions.

$$F_r = 1/2\ u_p^2 C_r A_p \rho_a \tag{22}$$

$$Re_p = \frac{d_p \rho_a (u_a)^2}{\mu} \tag{23}$$

Equations (22) and (23) were developed for free-falling bodies, i.e., zero gas velocity. In the case of pneumatic conveying, however, the resistance or drag force is defined as in equation (17). To have a consistent analysis, then, the particle Reynolds number should involve relative velocity instead of absolute velocity. Thus,

$$Re_p = \frac{d_p \rho_a (u_a - u_p)}{\mu} \qquad (24)$$

Replacement of the particle velocity by the relative velocity in equations (22) and (23) permits use of the tabulated and graphical data of C_r versus Re_p, and hence equation (21) can be integrated graphically. As pointed out by DallaValle (8), however, Reynolds number information must be carefully analyzed. The Reynolds criterion for pipes which distinguishes turbulent from streamline flow has a value of approximately 2500, while the value of the criterion for particles is about 1.0, as may be seen in Figures 30 and 31. Turbulence of a particle in a quiet fluid is a localized condition, whereas turbulence in a fluid in motion is general. Turbulence denotes a destruction of parallel shearing elements in the fluid so that motion becomes a function of the fluid density only. Hence a particle injected into a turbulent stream behaves as though its Reynolds number is greater than 1.0, even though its true value may be considerably less. DallaValle has set forth the following summary of the Reynolds criteria:

(1) If a fluid is in streamline motion, the motion of a particle injected into it may be either streamline or turbulent, depending on whether the particle Reynolds number is greater or less than 1.0. Thus, for streamline motion,

$$Re_p = \frac{d_p \rho_a (u_a - u_p)}{\mu} \quad 1.0$$

and for turbulent motion,

$$Re_p = \frac{d_p \rho_a (u_a - u_p)}{\mu} \quad 1.0$$

(2) If the fluid is in turbulent motion, the motion of a particle injected into it will be turbulent, regardless of the particle Reynolds number.

In the present study, the air Reynolds number was in the turbulent region in all experiments, and therefore the coefficients of resistance were independent of the particle Reynolds numbers. Some of the earlier investigators of pneumatic conveying, however, have utilized conditions in which the air Reynolds number was less than 2500; in these cases it is necessary to re-examine the coefficient of resistance for possible dependence on the particle Reynolds number.

Reference to Figures 30 and 35 will show that the coefficient of resistance in the turbulent region is independent of Re_p but is strongly influenced by the shape of the particle. Pettyjohn and Christiansen (21) developed the relation between the coefficient of resistance and the particle shape, expressed as sphericity, and their results are presented in Figure 35 for convenience. Methods for estimating the sphericity have been discussed previously.

Treatment of C_r as a constant for a specific particle shape simplifies equation (21). For the case of spherical particles, A_p may be replaced by $\pi/4 \cdot d_p^2$ and m by $\pi/6 \cdot d_p^3 \rho_p$, thus reducing the equation to

$$dL = \frac{u_p du_p}{3\rho_a C_r \frac{(u_a - u_p)^2}{4 d_p \rho_p}} \qquad (25)$$

Since C_r has a constant, finite value, equation (25) is readily inte-

grable but leads to the result that the ultimate particle velocity is equal to the gas velocity. This result does not conform to experimental observations, principally because particle-to-wall collisions and particle friction effects were not considered in the derivation. The effect of such frictional contacts would be to retard the acceleration of the particles, and an equilibrium velocity would be reached when the forces acting on the particle would equal the frictional force resisting motion. As the air expands, there is a corresponding increase in the air velocity; the effect of an increased air velocity on the drag force is partially offset, however, by the decrease in air density. The mechanism of friction effects at the pipe walls suggests an analogy with the familiar Fanning equation

$$\frac{dF_a}{dL} = \frac{f_a u_a^2}{2g_c D} \tag{26}$$

For the case of the solids phase in pneumatic transport, equation (26) can be modified to give

$$\frac{dF_p}{dL} = \frac{f_p u_p^2}{2g_c D} \tag{27}$$

Hence equation (25) can be altered by a term to account for the particle friction effects. Thus,

$$dL = \frac{u_p du_p}{\frac{3\rho_a C_r (u_a - u_p)^2}{4 d_p \rho_p} - \frac{f_p u_p^2}{2D}} \tag{28}$$

Or in integrated form,

$$\Delta L = \int_{u_{p1}}^{u_{p2}} \frac{u_p du_p}{\frac{3\rho_a C_r (u_a - u_p)^2}{4 d_p \rho_p} - \frac{f_p u_p^2}{2D}} \tag{29}$$

Equation (29) has been found to express accurately the length of pipe necessary to achieve a specific particle velocity. Because the nature of the term f_p was unknown during the investigation, it was necessary to make use of a relation between f_p and the pressure drop, as in equation (27). Rearrangement of equation (27) and substitution of $\Delta P_{fp}/\rho_{ds}$ for ΔF_p gives

$$f_p = \frac{\Delta P_{fp}}{\Delta L} \cdot \frac{2 g_c D}{u_p^2 \rho_{ds}} \tag{30}$$

where $\Delta P_{fp} = \Delta P_{ft} - \Delta P_{fa}$.

The continuity equation applied to the solids is

$$G_p/A = u_p \rho_{ds} \tag{31}$$

and substitution of G_p/A for $u_p \rho_{ds}$ in equation (30) yields

$$f_p = \frac{\Delta P_{fp}}{\Delta L} \cdot \frac{2 g_c D A}{u_p G_p} \tag{32}$$

Substitution of the value of f_p given by equation (32) into equation (25) leads to

$$\Delta L = \int_{u_{p1}}^{u_{p2}} \frac{u_p du_p}{\frac{3\rho_a C_r (u_a - u_p)^2}{4 d_p \rho_p} - \frac{\Delta P_{fp}/\Delta L \; g_c \Delta u_p}{G_p}} \tag{33}$$

where the term f_p has been replaced by terms easily evaluated from pressure drop measurements. The necessary length of pipe to achieve an equilibrium particle velocity is obtained by integrating between the limits of $u_{p1} = 0$ to $u_{p2} = u_p^*$. Equation (33) cannot be integrated directly or by graphical methods since the relation between the particle velocity and ΔP_{fp} is not known; hence a trial-and-error technique was used, and a sample solution is given in a later section. Photographs showing the decrease in disperse-density as the particles accelerate are given in Figures 7 through 10.

In agreement with the results of other investigators, the data of the present investigation show that, for a specific air velocity, the ultimate particle velocity is independent of the loading. For example, if for a constant air flow the weight of the solids feed was increased, the particles would accelerate more slowly but would eventually attain the same velocity as in the case of the lighter loading. The effect of loading on the acceleration of the Tenite particles is shown for five different solid feed rates in Figure 11. Photographs showing the increase in the disperse-density with increased solids loadings are given in Figures 12 through 16.

B. Equilibrium Particle Velocity and Friction Factors

The equilibrium particle velocity may be readily determined from equation (33). Recognizing that $dL = udu/a$, it is apparent that the denominator of the right hand side of equation (33) represents the acceleration of the solids. Since the equilibrium particle velocity will

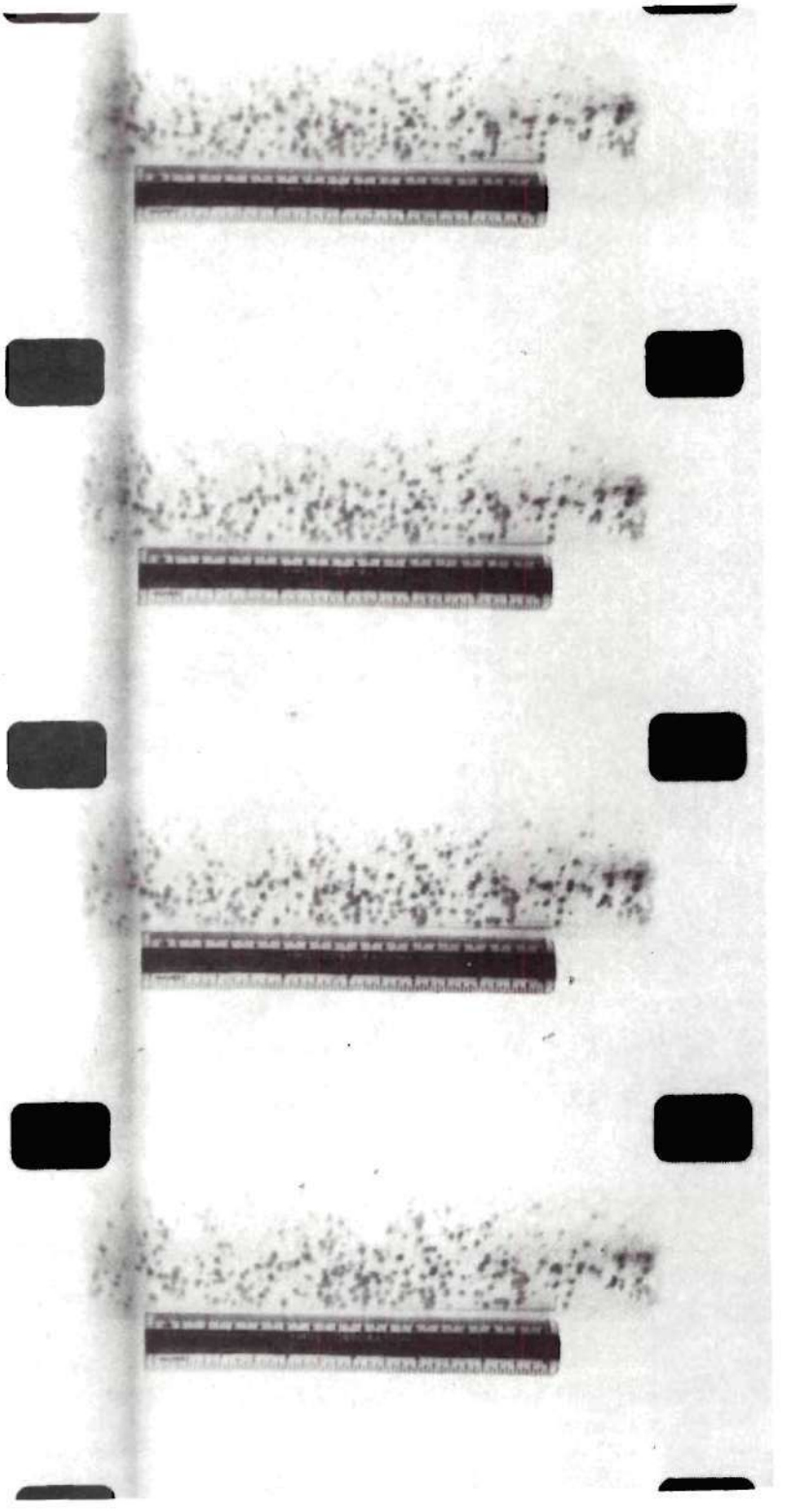

Figure 7. Tenite Particles at a Distance of Two Feet from the Solids Inlet. Air Velocity, 110 ft./sec. Solids Rate, 13.8 lb./min.

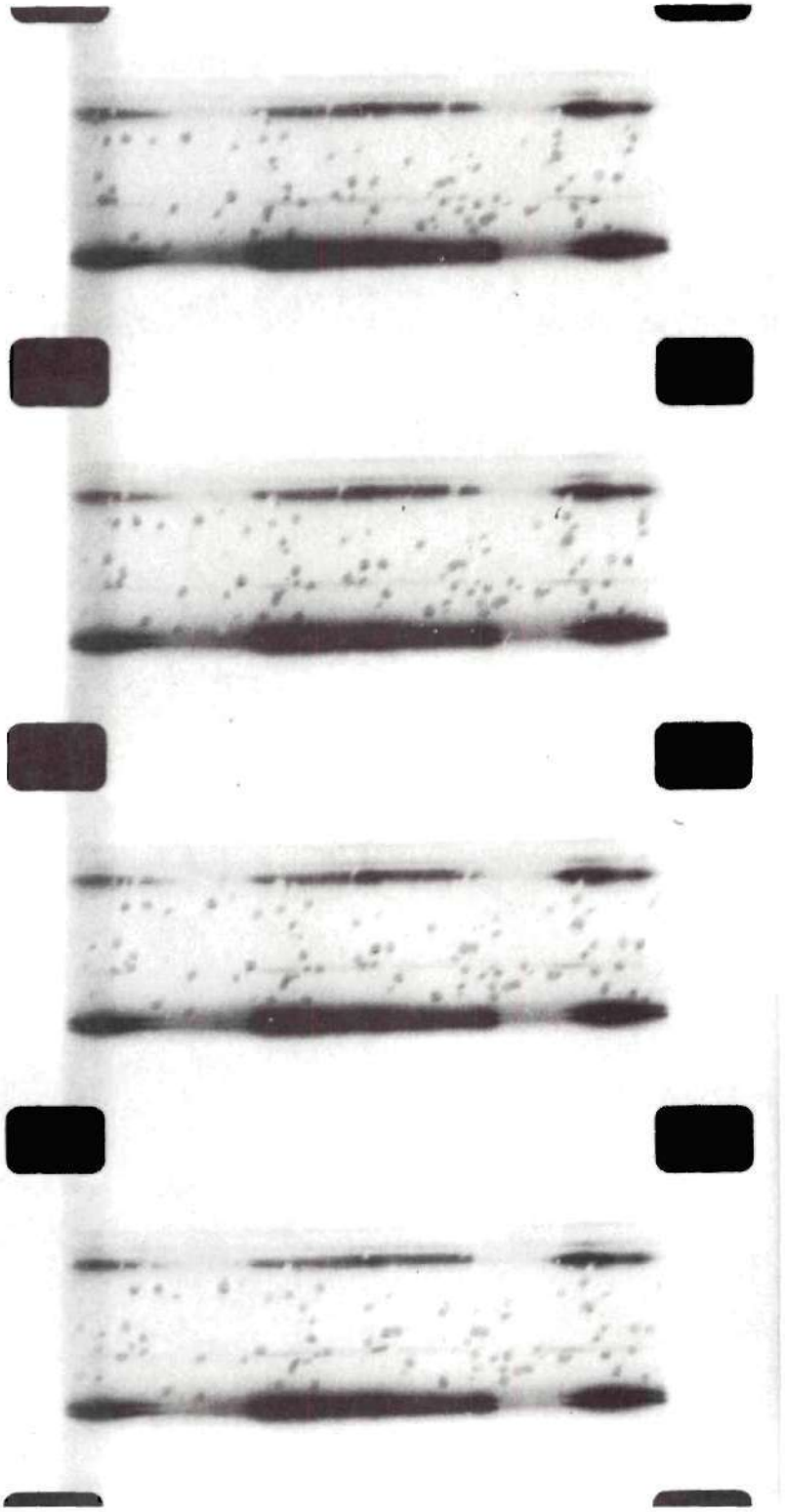

Figure 8. Tenite Particles at a Distance of Seven Feet from the Solids Inlet. Air Velocity, 110 ft./sec. Solids Rate, 13.8 lb./min.

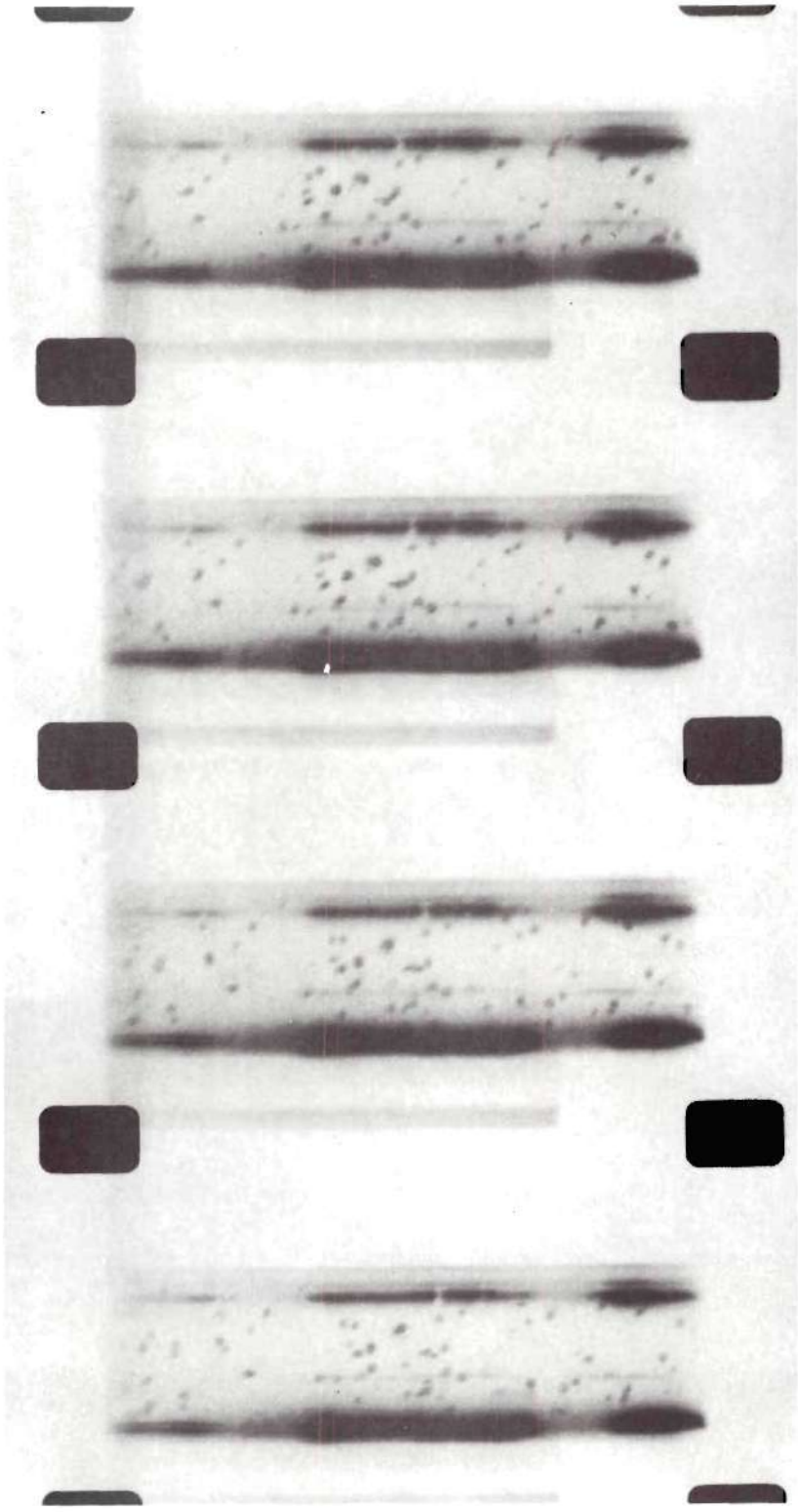

Figure 9. Tenite Particles at a Distance of Fourteen Feet from the Solids Inlet. Air Velocity, 110ft./sec. Solids Rate, 13.8 lb./min.

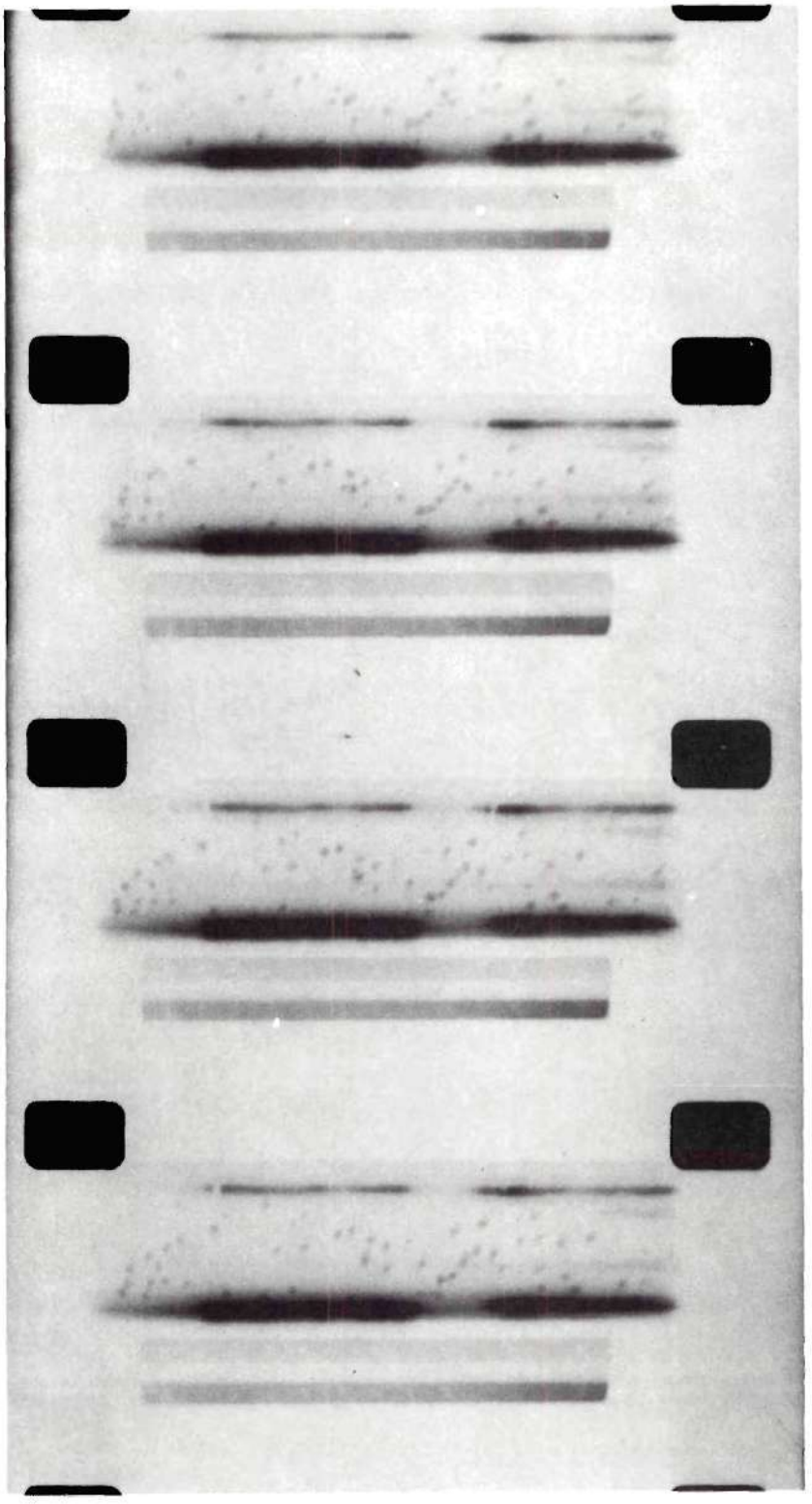

Figure 10. Tenite Particles at a Distance of Twenty Feet from the Solids Inlet. Air Velocity, 110 ft./sec. Solids Rate, 13.8 lb./min.

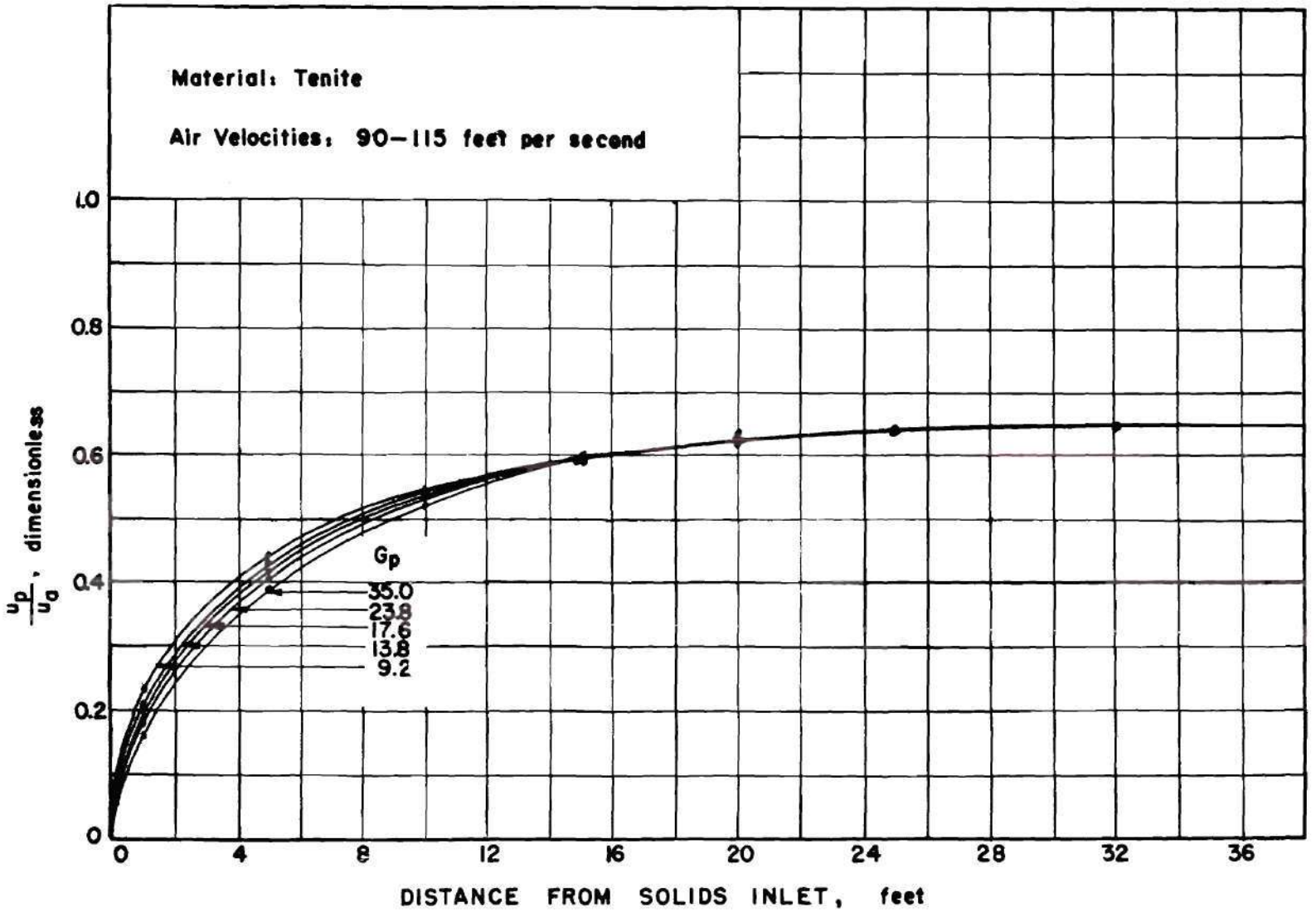

Figure 11. The Effect of Loading on the Acceleration of Tenite Particles.

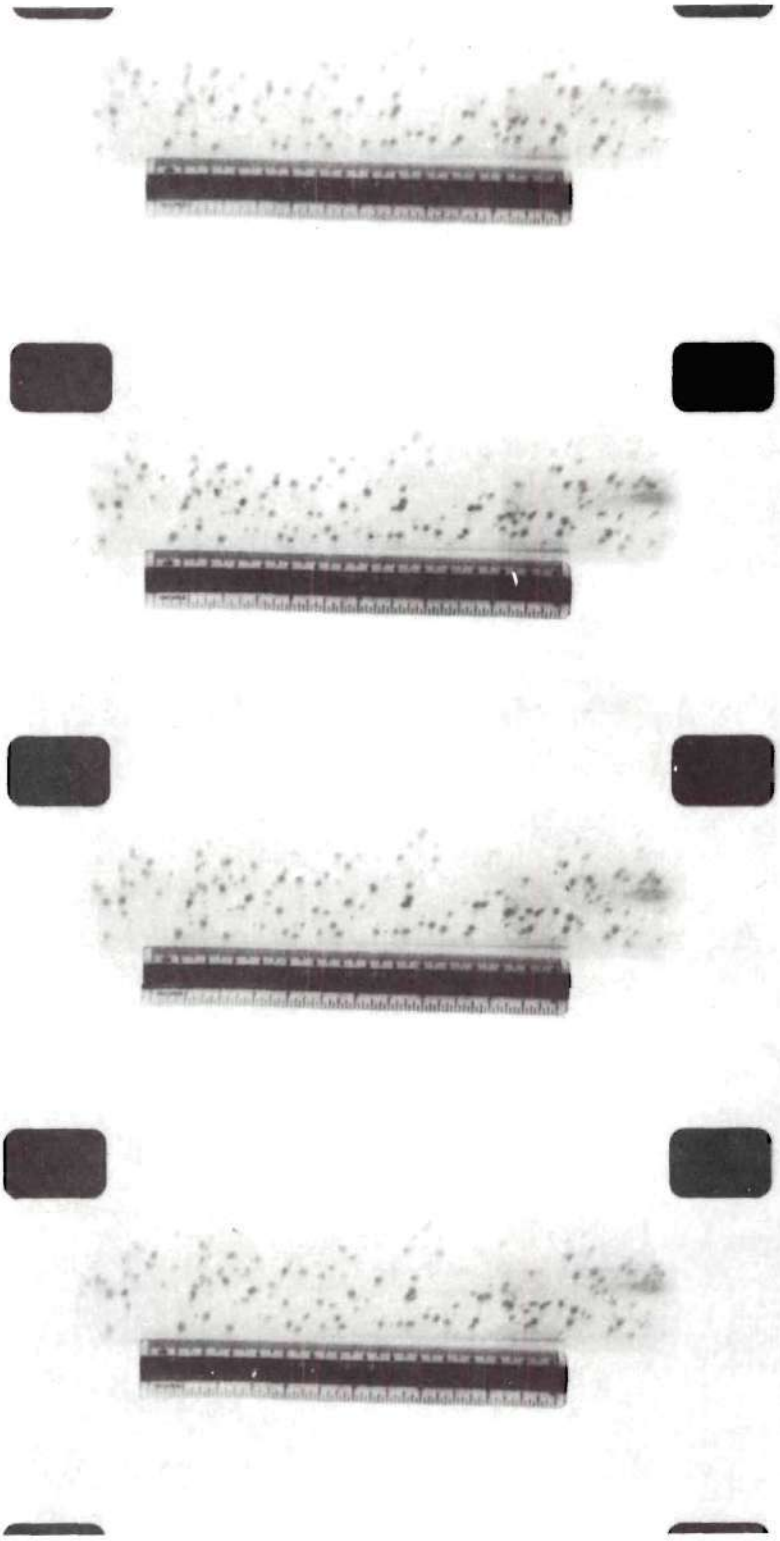

Figure 12. The Motion of Tenite Particles in a Two-Inch Pipe at a Loading Rate of 9.2 lb./min.

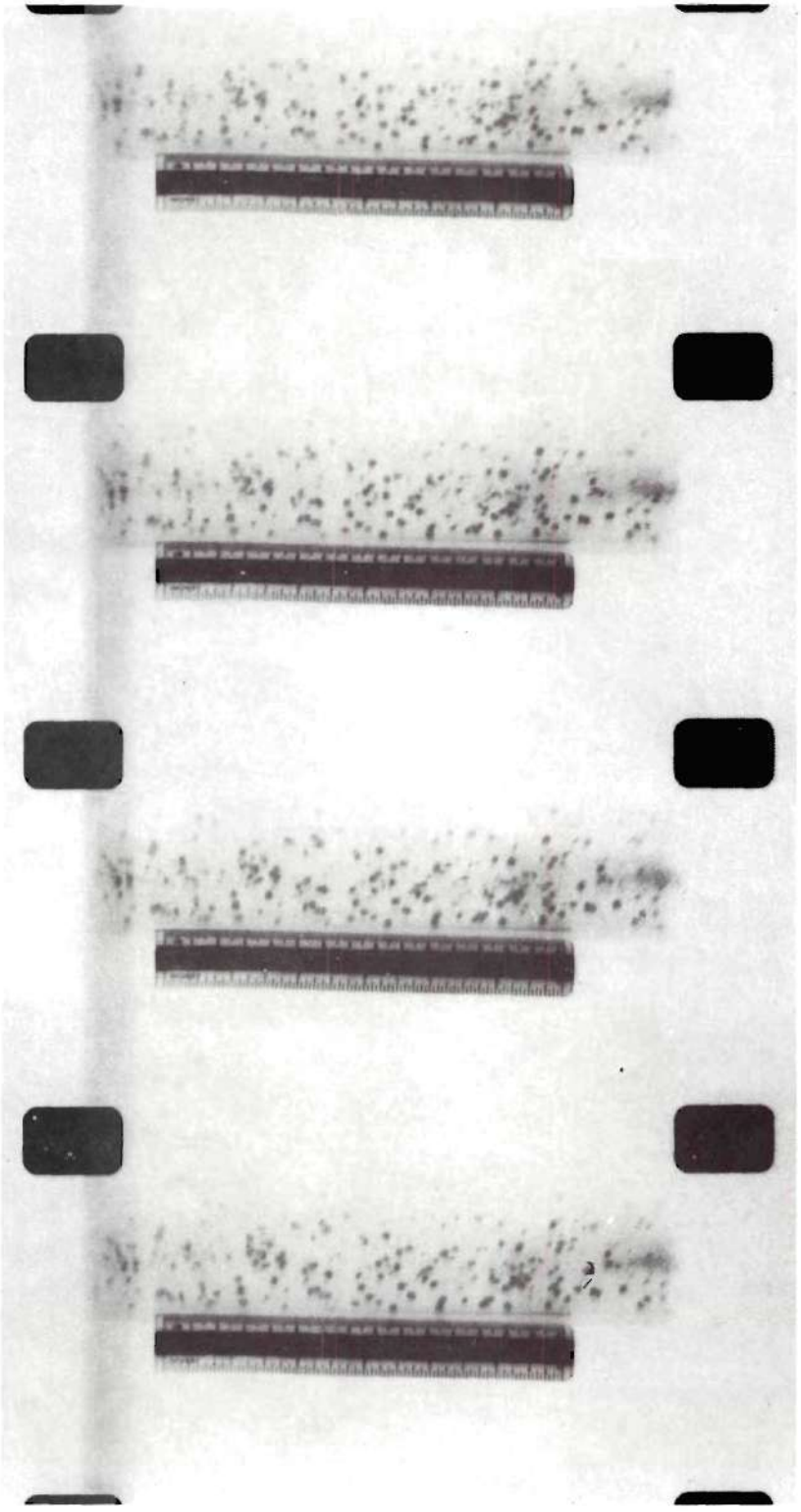

Figure 13. The Motion of Tenite Particles in a Two-Inch Pipe at a Loading Rate of 13.8 lb./min.

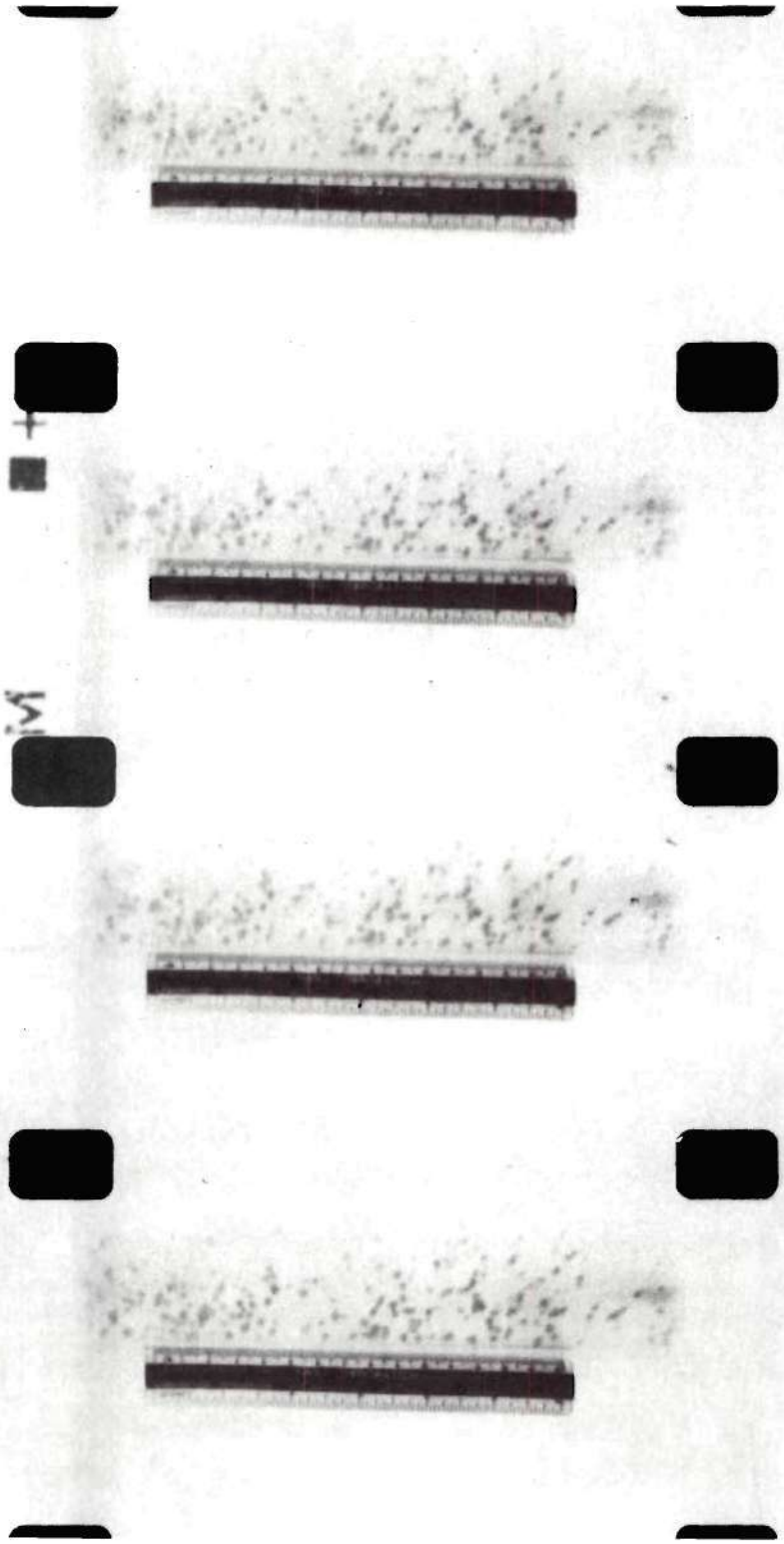

Figure 14. The Motion of Tenite Particles in a Two-Inch Pipe at a Loading Rate of 17.6 lb./min.

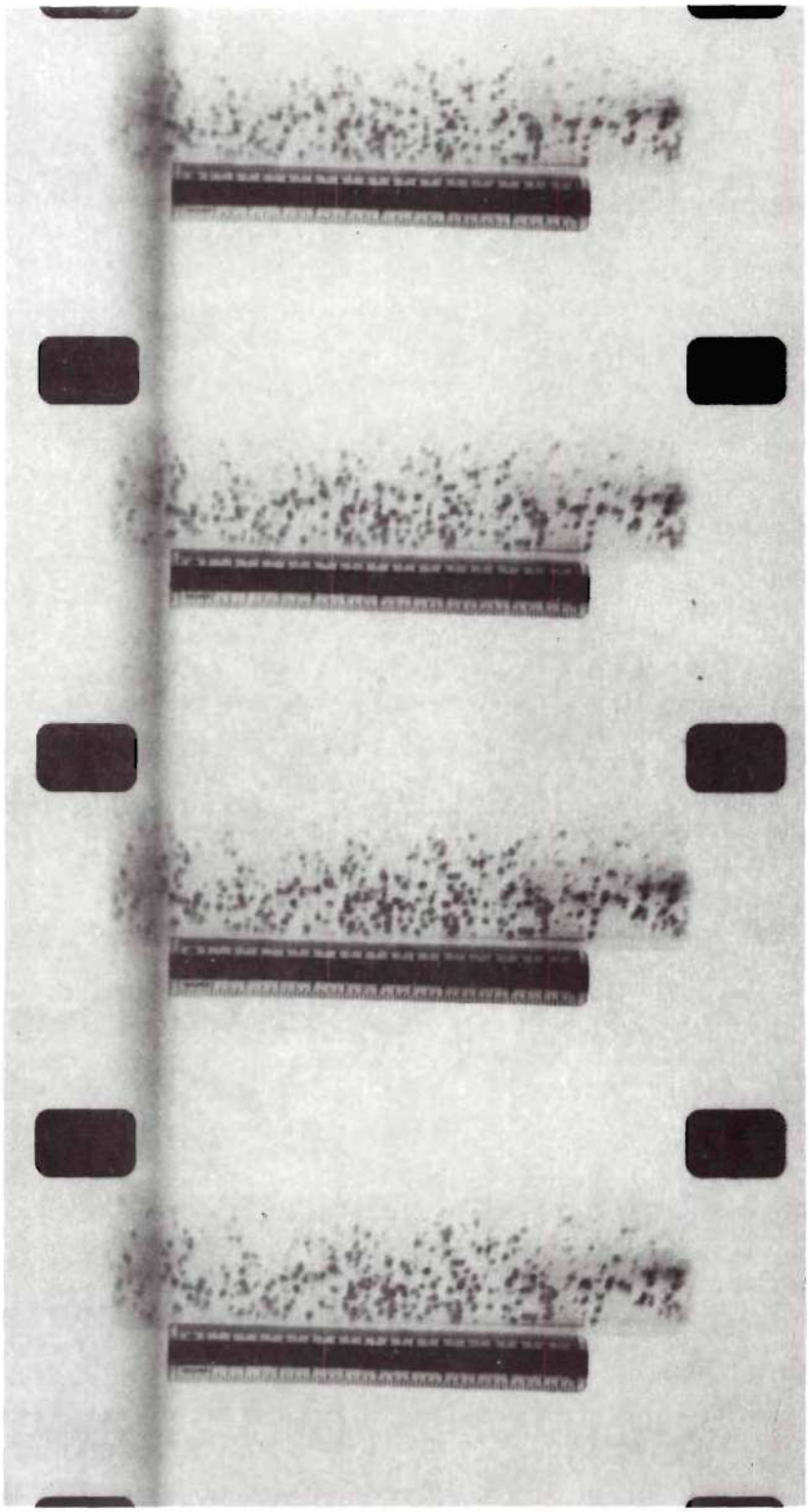

Figure 15. The Motion of Tenite Particles in a Two-Inch Pipe at a Loading Rate of 23.8 lb./min.

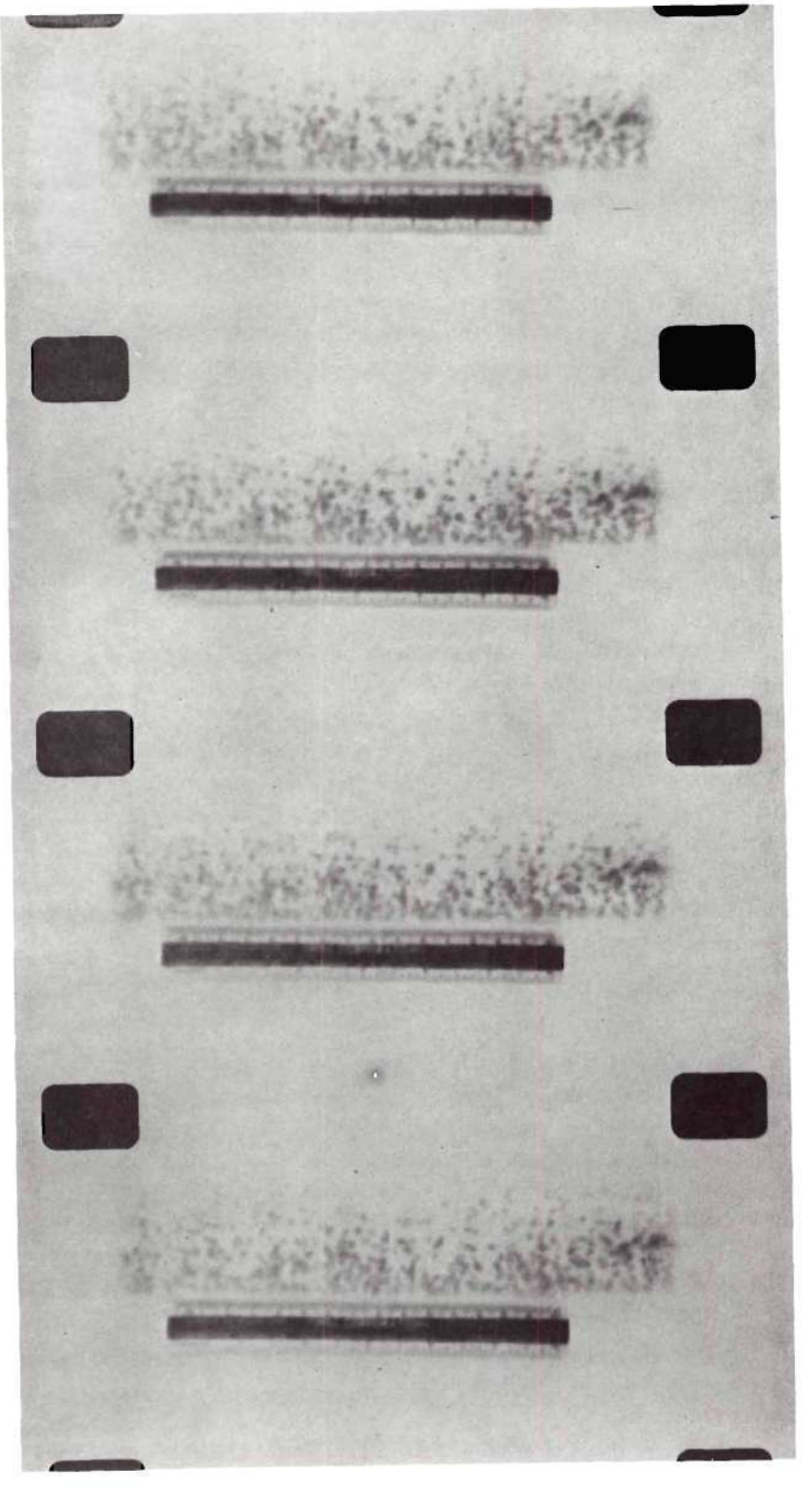

Figure 16. The Motion of Tenite Particles in a Two-Inch Pipe at a Loading Rate of 35.0 lb./min.

be attained when the acceleration is zero, the denominator of the right side of equation (33) may be set equal to zero and solved for the particle velocity. Since from equation (29) it is evident that the acceleration may be expressed as

$$a = \frac{3\rho_a C_r (u_a - u_p)^2}{4 d_p \rho_p} - \frac{f_p u_p^2}{2D} \quad , \tag{34}$$

the friction factor corresponding to this equilibrium velocity (zero acceleration) may be obtained from equation (34). Thus,

$$f_p^* = \frac{3\rho_a C_r D (u_a - u_p^*)^2}{2 d_p \rho_p (u_p^*)^2} \tag{35}$$

C. Pressure Drops in Pneumatic Conveying

The pressure drops to be considered in a pneumatic conveying process have been summarized by Lapple (18). Thus,

$$\Delta P_T = \Delta P_{aa} + \Delta P_{ap} + \Delta P_{fa} + \Delta P_{fp} \tag{36}$$

for horizontal conveying.

The pressure drop encountered in accelerating the conveying air, ΔP_{aa}, is obtained from an energy balance over the acceleration region, considering only the gas phase, and may be expressed by

$$\Delta P_{aa} = \frac{u_a^2}{2 g_c} \rho_a \tag{37}$$

where u_a is the final air velocity.

The pressure drop which occurs during the acceleration of the solids

may be calculated from a momentum balance. Thus,

$$\Delta P_{ap} = \frac{G_p u_p^*}{A g_c} \tag{38}$$

The pressure drop due to friction of the air passing through the pipe may be calculated using the Fanning relation, as in equation (26), using the appropriate friction factors in conformity with the Reynolds number. Because of the ease with which pressure drops may be calculated in this manner, most investigators have attempted to treat the friction effects of the air and of the solids jointly, rather than separately, by modifying the Reynolds number in diverse ways, but no single development has met with wide acceptance.

If consideration is limited to the friction pressure drop effects at the sections of the pipe where acceleration has been completed, equation (36) may be re-written as

$$\Delta P_T/\Delta L = \Delta P_{fa}/\Delta L + \Delta P_{fp}/\Delta L \tag{39}$$

Dividing both sides of equation (39) by $\Delta P_{fa}/\Delta L$ leads to

$$\frac{\Delta P_{ft}/\Delta L}{\Delta P_{fa}/\Delta L} = 1 + \frac{\Delta P_{fp}/\Delta L}{\Delta P_{fa}/\Delta L} \tag{40}$$

As noted earlier, most of the investigators have followed the practice of Gasterstadt (11) in plotting the specific pressure drop, $\Delta P_{ft}/\Delta P_{fa}$, against the specific loading R. Since Gasterstadt obtained linear relations, it would seem that $\Delta P_{fp}/\Delta P_{fa}$ is equal to R multiplied by a constant, but the results of others, e.g., Farbar (10), showed no

such linearity. Examination of the Fanning equation shows that

$$\Delta P_{fa}/\Delta L = \frac{f_a u_a^2}{2g_c D} \rho_a \tag{41}$$

and the assumed analogy of the Fanning relation to the solids friction effects, justified by experiment, is given in equation (30) as

$$\Delta P_{fp}/\Delta L = \frac{f_p u_p^{*2}}{2g_c D} \rho_{ds} \tag{30}$$

Hence,

$$\frac{\Delta P_{fp}/\Delta L}{\Delta P_{fa}/\Delta L} = \frac{f_p u_p^{*2} \rho_{ds}}{f_a u_a^2 \rho_a} = \frac{f_p u_p^* (u_p^* \rho_{ds})}{f_a u_a (u_a \rho_a)} \tag{42}$$

From the continuity equations, $(u_p^* \rho_{ds})$ may be replaced by G_p/A and $(u_a \rho_a)$ by G_a/A. Substitution into equation (42) yields

$$\frac{\Delta P_{fp}/\Delta L}{\Delta P_{fa}/\Delta L} = \frac{f_p u_p^*}{f_a u_a} \cdot R \tag{43}$$

where $G_p/G_a = R$. Equation (40) then becomes

$$\frac{\Delta P_{ft}/\Delta L}{\Delta P_{fa}/\Delta L} = 1 + \frac{f_p u_p^*}{f_a u_a} \cdot R \tag{44}$$

It is evident from equation (44) that the specific pressure drop is dependent not only on R, but also on the relation between the particle and air velocities and between the solids and air friction factors. The specific pressure drop is plotted against R in the accustomed manner in Figure 17 and against $f_p u_p^* R/f_a u_a$ in Figure 18. Figure 17 resembles the

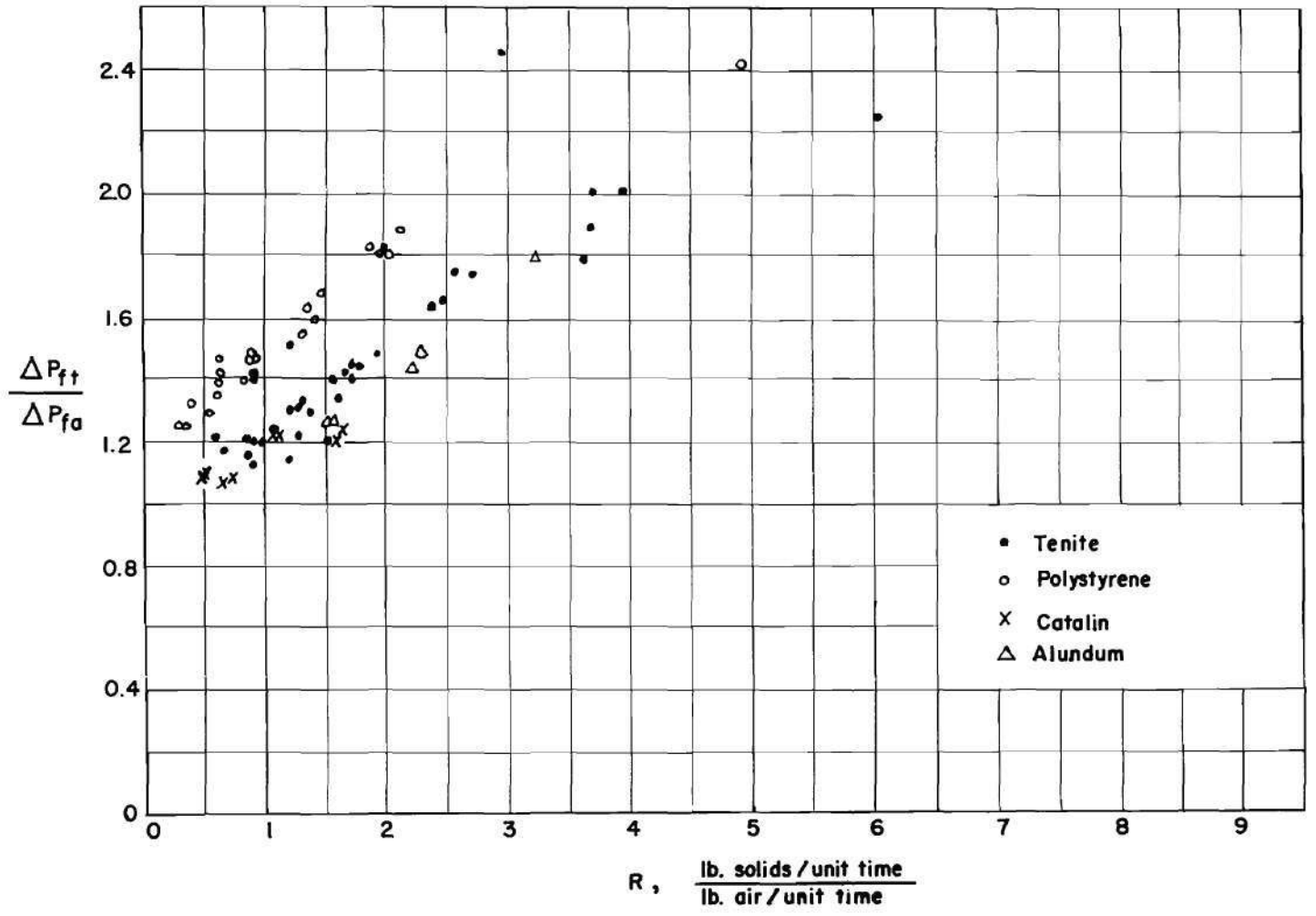

Figure 17. Specific Pressure Drop vs. Specific Loading for Horizontal Conveying.

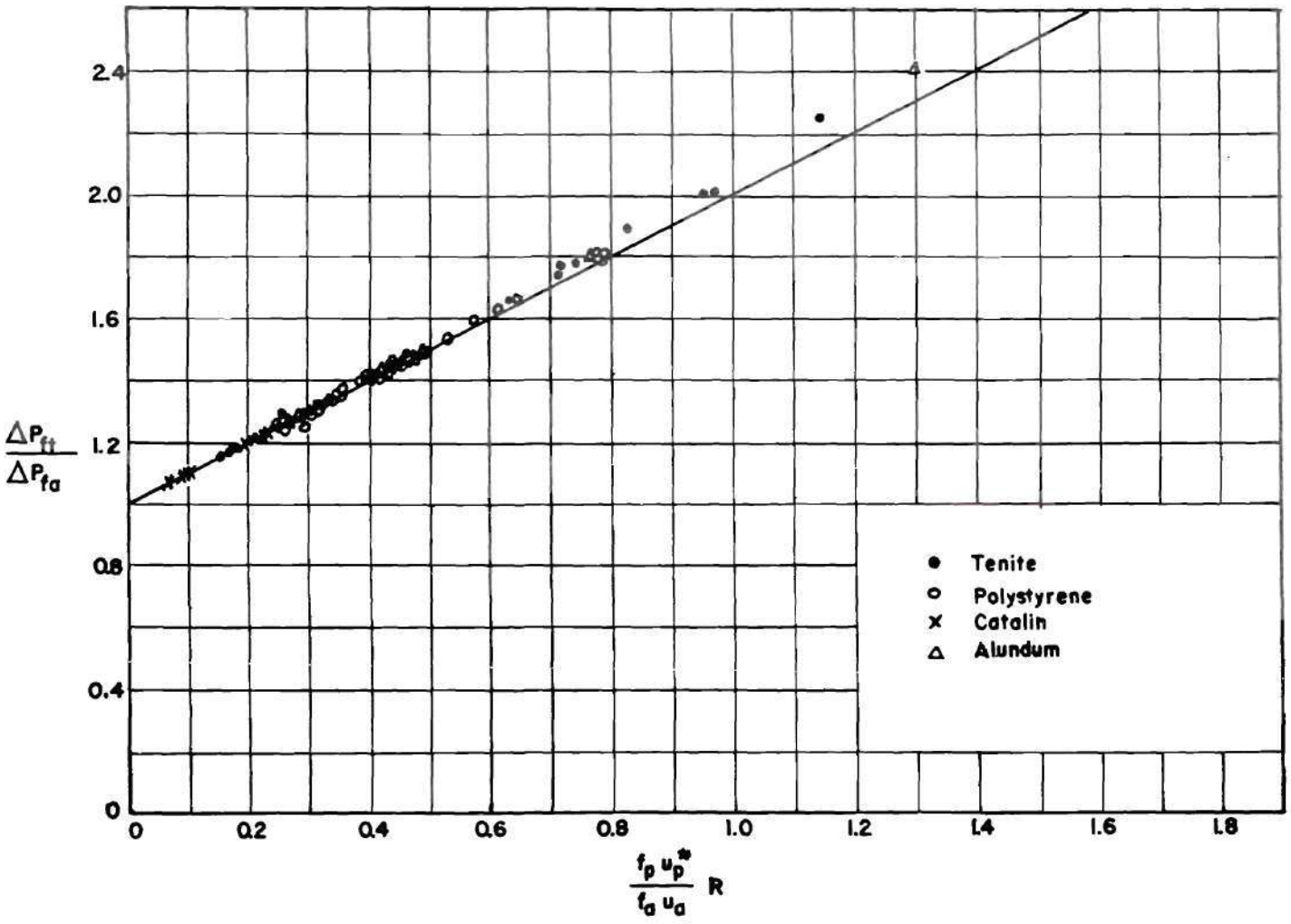

Figure 18. Specific Pressure Drop Plotted According to Equation (44) for Horizontal Conveying.

data presented by Farbar for horizontal pneumatic conveying but indicates little more than a general trend. Figure 18, on the other hand, accurately describes the observed pressure drops over a wide range of particle sizes and densities, and thus is appropriate for use in design problems. The apparent difference between Gasterstadt's linear specific pressure drop-loading results and the non-linear results obtained by others is fully clarified by examination of equation (44). Gasterstadt's data were obtained with grains of similar size, shape and density. It has already been pointed out that the equilibrium particle velocity is independent of the loading for a constant air velocity, and that the friction factor corresponding to the equilibrium particle velocity is also independent of the loading (See equation 35). Hence, for the case of horizontal pneumatic conveying of a specific material at a constant air velocity, the term $f_p u_p^*/f_a u_a$ is constant and equation (44) reduces to the result obtained by Gasterstadt,

$$\frac{\Delta P_{ft}/\Delta L}{\Delta P_{fa}/\Delta L} = 1 + kR \qquad (45)$$

where k is a constant. Other investigators, working with materials having different sizes and densities, have not obtained linear specific pressure drop-loading results because the term involving velocities and friction factors was not constant from one material to another. Both f_p and u_p are dependent on the particle diameter and density; hence, for a certain air velocity, one would not expect the equilibrium velocity of a large, heavy particle to be the same as the velocity of a small, light particle.

Although experiments on vertical pneumatic conveying were not conducted in the present study, the agreement of observed pressure drop data with theoretical developments for the case of horizontal conveying suggested extension of the the theory to the vertical conveying problem. The individual pressure drops encountered in vertical conveying may be expressed by a relation similar to equation (36). Thus,

$$\Delta P_T = \Delta P_{aa} + \Delta P_{ap} + \Delta P_{fa} + \Delta P_{fp} + \Delta P_{sa} + \Delta P_{sp} \tag{46}$$

where ΔP_{sa} and ΔP_{sp} are the pressure drops arising from the energy expended in supporting the static heads of the air and of the solids. ΔP_{sa} is negligible in comparison to the other pressure drops and may therefore be neglected. If, as before, consideration is limited to the regions where the acceleration of the gas and solids are completed, equation (46) becomes

$$\Delta P_{ft} = \Delta P_{fa} + \Delta P_{fp} + \Delta P_{sp} \tag{47}$$

and rearrangement to obtain a relation involving the specific pressure drop leads to

$$\frac{\Delta P_{ft}/\Delta L}{\Delta P_{fa}/\Delta L} = 1 + \frac{\Delta P_{fp}/\Delta L}{\Delta P_{fa}/\Delta L} + \frac{\Delta P_{sp}/\Delta L}{\Delta P_{fa}/\Delta L} \tag{48}$$

The pressure drop in the carrier gas due to supporting the solids may be regarded as a solids static head of density ρ_{ds}. Thus,

$$\Delta P_{sp}/\Delta L = \rho_{ds} = G_p/Au_p^* \tag{49}$$

Substituting the value of $\Delta P_{sp}/\Delta L$ given by equation (49) and the values of ΔP_{fp} and ΔP_{fa} given by equations (30) and (41) into equation (48) yields

$$\frac{\Delta P_{ft}/\Delta L}{\Delta P_{fa}/\Delta L} = 1 + \frac{f_p u_p^*}{f_a u_a} \cdot R + \frac{2 g_c D}{f_a u_a u_p^*} \cdot R \qquad (50)$$

Comparison of equations (50) and (44) shows that the only difference is the addition of the term $2g_cD/f_au_au_p^* \cdot R$ in the vertical conveying case to account for a pressure drop due to the solids static head. The experimental data of Hariu and Molstad (12) for vertical conveying are plotted according to equation (50) in Figure 19. The excellent agreement of the observed data with the theoretical equation establishes the validity of equation (50) for predicting pressure drops in vertical transport. Thus it is possible to predict the friction pressure drops in both horizontal and vertical pipes through the use of equations (44) and (50). The total pressure drop encountered in pneumatic conveying installations now may be expressed by using the developed relations for the individual quantities given in equations (36) and (46). Thus, for horizontal conveying,

$$\Delta P_T = \frac{u_a^2 \rho_a}{2 g_c} + \frac{G_p u_p^*}{g_c A} + \frac{f_a u_a {}^2 \rho_a L}{2 g_c D} \left[1 + \frac{f_p u_p^*}{f_a u_a} \cdot R \right] \qquad (51)$$

and for vertical conveying,

$$\Delta P_T = \frac{u_a {}^2 \rho_a}{2 g_c} + \frac{G_p u_p^*}{g_c A} + \frac{f_a u_a {}^2 \rho_a L}{2 g_c D} \left[1 + \frac{f_p u_p^*}{f_a u_a} \cdot R + \frac{2 g_c D}{f_a u_a u_p^*} \cdot R \right] (52)$$

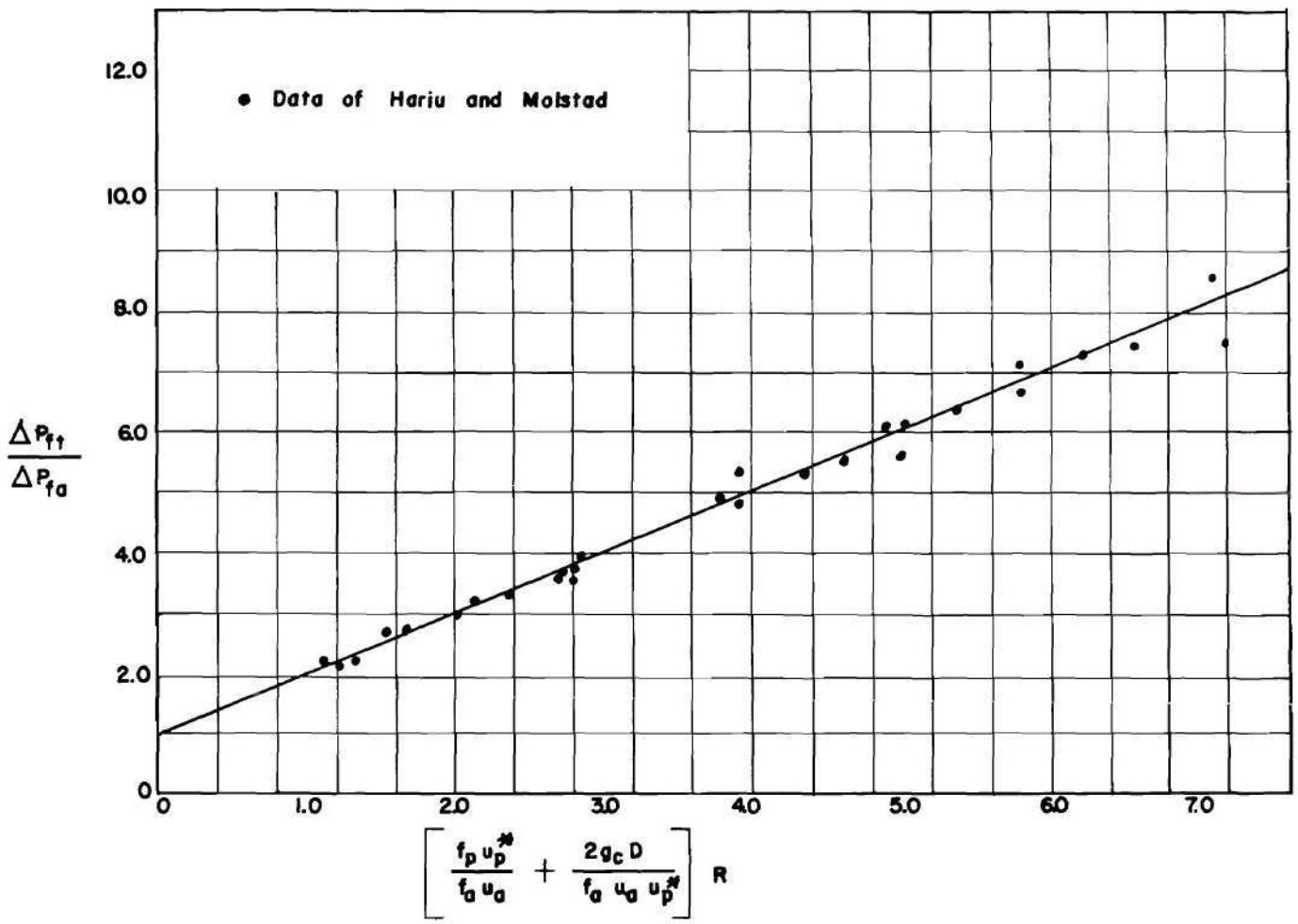

Figure 19. Specific Pressure Drop Plotted According to Equation (50) for Vertical Conveying.

The observed total pressure drop for a horizontal pipe length of 25 feet is plotted against the pressure drop calculated by equation (51) in Figure 20. The data represent materials varying in diameter from 0.0193 inch to 0.33 inch and in specific gravity from 1.05 to 1.82.

D. Estimation of Particle Velocity

The important relations developed thus far in this study involve the particle velocity, thus supporting the statements of many investigators that the solution to the problems of pneumatic conveying would depend on a knowledge of the particle velocity. Unfortunately, however, there is a dearth of information concerning particle velocities, due principally to the difficulties of measurement. In the absence of values of measured particle velocities, or pressure drop data, the successful application of equations (44) and (50) requires a means for estimating the equilibrium velocities, and therefore attempts were made to develop a method for predicting the ultimate solids velocity from the characteristics of the solid transported. The study of particle dynamics is most easily begun through analysis of the motion of particles in a vertical tube. If a single body falling under the action of gravity is considered, the body will attain a constant terminal velocity, u_t, when the resisting upward drag force, F_r, is equal to the net gravitational accelerating force, F_g. If the densities of the particle and the air are ρ_p and ρ_a, respectively, and the mass of the particle is m, the gravitational pull is

$$F_g = mg\left(\frac{\rho_p - \rho_g}{\rho_p}\right) \qquad (53)$$

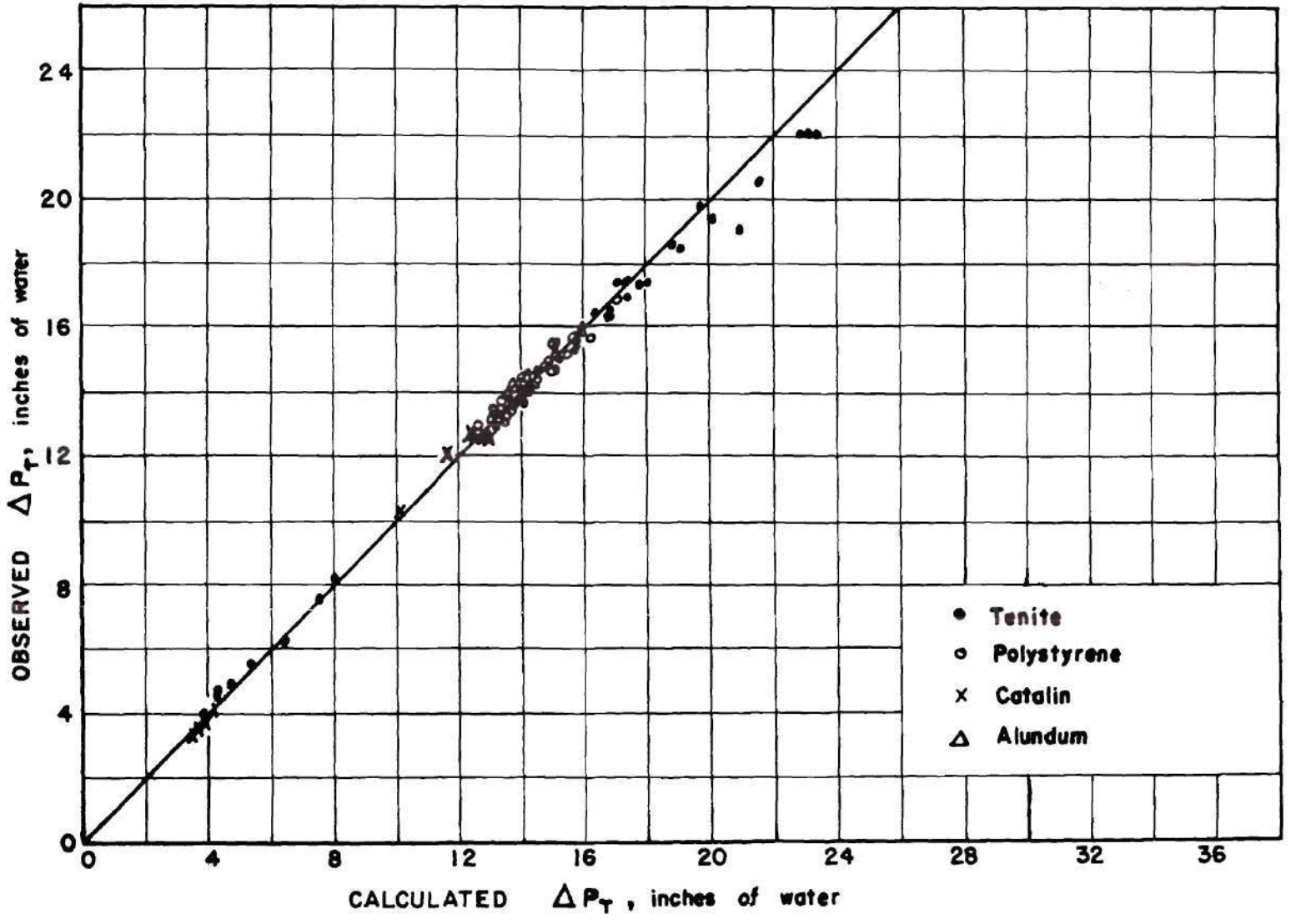

Figure 20. Comparison of Calculated and Observed Total Pressure Drops for a Horizontal Pipe Length of Twenty-Five Feet.

The drag force is given by equation (22). When $F_r = F_g$, $u_p = u_t$. Equating (53) and (22), and solving for u_t gives

$$u_t = \sqrt{\frac{2mg(\rho_p - \rho_a)}{C_r \rho_p \rho_a A_p}} \tag{54}$$

For spherical particles $m = d_p^3 \rho_p \pi/6$, and $A_p = d_p^2 \pi/4$. Then

$$u_t = \sqrt{\frac{4gd_p(\rho_p - \rho_a)}{3\rho_a C_r}} \tag{55}$$

Newton derived the following expression for the terminal velocity of a free-falling body under conditions of turbulent flow and negligible viscous forces.

$$u_t = \sqrt{\frac{\pi g d_p(\rho_p - \rho_a)}{6K_n \rho_a}} \tag{56}$$

where K_n is a constant indeterminate from theoretical study. As Lapple (18) points out, equation (56) is identical with equation (35) for a constant value of C_r when $K_n = \pi C_r/8$. Experimental data have indicated that this is a good approximation in the turbulent range of particle Reynolds numbers, where C_r is substantially constant with a value of about 0.44 for spherical particles. Then equation (56) becomes

$$u_t = 1.74 \sqrt{\frac{gd_p(\rho_p - \rho_a)}{\rho_a}} \tag{57}$$

Equations (54) through (57) were developed for terminal velocities in the turbulent particle Reynolds number region. In the streamline

region, where inertial terms are negligible, the drag force may be represented by Stokes law

$$F_r = 3\pi\mu u_p d_p \tag{58}$$

which, when equated to the gravitational forces on a particle, leads to the following expression for the terminal velocity.

$$u_t = \frac{d_p^2(\rho_p - \rho_a)g}{18\mu} \tag{59}$$

This relation has been shown to be accurate for particle Reynolds numbers ranging from less than 0.1 to nearly 2.0. There is no sharp definition between streamline and turbulent conditions, and hence an expression has been derived to approximate terminal velocities in the intermediate region, which includes Reynolds numbers ranging from 2.0, the upper limit of Stokes streamline law, to 1000, the lower limit of Newtons turbulent law. In the intermediate region the coefficient of resistance may be taken as

$$C_r = 18.5/Re_p^{0.6} \tag{60}$$

and substitution into equation (37) yields

$$u_t = 0.153\ g^{0.714} d_p^{1.142} (\rho_p - \rho_a)^{0.714} / \rho_a^{0.286} \mu^{0.428} \tag{61}$$

The minimum air velocity necessary to support a particle in the theoretical case is equal to the terminal velocity of the particle, and the actual particle velocity is the difference between the carrier gas

velocity and the terminal velocity. Chatley (3) and Lapple (18) use this concept in calculations of the energy requirements for the vertical transport of granular solids, and in calculations of the pressure drop encountered in the acceleration of particles, respectively. Lapple points out, however, that the equation

$$u_p = u_a - u_t \tag{62}$$

is only an approximation. The difference between the air velocity and the solids velocity is known as the "slip" between the air and the solids, and increases with increasing velocity of the air stream. The "slip" velocity is of the order of magnitude of the "choking" velocity, which is defined by Lapple as the air stream velocity when the velocity of the solids is just zero, or the minimum transport velocity. Wood and Bailey (31) report that the "choking" velocity is independent of the loading for relatively large particles.

The data of the present investigation, obtained in the turbulent regions of air Reynolds number and particle Reynolds number, and with horizontal tubes, supports the statement that the relative or "slip" velocity increases with increasing air velocity. Experimental data are shown in Figure 21. The studies of Hariu and Molstad (12) and Belden and Kassel (2) are at variance on this contention. Their data are difficult to interpret in terms of solids motion since both the air Reynolds numbers and the particle Reynolds numbers are in the intermediate region between streamline and turbulent flow. Hariu and Molstad found an increase in the relative velocity with an increase in the air velocity, but

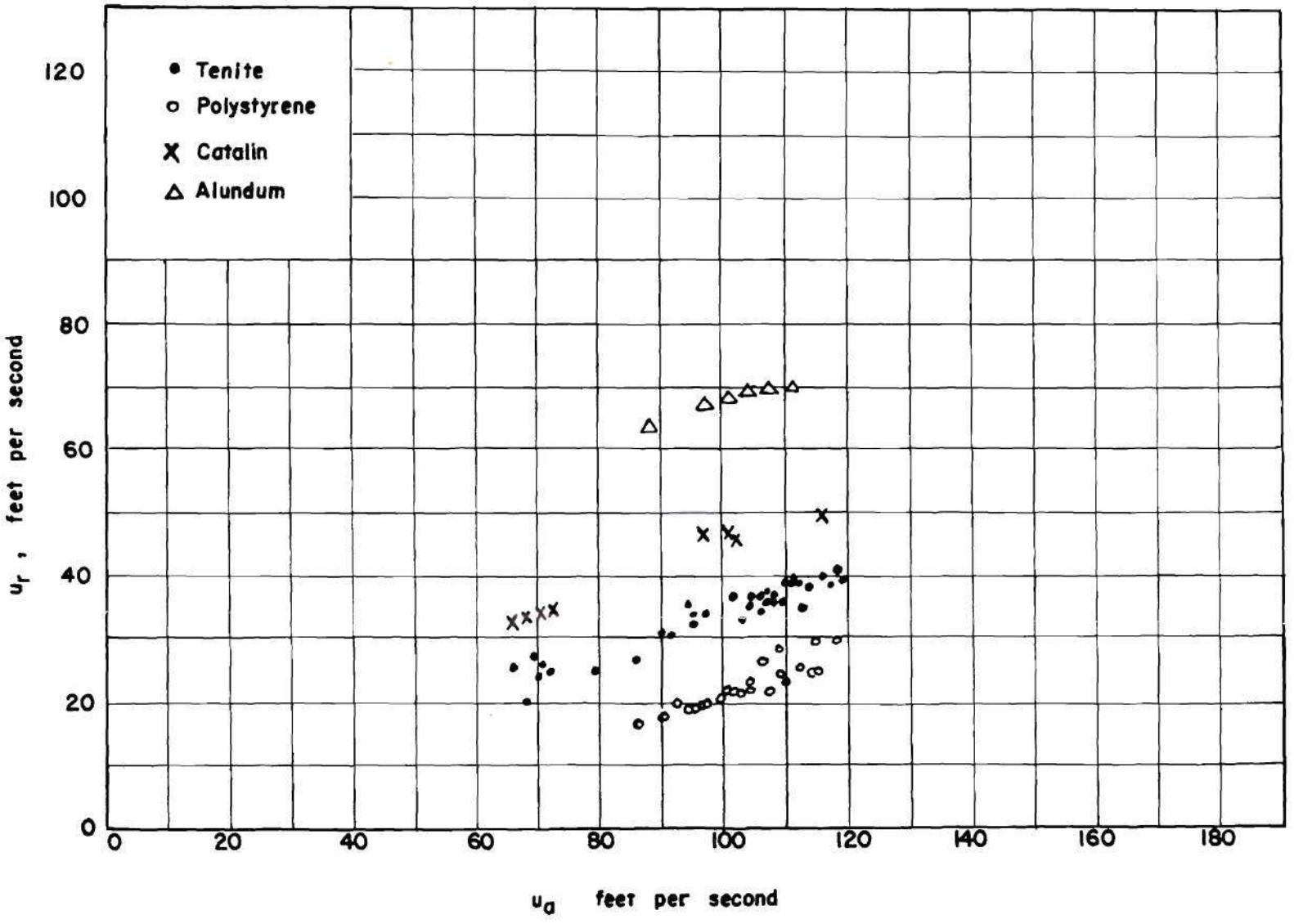

Figure 21. Influence of the Air Velocity on the Relative Velocity.

Belden and Kassel found that their relative velocities were all correlated by the equation

$$u_r = 1.32 \sqrt{\frac{g d_p (\rho_p - \rho_a)}{\rho_a}} \qquad (63)$$

which is in agreement with equation (55) corresponding to a coefficient of resistance of 0.77, a reasonable value considering the irregularity of the particles. Equation (63) does not involve a velocity term, and therefore the relative velocity is independent of the air velocity. Belden and Kassel were dealing with solids loading rates from one to ten pounds per square foot of pipe area per second, whereas Hariu and Molstad were studying solids rates ranging from ten to fifty pounds per square foot per second. Examination of the data of Hariu and Molstad for their light loadings (i.e., approximately ten pounds per square foot per second) reveals that the relative velocities are accurately predicted by Belden and Kassel's equation. Therefore it seems that, in the regions investigated by these authors, below some critical loading the relative velocity remains essentially constant and approximately equal to the terminal velocity as suggested by Wood and Bailey, and above the critical loading, the relative velocity increases with the air velocity, as stated by Lapple. DallaValle (7) developed empirical equations of the form

$$u_{mc} = k \left(\frac{s}{s + 1} \right) d^b \qquad (64)$$

where k and b are constants, and d is the diameter of the largest particle to be transported in inches. The velocity is defined as the minimum

air velocity necessary to transport the particles in feet per second. The constants for both horizontal and vertical conveying are given below.

	Vertical	Horizontal
K	222	100
b	0.60	0.40

The materials examined in DallaValle's studies ranged in specific gravity from 1.1 to 2.7 and in diameter from 0.055 to 0.32 inch. The loadings of the solids were light, and therefore the velocities predicted from equation (64) are only slightly higher than the terminal velocities.

The analysis of solids motion in horizontal pipes is even more complex than in vertical pipes. Chatley (3) points out that the difference between the fluid velocity along the pipe and the terminal velocity of the particle is a somewhat obscure factor in the transport of solids since the two velocities are at right angles. His subsequent energy requirement calculations for horizontal pipes were based upon estimations of the vertical components of the turbulence, and led to the result, often criticized and refuted, that more energy was required to transport the particles horizontally than vertically.

Zenz (32) has shown that correlation of pressure drop data can be achieved with a knowledge of the "saltation" velocity, which has been termed "slugging" or minimum conveying velocity by various authors. Unfortunately, no equation for estimating the minimum conveying velocity

has found wide application. Newton's, DallaValle's and Davis' relations for the minimum conveying velocity are independent of the loading, which limits their use to very light loadings. None was found to express accurately the relative velocities encountered in this study.

Correlation of the author's particle velocity data in terms of the density, pipe size, particle size and air velocity was first attempted through consideration of the acceleration term. It has already been shown that the acceleration of a particle in horizontal pneumatic transport may be expressed as

$$a = \frac{3\rho_a C_r (u_a - u_p)^2}{4 d_p \rho_p} - \frac{f_p u_p^2}{2D} \tag{65}$$

When the equilibrium velocity is reached, the acceleration will equal zero. Separating the velocity terms leads to

$$\frac{(u_a - u_p)^2}{u_p} = \frac{2 d_p \rho_p f_p}{3 D \rho_a C_r} \tag{66}$$

From the Fanning analogy, equation (32), f_p may be replaced by its equivalent, $\Delta P_{fp}/\Delta L \cdot 2g_c DA/u_p G_p$. Furthermore, it has been suggested that $\Delta P_{fp}/\Delta L$ is proportional to $G_p/Au_p{}^*$. Substitution of these quantities into equation (66) leads to

$$u_r = 1.15 \sqrt{\frac{d_p(\rho_p - \rho_a)g}{\rho_a C_r}} \tag{67}$$

which is equivalent to Newton's equation (57) for the terminal velocity of a free-falling body. According to equation (67), the relative velo-

city is independent of the air velocity, a condition which is not supported by experimental evidence. The observed values of relative velocity are plotted according to equation (67) in Figure 22. It is evident from Figure 22 that the relative velocity of a material in a horizontal pneumatic transport system cannot be determined solely from the size, shape and density characteristics of the material. Moreover, there seems to be an apparent dependence of the relative velocity on the tube diameter. Actually, however, the difference in the values of u_r for the two-inch and the three-inch pipes is due to the difference in air velocities. The greater part of the experiments with a two-inch pipe were carried out using air velocities of from 90 to 120 feet per second, while with the three-inch pipe, the air velocities varied from 66 to 72 feet per second. In a few tests with light loadings in the two-inch pipe, the gate valve controlling the air flow was closed to such a degree that the air velocity was of the order of 75 feet per second. The relative velocity in the two-inch pipe at this air velocity was equal to the relative velocity in the three-inch pipe at the same air velocity. Hence a relation such as equation (64), which does not consider the dependence of u_r on u_a, is of value only for a limited range of air velocities. The variation of the relative velocity with changes in the air velocity, shown in Figure 21, confirms the statement by Lapple (18) that the relative velocity increases with increasing air velocity.

As discussed earlier, a rough estimate of the particle velocity in a transport tube may be obtained by the use of equation (62). The experimental particle velocity data for the various materials studied

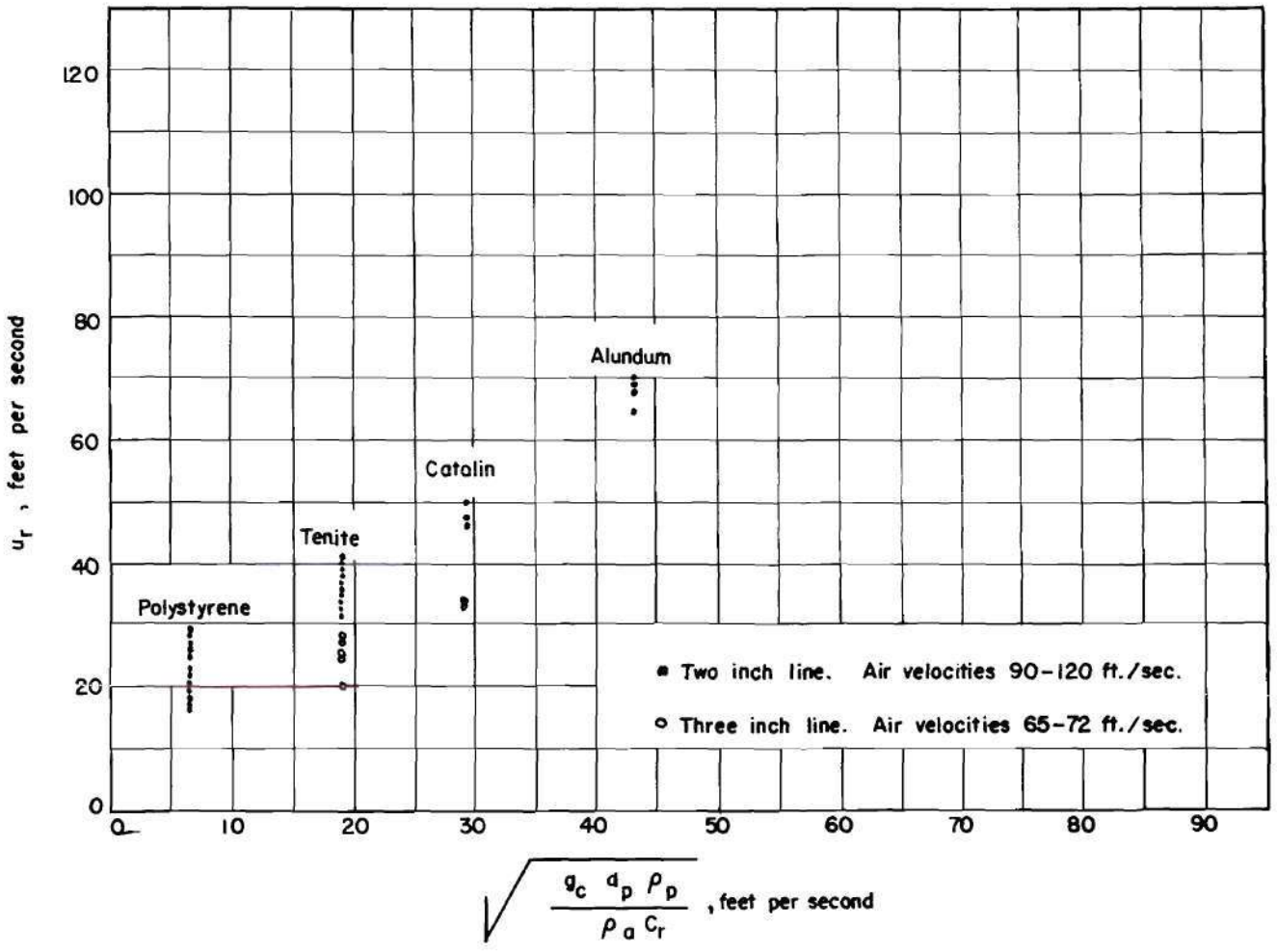

Figure 22. Variation of the Relative Velocity with the Function $(g_c d_p \rho_p / \rho_a C_r)^{0.5}$

are plotted against $u_a - u_t$ in Figure 23, where the terminal velocities were calculated by equation (55). The distinct pattern of the experimental data indicates a certain correlation, but the observed values of the particle velocity by no means fall on a straight line of unit slope passing through the origin, as predicted by equation (62). Particle velocities estimated by equation (62) were in all cases higher than the observed particle velocities. Similar results were obtained by Hariu and Molstad in studies of vertical conveying. From equations (35), (38) and (44), it is evident that the consequence of using a value of particle velocity higher than the true velocity in the equations for estimating pressure drop is an acceleration pressure drop higher, and a friction pressure drop lower, than those which would be observed. Hence, for design purposes, calculation of the energy requirements for a pneumatic conveying system requires a more accurate knowledge of particle velocity than that predicted by equation (62).

Segler (24) discussed a proposal by Gasterstadt (11) that the particle velocities in horizontal transport be correlated by the equation

$$u_p = u_a - \beta u_t \tag{68}$$

Gasterstadt obtained a linear relation between β and u_a, but a similar plot of the data of the present investigation, given in Figure 24, shows no such clear relationship. The pattern of the experimental points in Figure 24, and the deviation of the particle velocities from equation (62) as shown in Figure 23, suggests that the relative velocity is a

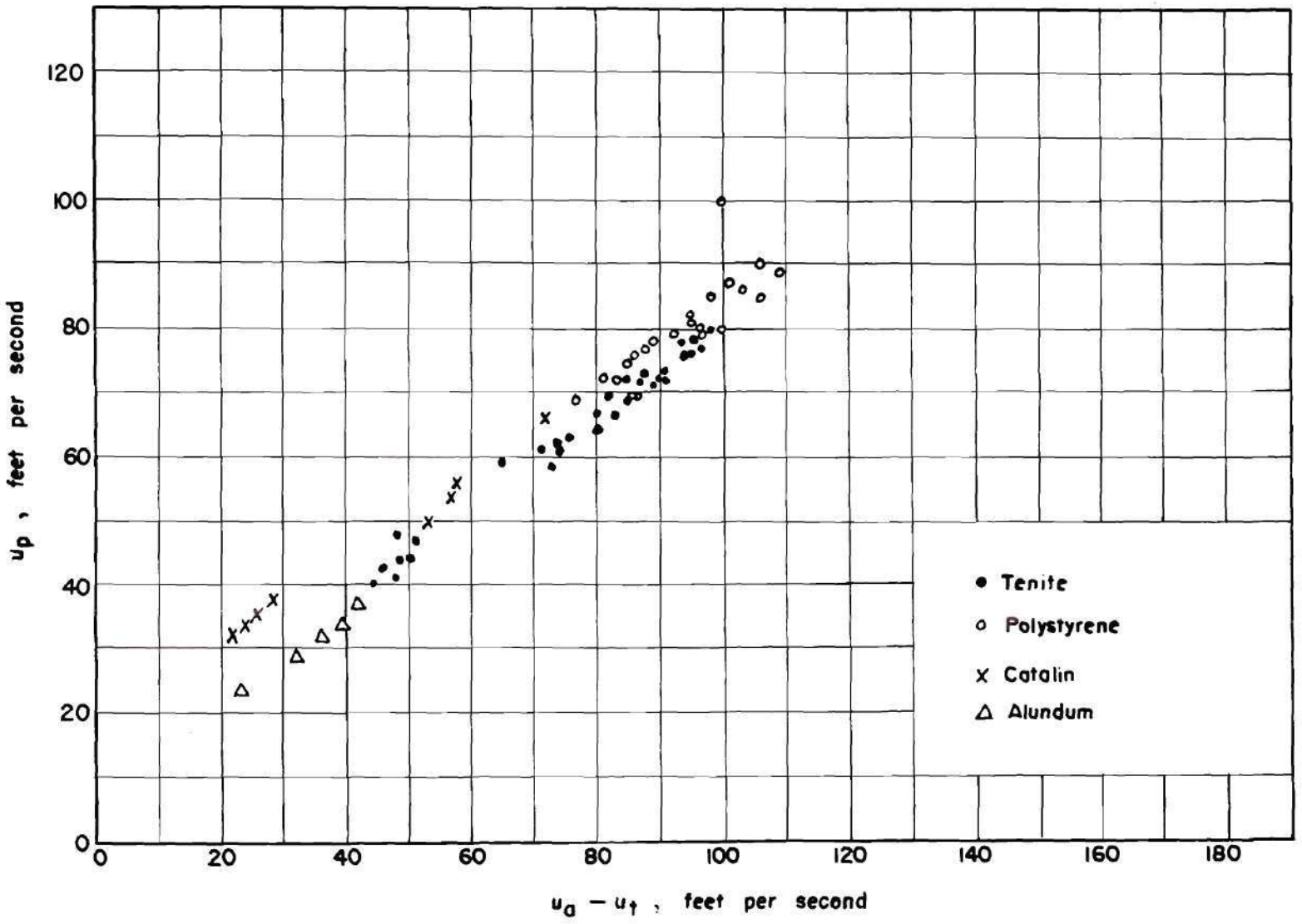

Figure 23. Particle Velocities Plotted According to Equation (62).

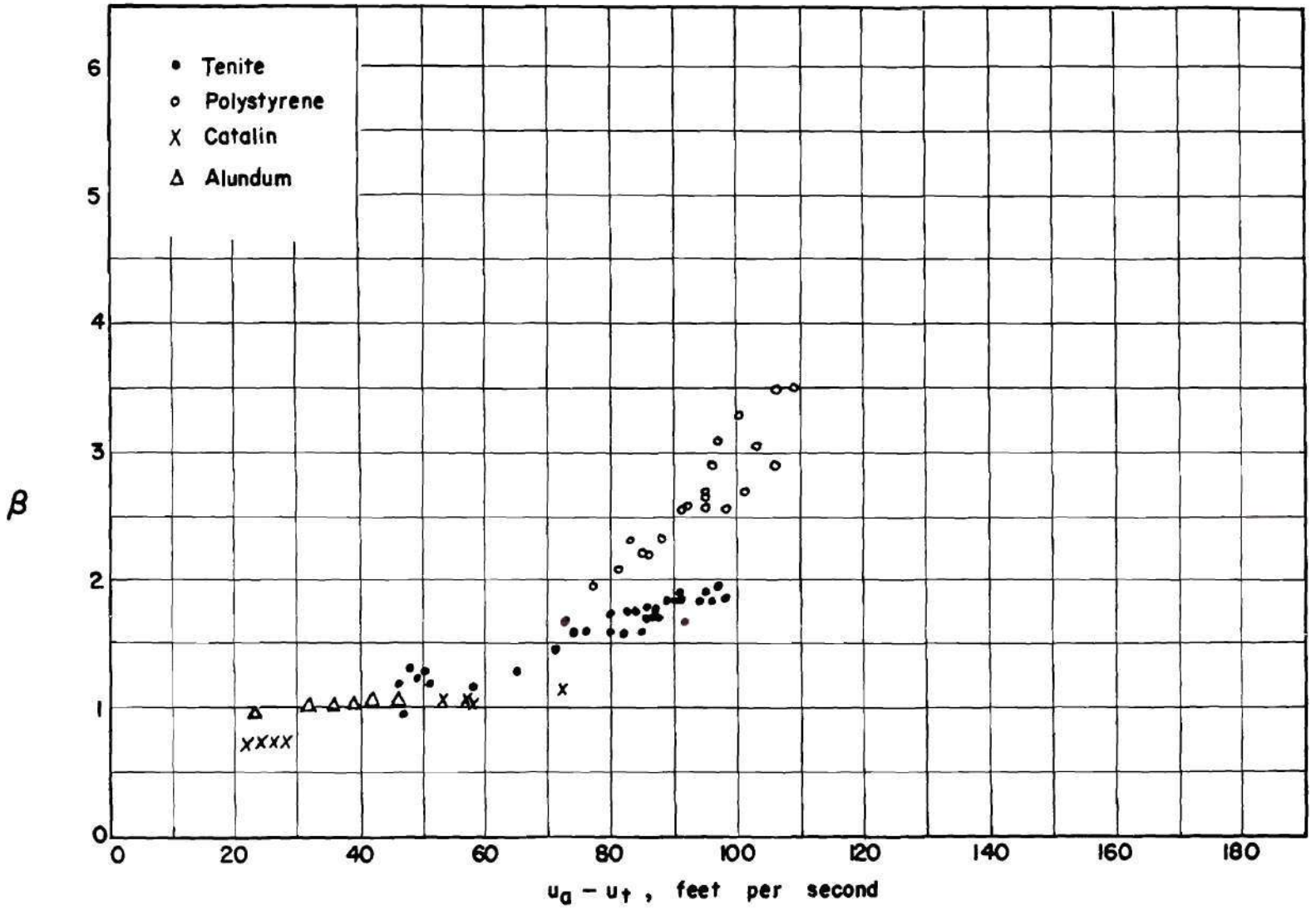

Figure 24. Variation of the Term β with Air Velocity.

function not only of a minimum conveying velocity, but also of the amount by which the actual conveying velocity exceeds the minimum conveying velocity; that is,

$$u_r = f(u_{mc},\ u_a/u_{mc}) \tag{69}$$

This functional relation is supported by the evidence that the deviation of the particle velocities predicted by equation (62) is greatest in the case of the polystyrene beads, where the ratio u_a/u_t was greatest, and is in agreement with the results of Zenz (32), which show the dependence of pressure drops on the ratio u_a/u_{mc}. Unfortunately, equation (69) could not be examined adequately since there is no accepted method for calculating the minimum conveying velocity. Attempts to replace u_{mc} by u_t in equation (69) were unsuccessful, a result which is not surprising, since u_t, while related to u_{mc}, is strictly applicable only to a vertical conveying system.

The relative velocity data were correlated through recognition of the fact that the ratio u_r/u_a for a specific material varied only slightly with relatively large changes in the air velocity, and that u_r/u_a for roughly spherical particles was primarily a function of the particle size and the density; that is,

$$u_r/u_a = f(d_p,\ \rho_p) \tag{70}$$

Hariu and Molstad, in their studies of vertical conveying, reported a nearly constant value of u_r/u_a for a specific granular solid, although others, using air velocities in vertical systems which led to streamline

flow conditions, have found that the relative velocity is constant, rather than the ratio u_r/u_a.

The experimental data for the turbulent conditions in the two-inch and the three-inch horizontal tubes used in the present study were found to be correlated by the empirical equation

$$u_r = 1.41\, u_a d_p^{0.3} s^{0.5} \qquad (71)$$

The relative velocities predicted from equation (71) generally differed from the observed relative velocities by less than five per cent, the order of magnitude of the experimental error in measuring the velocities. The observed relative velocities are plotted according to equation (71) in Figure 25. The ranges of variables in the development of the equation were as follows: air velocity, 66 to 119 feet per second; particle diameter, 0.014 to 0.33 inch; and particle specific gravity, 1.05 to 1.82. Although the accuracy of equation (71) outside the specified ranges is unknown, the conditions in most pneumatic conveying systems will be within the areas examined in this investigation. Of the literature references, only Uspenskii (26) cites particle velocity data for a horizontal system. His value of u_p/u_a for coal particles 0.105 mm. diameter is but ten per cent higher than the value calculated from equation (71), which indicates that the range of usefulness of the empirical equation may be extended to particle diameters smaller than those investigated in this work. More accurate methods for predicting the minimum conveying velocity will permit more accurate estimations of the particle velocity.

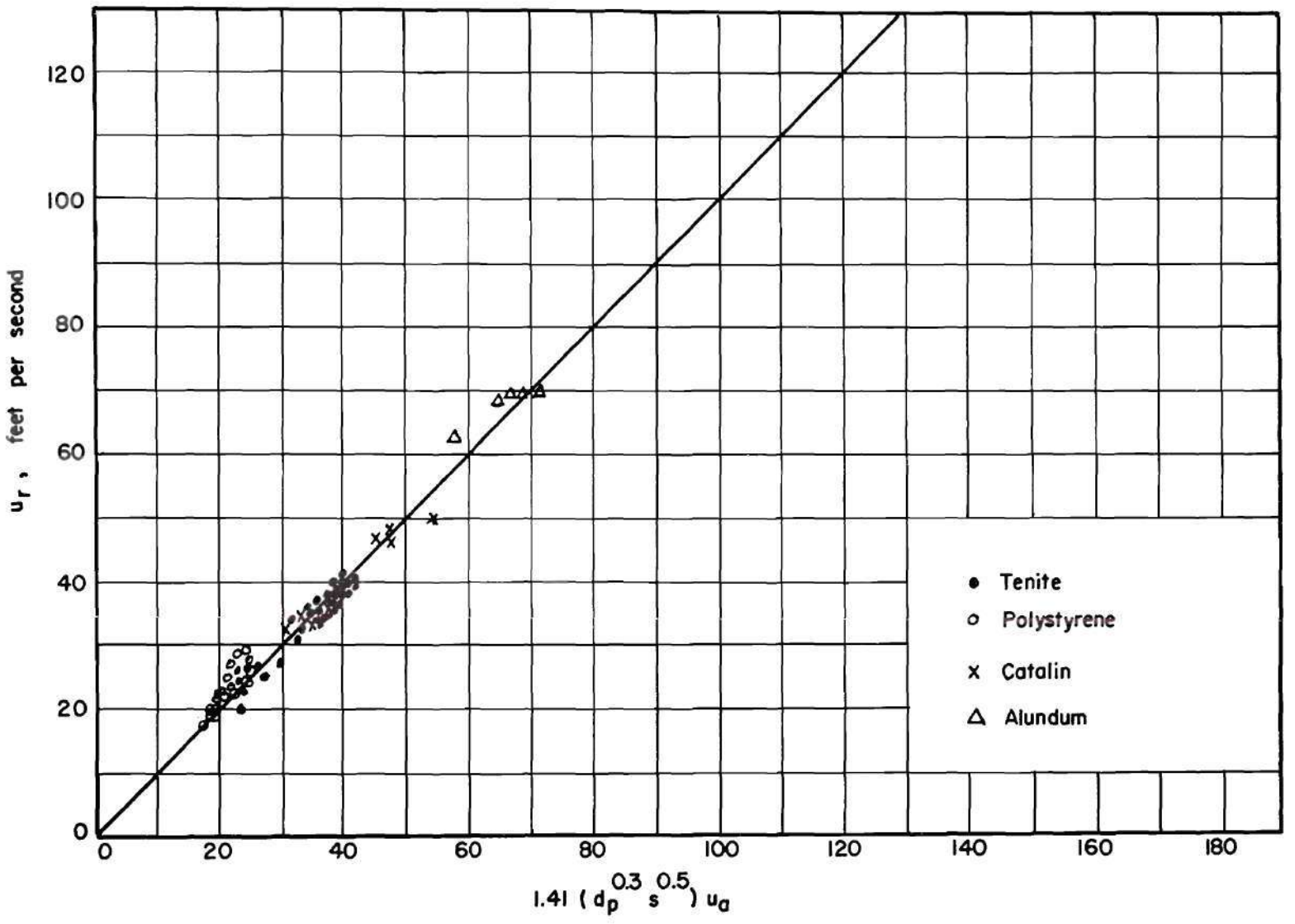

Figure 25. Relative Velocities Plotted According to Equation (71).

V. CONCLUSIONS

The following conclusions may be drawn as a result of this investigation of the pressure drops and the particle velocities encountered in horizontal pneumatic conveying:

1. The necessary length of pipe to achieve acceleration of the particles depends on the solids loading rate and may be estimated by the equation

$$L = \int_0^{u_p^*} \frac{u_p du_p}{\frac{3\rho_a C_r (u_a - u_p)^2}{4 d_p \rho_p} - \frac{\Delta P_{fp}/\Delta L \; g_c A u_p}{G_p}}$$

In all cases, with loadings ranging from 4 to 40 pounds of solids per minute, 99 per cent of the acceleration had been achieved in a pipe length from 30 to 65 diameters from the feed entrance.

2. The equilibrium particle velocity may be calculated from the equation

$$\frac{u_r^2}{u_p} = \frac{4 \Delta P_{fp}/\Delta L \; g_c A d_p \rho_p}{3 G_p \rho_a C_r}$$

if pressure drop measurements are available. In the absence of pressure drop data, the equilibrium particle velocity may be estimated by the empirical relation

$$u_r = 1.41 \; u_a d_p^{0.3} s^{0.5}$$

where the diameter is expressed in feet and the relative velocity in feet

per second.

3. The pressure drop due to sustaining the particles in suspension and overcoming the friction effects in a horizontal pipe may be calculated from the equation

$$\Delta P_{ft} = \frac{f_a u_a^2 \rho_a L}{2 g_c D} \left[1 + \frac{f_p u_p^*}{f_a u_a} R \right]$$

For vertical transport the equation becomes

$$\Delta P_{ft} = \frac{f_a u_a^2 \rho_a L}{2 g_c D} \left[1 + \frac{f_p u_p^*}{f_a u_a} R + \frac{2 g_c D}{f_a u_a u_p^*} R \right]$$

4. The equilibrium particle velocity of a given material is constant for a constant air flow and is relatively independent of the solids loading, as long as the air velocity is above the "slugging" velocity.

VI. RECOMMENDATIONS

Relations have been developed in the present investigation which permit accurate estimation of the pressure drops encountered in both horizontal and vertical pneumatic conveying. The energy requirements thus predicted are shown to be functions of the particle velocity, and hence a precise method for estimating the velocity of the solids, in terms of measurable quantities such as particle size, density, air velocity, etc., is obviously essential. The results obtained in the present investigation and earlier literature references indicate that the equilibrium particle velocity attained in a pneumatic transport system is also related to the difference between the prevailing air velocity and the minimum conveying or "slugging" velocity. These indications warrant a thorough investigation which should encompass the following phases: (1) a study of the equilibrium particle velocity and the relative velocity in relation to the particle size, shape, density, pipe size and the air velocity; (2) a study of the minimum conveying velocity in horizontal pipes, the relation between particle velocity and minimum conveying velocity, and the dependence of the minimum conveying velocity on the loading and on the characteristics of the solid; and (3) a study of the pressure drops encountered in "slugging" conditions to determine the nature of the flow in this region.

VII. BIBLIOGRAPHY

1. Albright, C.W., Holden, J.H., Simons, H.P., and Schmidt, L.D., "Pressure Drop in Flow of Dense Coal-Air Mixtures." Ind. Eng. Chem. 43, 1837-40 (1951).

2. Belden, D.H. and Kassel, L.S., "Pressure Drops Encountered in Conveying Particles of Large Diameter in Vertical Transfer Lines." Ind. Eng. Chem. 41, 1174-8 (1949).

3. Chatley, H., "The Pumping of Granular Solids in Fluid Suspension." Engineering 149, 230-1 (1940).

4. Cramp, W., "Pneumatic Transport Plants." Chem. and Ind. 44, 207-11T, 211-13T (1925).

5. Cramp, W. and Priestly, A., "Pneumatic Grain Elevators." The Engineer 137, 89 (1924).

6. Culgan, J.M., "Pneumatic Conveying of Materials of Unit Density in a Three-Inch Pipe." Ph.D. Thesis in the School of Chemical Engineering, Georgia Institute of Technology, 1952.

7. DallaValle, J.M., "The Theory and Practice of Pneumatic Conveying." Heating and Ventilating 39, No. 11, 28-32 (1942).

8. DallaValle, J.M., Micromeritics. Pitman Publishing Company, New York, 1948.

9. Davis, H.F., "The Conveyance of Solid Particles by Fluid Suspension." Engineering 140, 1, 124 (1935).

10. Farbar, L., "Flow Characteristics of Solids-Gas Mixtures in a Horizontal and Vertical Circular Conduit." Ind. Eng. Chem. 41, 1184-91 (1949).

11. Gasterstadt, J., "Die Experimentelle Untersuchung des Pneumatischen Fordervorganges." Zeit. Vereinigung Deutschen Ingenieurw. 68, 617-24 (1924).

12. Hariu, O.H., and Molstad, M.C., "Pressure Drop in Vertical Tubes in Transport of Solids by Gases." Ind. Eng. Chem. 41, 1148-60 (1949).

13. Hudson, W.G., Conveyors and Related Equipment. John Wiley and Sons, New York, 1944.

14. Hunsaker, J.C. and Rightmire, B.G., Engineering Applications of Fluid Mechanics. McGraw-Hill Book Co., Inc., New York, 1947.

15. Jennings, M., "Pneumatic Conveying in Theory and Practice." Engineering 150, 361-3 (1940).

16. Khudyakov, G.N. and Chukhanov, Z.F., "The Motion of Solid Particles in Gas Streams." Doklady Akad. Nauk. SSSR 78, 681-4 (1951).

17. Korn, A.H., "How Solids Flow in Pneumatic Handling Systems." Chem. Eng. 57, No. 3, 108-11 (1950).

18. Lapple, C.E., Fluid and Particle Mechanics. University of Delaware, Newark, Delaware, 1951.

19. Lapple, C.E. and Shepherd, C.B., "Calculation of Particle Trajectories." Ind. Eng. Chem. 32, 605-17 (1940).

20. Perry, J.H., ed., Chemical Engineers Handbook. 3rd ed., McGraw-Hill Book Co., Inc., New York, 1950.

21. Pettyjohn, E.S. and Christiansen, E.E., "Effect of Particle Shape on Free Settling Rates of Isometric Particles." Chem. Eng. Progress 44, 157-72 (1948).

22. Russ, G.H., "Pneumatic Transport of Granular Materials." J. Imp. Coll. Chem. Eng. Soc. 2, 48-57 (1946).

23. Sadler, A.M., "Gas-Solids Fluidizing for Transport." Chem. Eng. 56, No. 5, 110 (1949).

24. Segler, G., "Untersuchungen an Kornergeblasen und Grundlagen fur die Berechnung." Zeit. Vereinigung Deutschen Ingenieurw. 79, 558-9 (1935).

25. Stearns, R.F., Jackson, R.M., Johnson, R.R., and Larson, C.A., Flow Measurement with Orifice Meters. D. VanNostrand Co., New York, 1951.

26. Uspenskii, V.A., "Velocity of Particles and Coefficients of Resistance in Pneumatic Conveying." Za Ekonomiyu Topliva 8, No. 3, 26-30 (1951).

27. Vogt, E.G. and White, R.R., "Friction in the Flow of Suspensions: Granular Solids in Gases Through Pipe." Ind. Eng. Chem. 40, 1731-8 (1948).

28. Wadell, H., "The Coefficient of Resistance as a Function of Reynolds Number for Solid Particles of Various Shapes." J. Franklin Inst. 217, 459-90 (1934).

29. Wagon, H., "Zur Bestimmung der Schwebegeschwindigkeit von Schuttgutern in Pneumatischen Forderanlagen." Zeit. Vereinigung Deutschen Ingenieurw. 92, 577-80 (1950).

30. Wilhelm, R.H. and Valentine, S., "The Fluidized Bed. Transition States in the Vertical Pneumatic Transport of Particles." Ind. Eng. Chem. 43, 1199-1203 (1951).

31. Wood, S.A. and Bailey, A., "The Horizontal Carriage of Granular Material by an Injector-Driven Air Stream." Proc. Inst. Mech. Engrs. (London) 142, 149-64 (1939).

32. Zenz, F.A., "Two Phase Fluid-Solid Flow." Ind. Eng. Chem. 41, 2801-6 (1949).

VIII. SAMPLE CALCULATION

The following illustrative calculations refer to Run No. 18.

1. Specific loading.

$$R = G_p/G_a = 1.71$$

2. Air friction loss.

The pressure drop due to the air friction is calculated by the Fanning method, equation (41).

$$\frac{\Delta P_{fa}}{\Delta L} = \frac{f_a u_a^2 \rho_a}{2 g_c D} \cdot \frac{12}{62.4} = 0.262 \text{ in. } H_2O/\text{ft.}$$

3. Total friction loss.

The friction pressure drop due to the air and the solids is taken from the slope of the straight-line section of the pressure drop versus length of pipe curve, as in Figure 26.

$$\frac{\Delta P_{ft}}{\Delta L} = 0.385 \text{ in. } H_2O/\text{ft.}$$

4. Specific pressure drop.

$$\frac{\Delta P_{ft}/\Delta L}{\Delta P_{fa}/\Delta L} = 1.47$$

5. Pressure drop due to the solids.

$$\Delta P_{fp} = \Delta P_{ft} - \Delta P_{fa} = 0.123 \text{ in. } H_2O/\text{ft.}$$

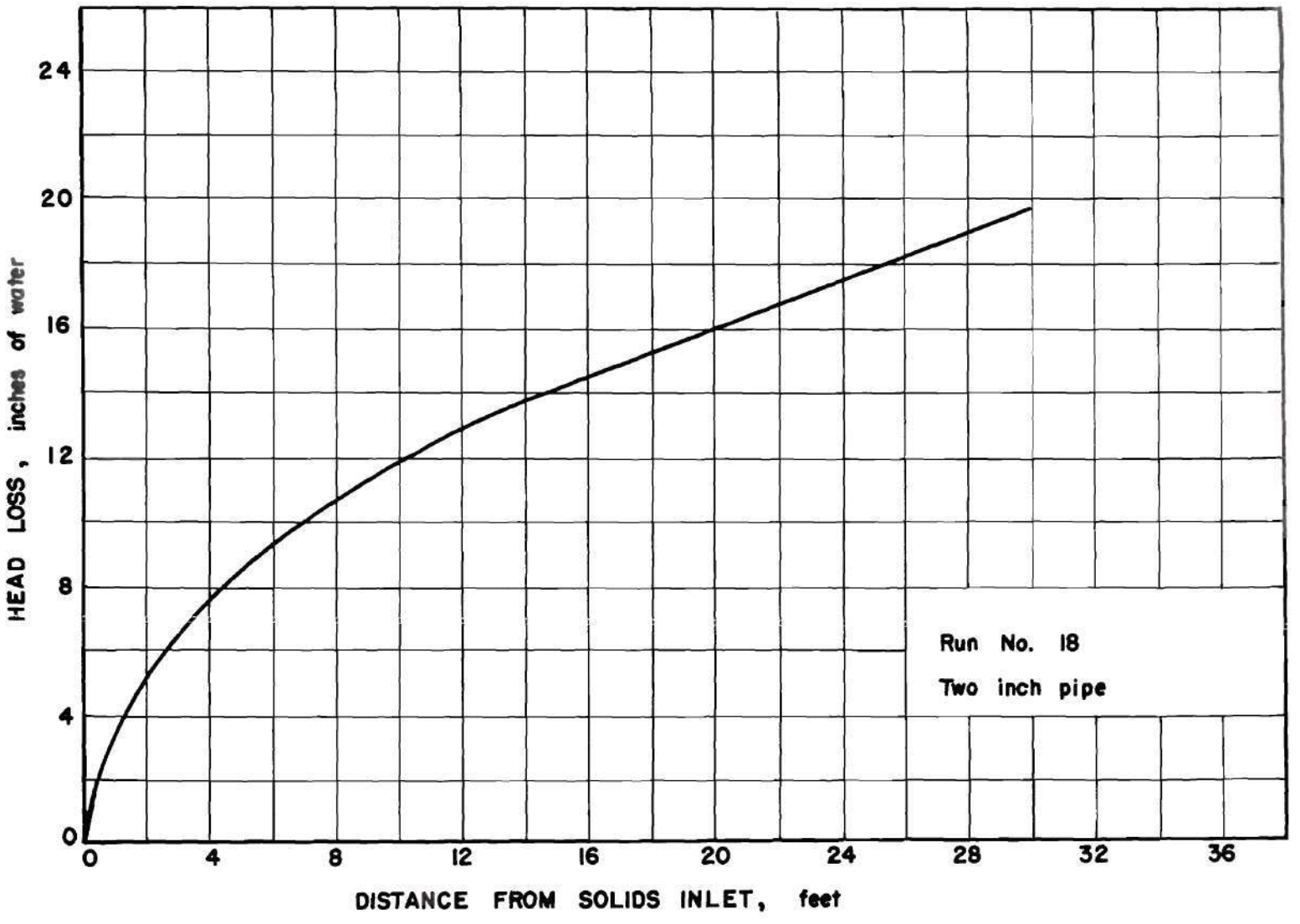

Figure 26. Pressure Drop-Pipe Length Data for Run No. 18.

6. Equilibrium particle velocity.

The equilibrium particle velocity may be determined by setting the denominator of equation (33) equal to zero and solving for the particle velocity.

$$\frac{3\rho_a C_r (u_a - u_p^*)^2}{4 d_p \rho_p} = \frac{\Delta P_{fp}/\Delta L \; g_c A u_p^*}{G_p}$$

$$u_p^* = 71 \text{ ft./sec.}$$

7. Solids friction factor.

The solids friction factor may now be calculated from equation (32).

$$f_p = \frac{2\Delta P_{fp}/\Delta L \; g_c D A}{u_p G_p}$$

8. Acceleration of a particle.

The acceleration of a particle along the pipe may be determined by equation (33), modified for use in a trial-and-error calculation. Thus,

$$\Delta L = \frac{(u_p)_{av} \; u_p}{\frac{3\rho_a C_r \left(u_a - (u_p)_{av}\right)^2}{4 d_p \rho_p} - \frac{\Delta P_{fp}/\Delta L \; g_c A (u_p)_{av}}{G_p}}$$

The procedure was as follows: first, a specific distance from the solids inlet was chosen; next, a particle velocity was assumed at this specified distance. The average particle velocity along the increment of pipe length was determined. The pressure drop due to

the solids was obtained in the manner shown in Item 5, where $\Delta P_{ft}/\Delta L$ was taken from a plot such as Figure 26, corresponding to the specified distance from the solids inlet. When the assumed particle velocity satisfied the above equation within five per cent, another increment of pipe length was specified and the procedure repeated. An illustration of the method is given below.

Run No. 18

Specified L, ft.	ΔL, ft.	Assumed u_p, ft./sec.	$(u_p)_{av}$, ft./sec.	$\Delta P_T/\Delta L$, (Fig. 26) in. H_2O/ft.	$\Delta P_{fp}/\Delta L$, in. H_2O/ft.	$(u_p)_{av}\Delta u_p/a$, ft.
1.0	1.0	26	13	2.15[a]	1.89[a]	0.97
2.5	1.5	34 36	30 31	0.82[a]	0.56[a]	1.03 1.45
5.0	2.5	48	42	0.50[a]	0.24[a]	2.57
10.0	5.0	62 60	55 54	0.40[a]	0.14[a]	6.75 5.20
20.0	10.0	70 68	65 64	0.385	0.123	15.5 10.4
80.0	60.0	72	70	0.385	0.123	56.4

[a] Includes acceleration pressure drop

IX. APPENDIX

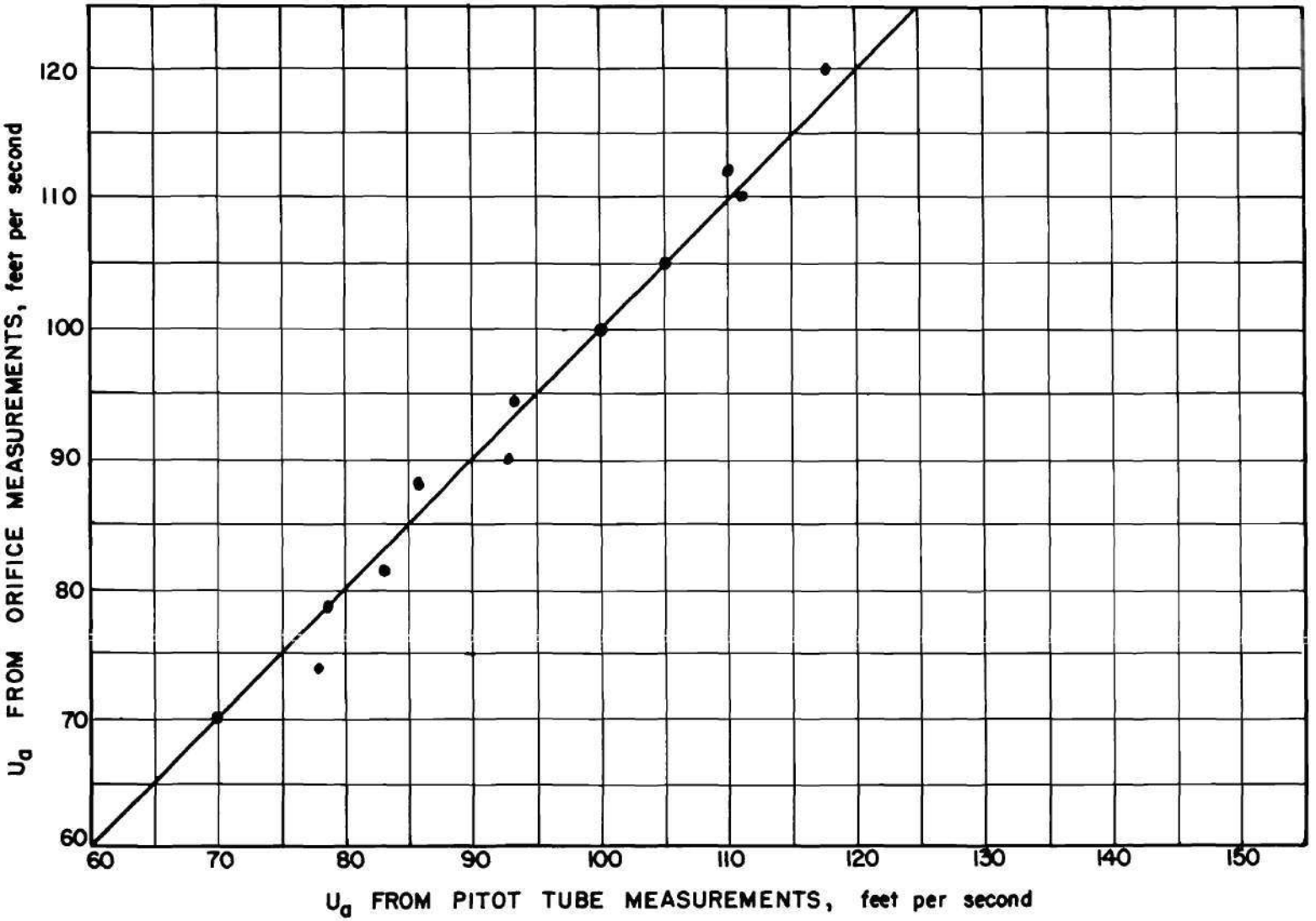

Figure 27. Comparison of Air Velocities Measured with the Orifice Meter and Pitot Tube.

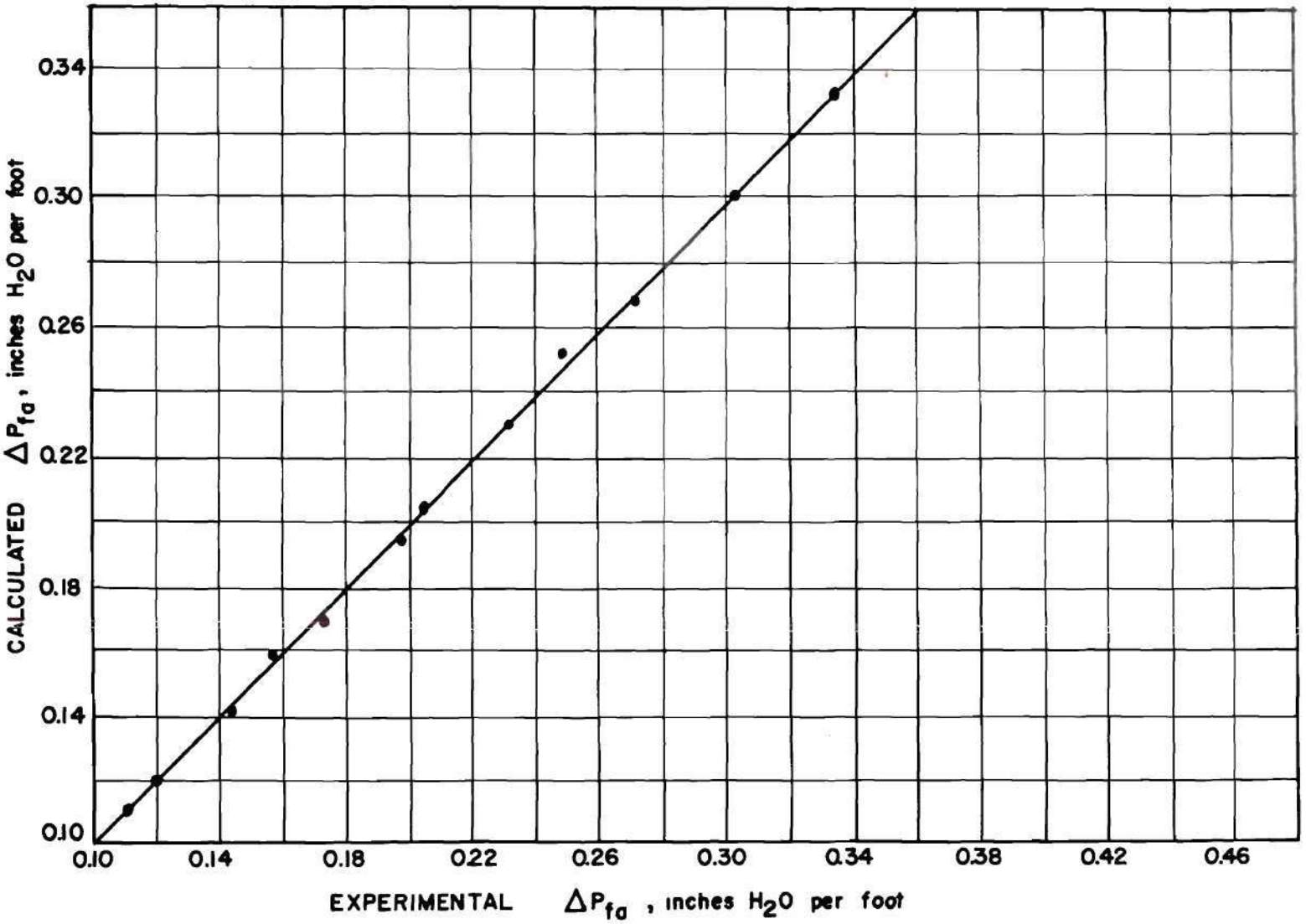

Figure 28. Comparison of the Experimental and Calculated Pressure Drops for the Conveying Air in the Two-Inch Pipe.

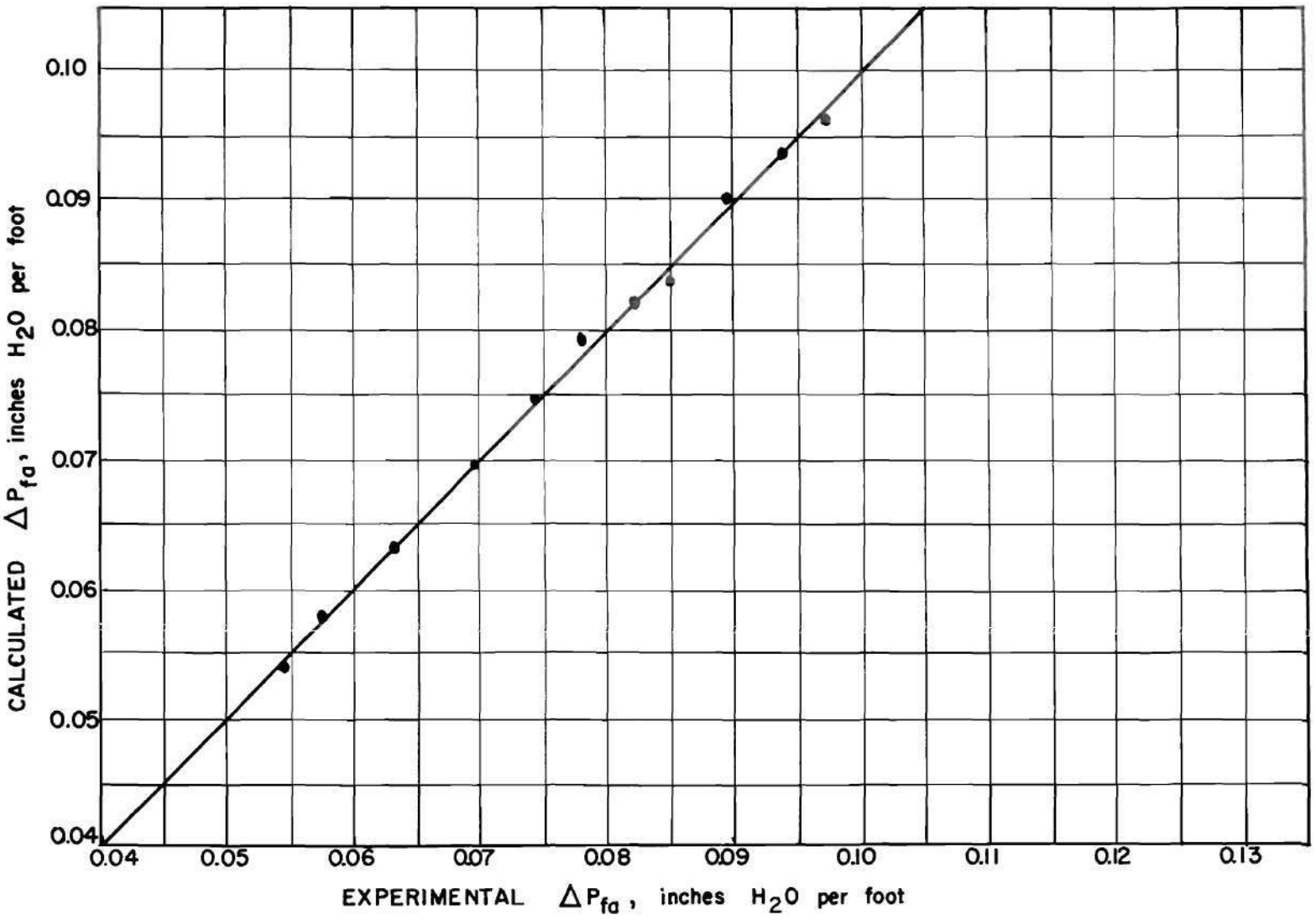

Figure 29. Comparison of the Experimental and Calculated Pressure Drops for the Conveying Air in the Three-Inch Pipe.

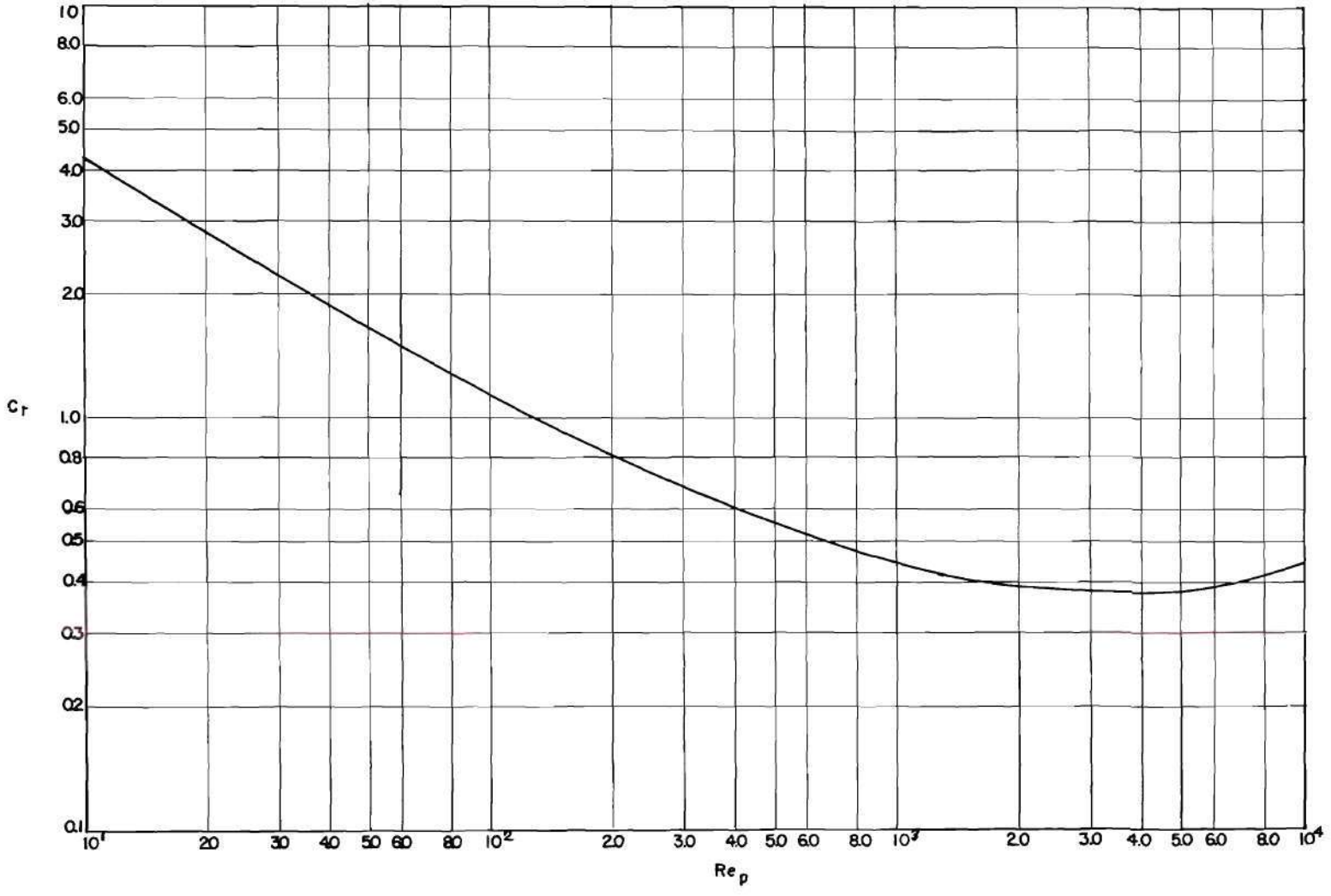

Figure 30. Coefficient of Resistance vs. Particle Reynolds Number.

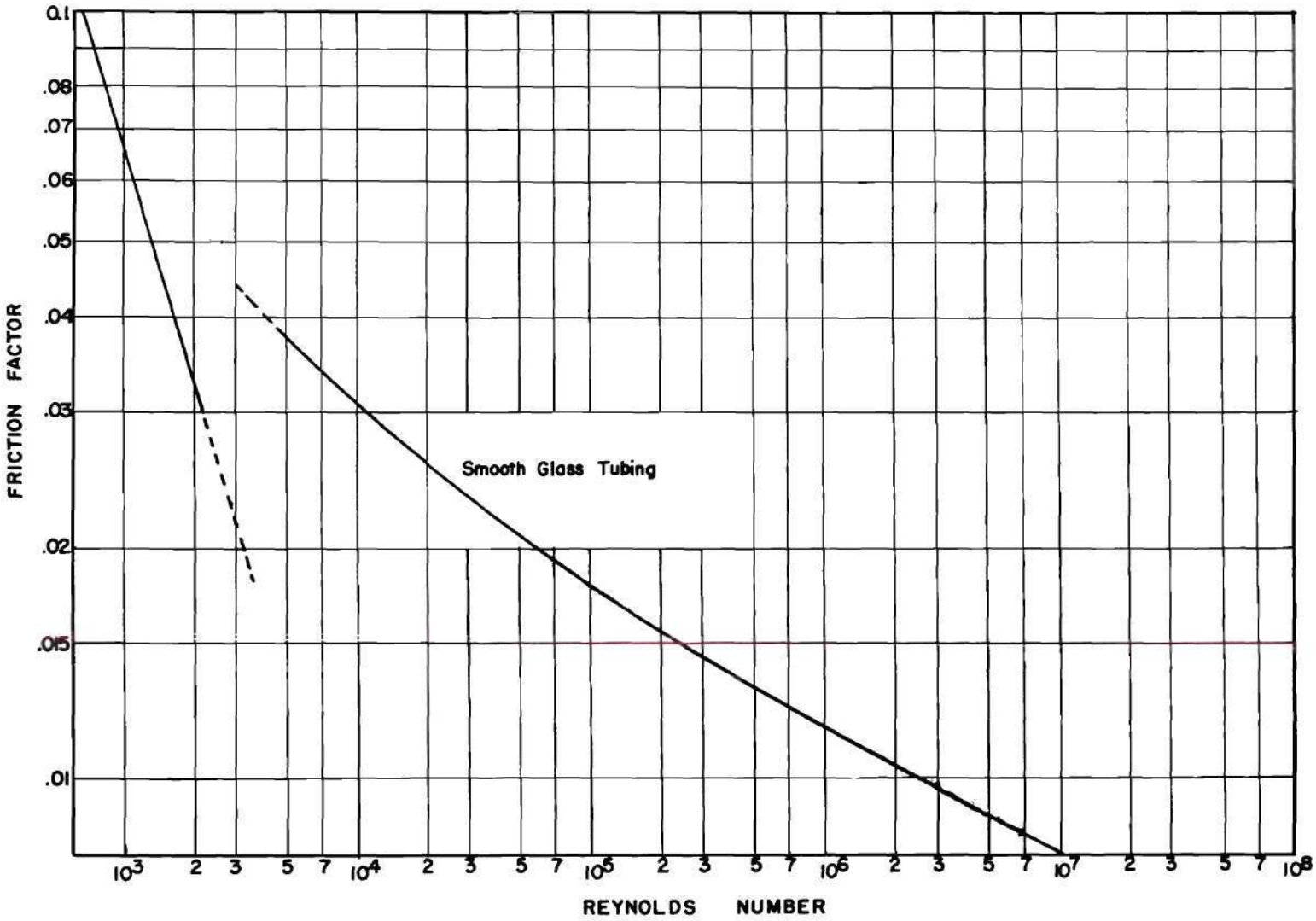

Figure 31. Air Reynolds Number-Fanning Friction Factor Relation.

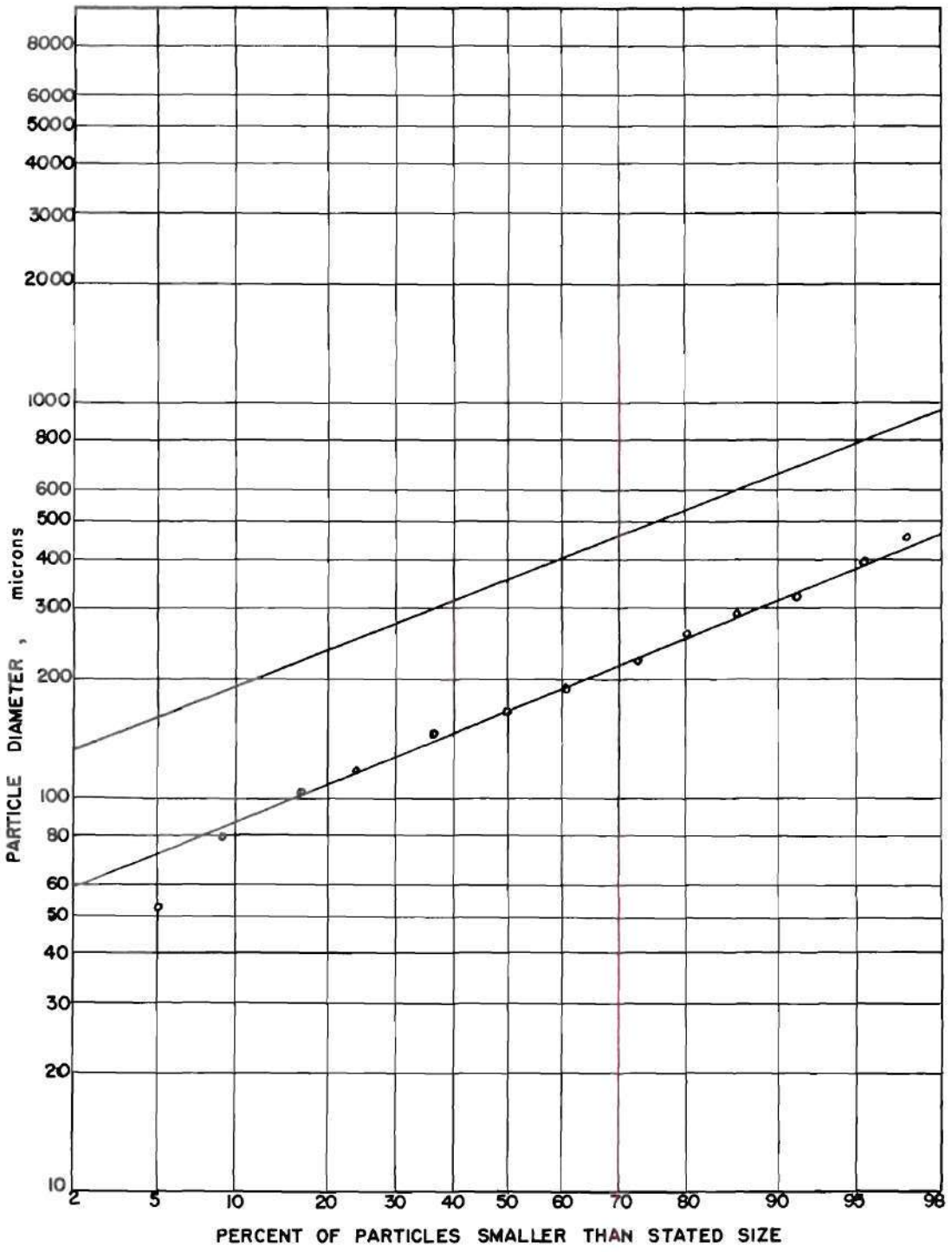

Figure 32. Size Distribution of Polystyrene Beads.

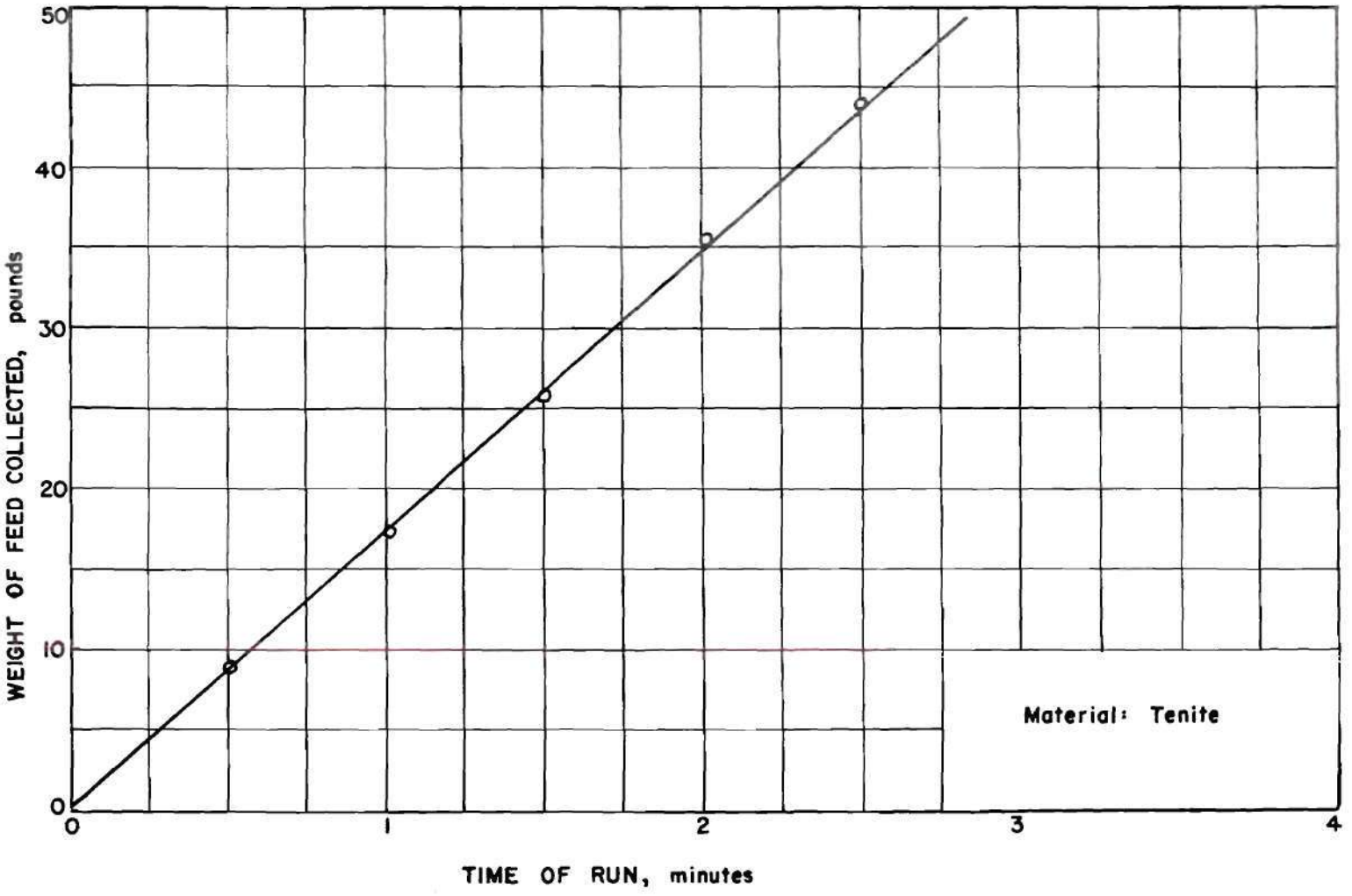

Figure 33. Calibration Curve for the Screw Feeder.

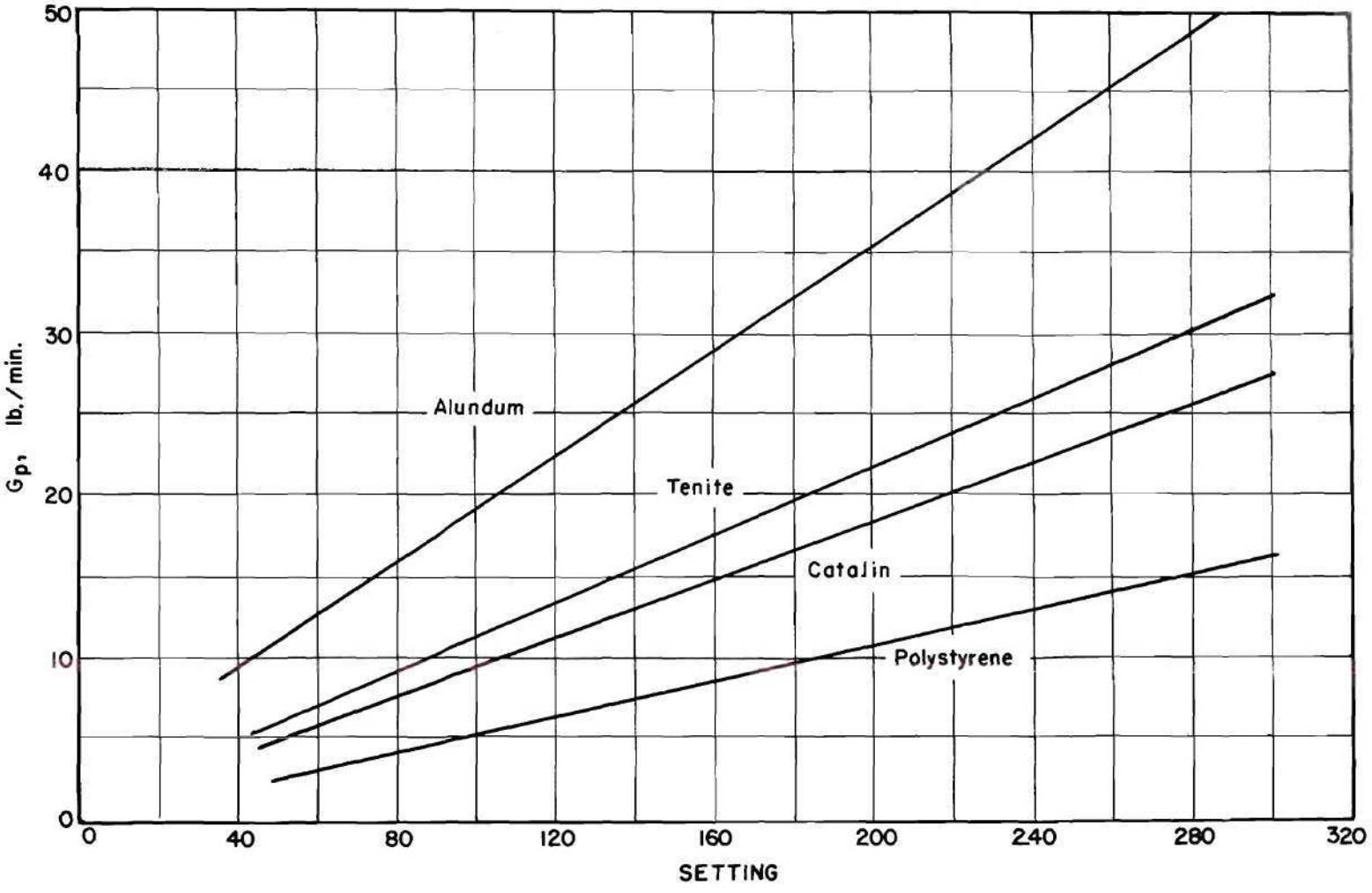

Figure 34. Calibration Curves for the Gear Reducer Settings.

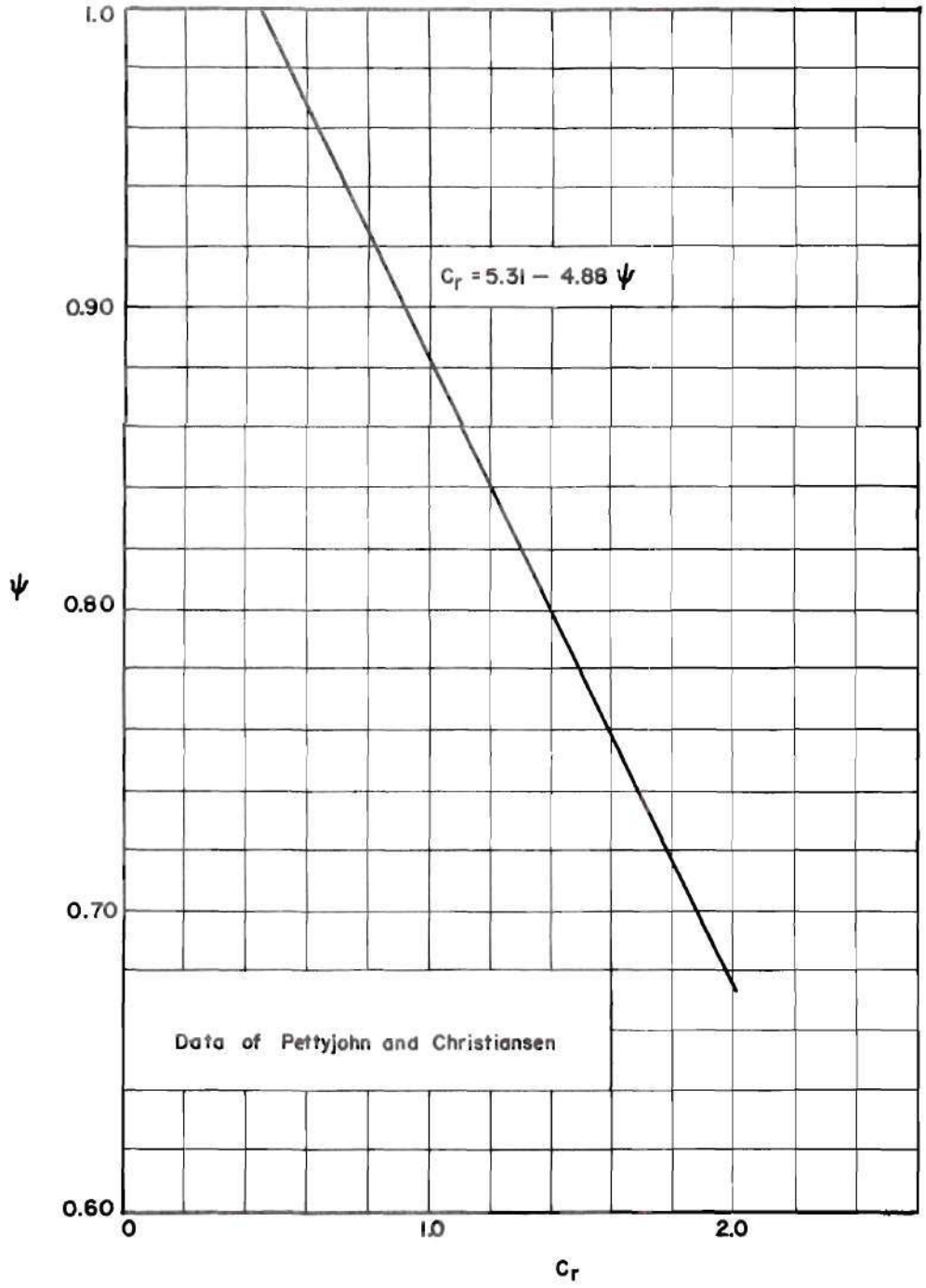

Figure 35. Coefficient of Resistance vs. Sphericity.